SEQUENCE STRATIGRAPHY AND DETRITAL ZIRCON PROVENANCE OF THE EUREKA QUARTZITE IN SOUTH-CENTRAL NEVADA AND EASTERN CALIFORNIA

A Thesis

by

BENJAMIN DAVID WORKMAN

Submitted to the Office of Graduate Studies of
Texas A&M University
in partial fulfillment of the requirements for the degree of

MASTER OF SCIENCE

May 2012

Major Subject: Geology

Sequence Stratigraphy and Detrital Zircon Provenance of the Eureka Quartzite in South-Central Nevada and Eastern California

SEQUENCE STRATIGRAPHY AND DETRITAL ZIRCON PROVENANCE OF THE EUREKA QUARTZITE IN SOUTH-CENTRAL NEVADA AND EASTERN CALIFORNIA

A Thesis

by

BENJAMIN DAVID WORKMAN

Submitted to the Office of Graduate Studies of
Texas A&M University
in partial fulfillment of the requirements for the degree of

MASTER OF SCIENCE

Approved by:

Chair of Committee,	Michael Pope
Committee Members,	Brent Miller
	Deborah Thomas
Head of Department,	John Giardino

May 2012

Major Subject: Geology

ABSTRACT

Sequence Stratigraphy and Detrital Zircon Provenance of the Eureka Quartzite in South-Central Nevada and Eastern California. (May 2012)

Benjamin David Workman, B.S., Calvin College

Chair of Advisory Committee: Dr. Michael Pope

The Middle-Late Ordovician Eureka Quartzite in south-central Nevada and eastern California is a supermature quartz arenite that was deposited along the Lower Paleozoic western passive margin of Laurentia. Measured section descriptions and facies stacking patterns indicate that the Eureka Quartzite represents a 3rd-order sequence and contains three ~2-4 m.y. sequences and many small parasequences. Detrital zircon analysis of eight samples from the base and top of four locations contains three main populations of ~1.8-2.0 Ga, ~2.6-2.8 Ga, and ~2.0-2.3 Ga, and a smaller infrequent population of ~1.6-1.8 Ga grains. These peaks are interpreted to represent sediment sourced from exposed proximal basement to the east, likely from the Yavapai and Mazatzal Provinces (~1.6-1.7 Ga), the Trans-Hudson Orogen (~1.8-1.9 Ga), Paleoproterozoic crusts (~2.0-2.3 Ga), and underlying or proximal Archean (~2.6-2.8 Ga) sources. Sediment likely was transported to the shoreline and across Archean basement by rivers draining the Transcontinental Arch. Long-shore currents played an important role in deposition and likely account for the similarity of Middle-Late Ordovician, supermature, quartz arenite deposits on western Laurentia. Although the

Peace River Arch likely provided some sediment for the Eureka Quartzite, it is apparent its provenance was mostly Trans-Hudson Orogen and Archean basement. Temporal and spatial provenance changes are inferred from probability-density plots of the detrital zircon analyses to indicate sea-level changes covered or exposed possible sediment sources during deposition.

DEDICATION

To my wife who stood by my side and encouraged me to the end.

ACKNOWLEDGEMENTS

I would like to thank the chair of my committee, Dr. Mike Pope, and my committee members, Dr. Brent Miller and Dr. Debbie Thomas, for their assistance and support throughout the course of my research and studies.

I would also like to thank my friends, fellow students, and faculty for providing a great experience and learning environment at Texas A&M University.

Finally, I would like to thank my family for their encouragement, and my wife, Diane Workman, for her continued support, love, and patience throughout the course of my studies and research.

TABLE OF CONTENTS

Page

LIST OF FIGURES

LIST OF TABLES

INTRODUCTION

The Middle-Late Ordovician Eureka Quartzite is a supermature quartz arenite deposited along the passive margin of western Laurentia (Fig. 1) and is well exposed in the southern Great Basin of Nevada and eastern California (Zimmerman and Cooper, 1999). The Eureka Quartzite and its equivalents are the only significant siliciclastic deposits within carbonate-dominated Cambrian-Devonian deposits along the Cordilleran margin (Webb, 1956; Druschke et al., 2009). Deposition of the Eureka Quartzite and its equivalents also are unique because of their extent, uniformity, and textural and compositional maturity (Ketner, 1966, 1968); these two characteristics have made the Eureka Quartzite the focus of many studies (e.g., Webb, 1958; Ketner, 1968; Zimmerman and Cooper, 1999; Wallin, 1990) and its provenance was previously studied by detrital zircon geochronology (Gehrels et al, 1995; Gehrels and Dickenson, 1995; Gehrels, 2000). Initial detrital zircon populations of the Eureka Quartzite and other Ordovician quartzites were based on four samples (Fig. 1), a total of 158 zircon grains, analyzed using thermal ionization mass spectrometry (TIMS) (Gehrels et al., 1995; Gehrels and Dickenson, 1995; Gehrels, 2000). These data were augmented and verified by a subsequent study of 400 grains using laser ablation inductively coupled plasma mass spectrometry (LA-ICP-MS) (Gehrels pers. com., 2008). The zircons analyzed by Gehrels show a bimodal age distribution dominated by both 1.8-2.0 Ga and 2.5-2.8 Ga

---

This thesis follows the style of Journal of Sedimentary Research.

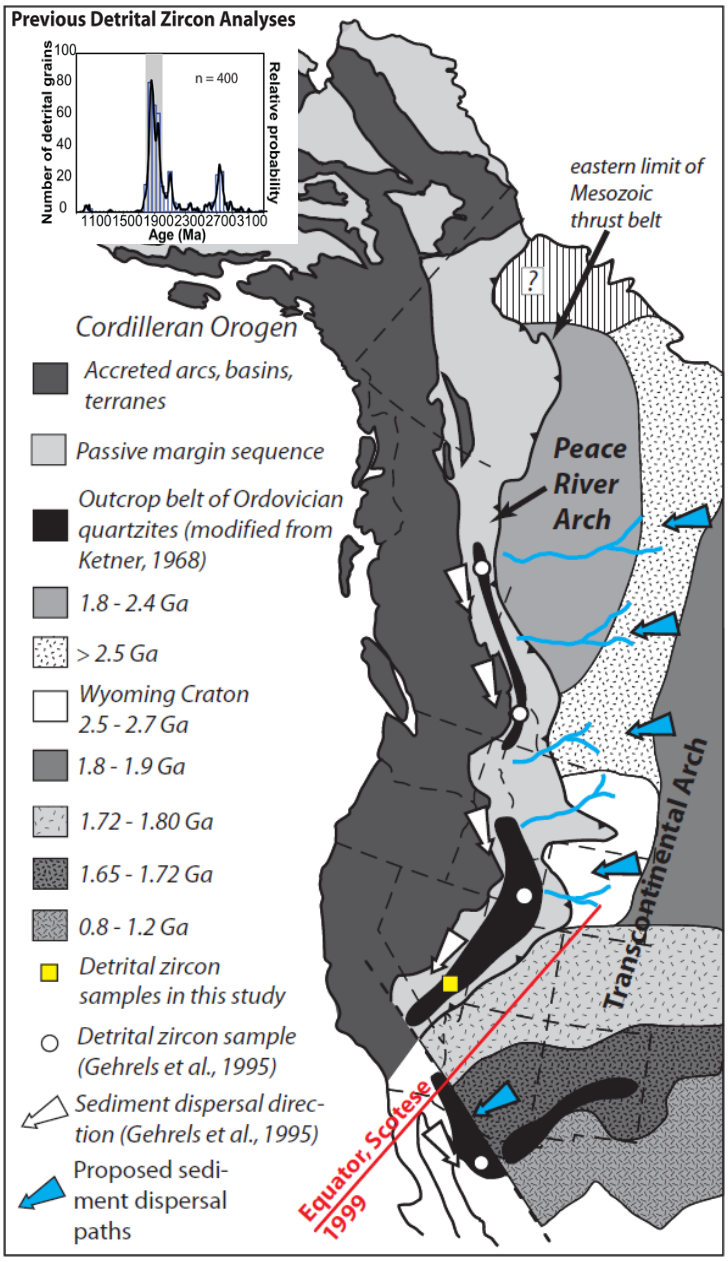

FIG. 1. - Map of western North America. Outcrops of Middle-Upper Ordovician quartz arenites (black) plotted on the Paleozoic passive margin (modified from McClelland, unpub.). Basement units from Hoffman (1989), Ross and Villeneuve (2003) and Van Schmus et al. (1993). Previous detrital zircon studies by Gehrels indicate that Middle-Late Ordovician quartz arenites of western North America have a unique provenance dominated by 1.8-2.0 Ga and 2.5-2.8 Ga grains with another small but persistent population of 2.1 Ga grains and locally rare 0.9-1.2 Ga grains. These studies indicate a uniform source area with little recycling of underlying Mesoproterozoic, Neoproterozoic, or Cambrian sandstones that contain a wide array of 1.7-0.6 Ga grains. The histogram and relative probability curve below for Middle-Late Ordovician quartz arenites of four samples along western N.A. Cordillera (Gehrels, unpub. data).

populations; however, a smaller yet prevalent 2.05-2.1 Ga population and a locally rare 0.9-1.2 Ga population also occurred. These data (Fig. 1) were interpreted to suggest that the source of sediment for these units was the Peace River Arch in northern British Columbia (Gehrels et al., 1995; Gehrels and Dickinson, 1995; Gehrels, 2000).

This paper refines the provenance and depositional settings of the Eureka Quartzite in south-central Nevada and eastern California. The depositional patterns recognized in measured sections provide insights into sediment transport and depositional environments of Middle-Late Ordovician siliciclastic systems in western Laurentia. Furthermore, sequence stratigraphy in this unit provides a framework for understanding depositional processes of similar supermature siliciclastic sediments.

Geologic Setting

A passive margin developed along the western margin of the North American Cordillera from the latest Neoproterozoic to Late Devonian (Druschke et al., 2009 and references therein). During the Ordovician, deposition along the western and eastern margins of Laurentia occurred at, or near, the equator, on either side of the Transcontinental Arch (Witzke, 1990). Most Ordovician quartz arenites deposited along the western passive margin are less than 250 m thick, but they range from as much as 500 m thick near Peace River Arch, Canada to less than 40 m thick in northern Nevada (Ketner, 1968). Depositional environments for these units range from non-marine settings to nearshore and shallow marine shelf environments that interfinger with deep-water carbonate and shale basinward (Webb, 1958; Ketner, 1968). Originally, these quartz arenites were thought to have been part of a regressive sequence (Ross, 1964;

Ketner, 1968) deposited during the Middle Ordovician sea-level lowstand (Webb, 1958); with regressive basal deposits and transgressive upper deposits (Webb, 1956). Recent biostratigraphy and carbon isotope stratigraphy (Fig. 2) indicates that basal deposits of the Eureka Quartzite are Whiterockian to late Chatfieldian (middle Mohawkian) whereas upper deposits are Cincinnatian (Druschke et al., 2008; Saltzman et al., 2003; Sweet, 2000). The Eureka Quartzite was deposited during the time of the most extensive Paleozoic continental flooding (Algeo and Seslavinsky, 1995).

The Eureka Quartzite was originally named by Hague in the Eureka district (Webb, 1956), however the term 'quartzite' is a misnomer as it was not metamorphosed. Middle-Late Ordovician quartz arenites of Laurentia record widespread texturally mature siliciclastic deposition (Ketner, 1966, 1968; Webb, 1958; Dott et al., 1986; Druschke et al., 2008). Previous sedimentological studies described the Eureka Quartzite and its counterparts to be more than 99% quartz (Wallin, 1990) with extremely low heavy mineral content; however, non-detrital pyrite and collophane (phosphate) accessory minerals locally are common (Ketner, 1966). The quartz arenite is silica cemented and consists of very fine to medium grains that are very well-sorted and well-rounded (Webb, 1956; Ketner, 1966). The Eureka Quartzite has three locally recognizable units: 1) a basal reddish brown-weathered cross-bedded quartz arenite and calcareous quartz arenite with some argillaceous beds, 2) a widespread medial vitreous white quartz arenite, and 3) an uppermost dolomitic quartz arenite (Webb, 1956). The upper dolomitic quartz arenite commonly is considered the basal unit of the overlying Ely Springs Dolomite (Langenheim et al., 1962).

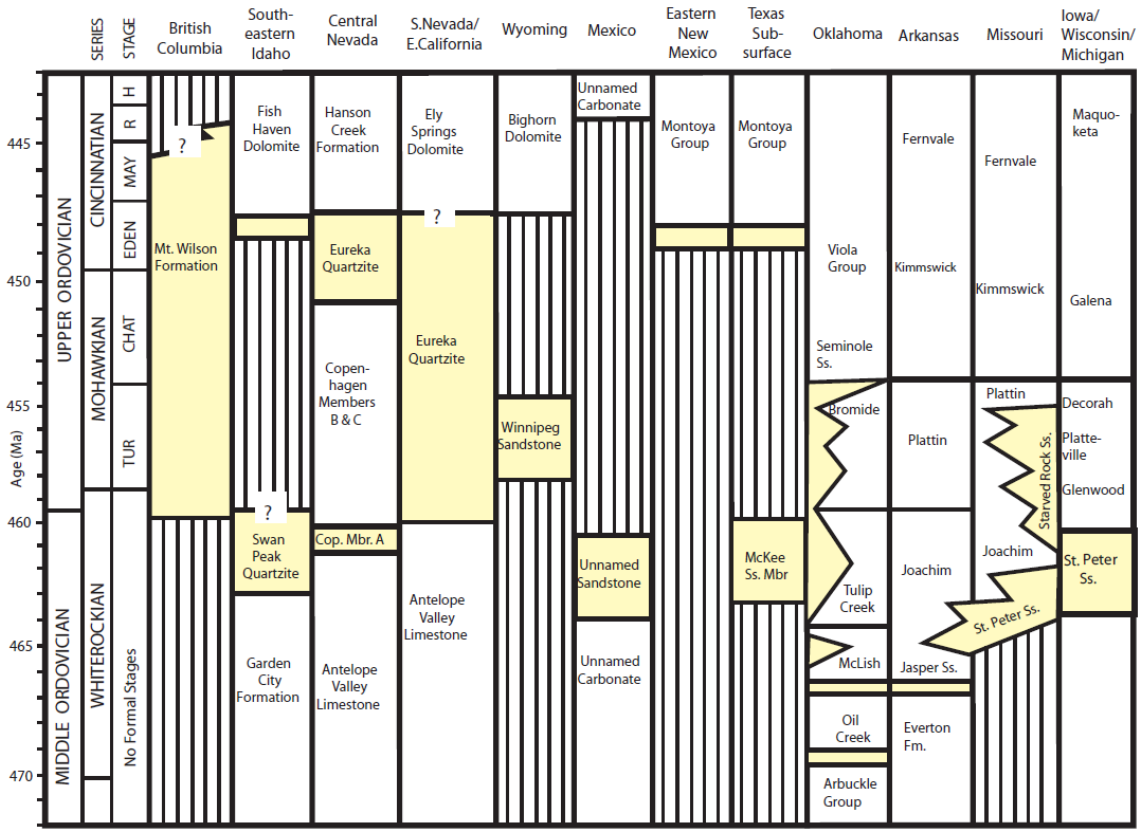

FIG. 2. - Biostratigraphic correlation chart for Middle-Upper Ordovician quartz arenites of western U.S. and U.S. Midcontinent. Duration of units modified from Norford (1969) James and Oaks (1997), Churkin (1962), Hobbs et al. (1968), Biek (1999), Poole et al. (1995), Suhm (1997), Saltzman and Young (2005), Harris et al. (1979).

The Eureka Quartzite and its equivalents were originally thought to be massive and featureless (Dapples, 1955; Webb, 1958; Ketner, 1968), but recent studies indicate these units contain an abundance of sedimentary structures: bimodal cross-bedding, hummocky cross-stratification (HCS), low-angle to planar cross-stratification, a variety of trace fossils and stromatolites (Druschke et al., 2008; Zimmerman and Cooper, 1999). Stromatolite structures were previously described as load structures and hummocky

cross-stratification (Druschke et al., 2008 and references therein). Sedimentary structures within the Eureka Quartzite are consistent with a transition in deposition from high-energy nearshore environments to lower energy offshore environments (Dott et al., 1986; Hall, 1989; Zimmerman and Cooper, 1999; and Druschke et al., 2008). Basal contacts of the Eureka Quartzite and its equivalents generally are sharp, unconformably overlying carbonate units below. Locally conformable and gradational basal contacts occur where carbonate is interbedded with the quartz arenite. The upper contact is nearly always a sharp surface marked by silicified quartz arenite overlain by Upper Ordovician sandy dolomite that grades upward into massive carbonate units containing little to no siliciclastic material (Harris et al., 1995; Leatham, 1985; Measures, 1992). In the study area, the lower boundary of the Eureka Quartzite is a major karst surface (Cooper and Keller, 2001) unconformably overlying the Pogonip Group (Fig. 2). The upper boundary is unconformably overlain by the Upper Ordovician Ely Springs Dolomite (Fig. 2).

In south-central Nevada and eastern California, a series of Late Cretaceous (90-75 Ma) thrust faults associated with the Sevier Orogeny caused crustal shortening up to 64 km (Fleck, 1970). In the study area, the post-Oligocene right-lateral Las Vegas shear zone (Fig. 3) marks an abrupt change in section displacing the Sevier Orogenic belt by as much as 40-75 kilometers (Stewart et al., 1968; Fleck, 1970; Miller and Zilinsky, 1981). Movement along the Las Vegas shear zone juxtaposed thick basinal deposits with thin landward deposits (Fleck, 1970). South of the Las Vegas shear zone in the

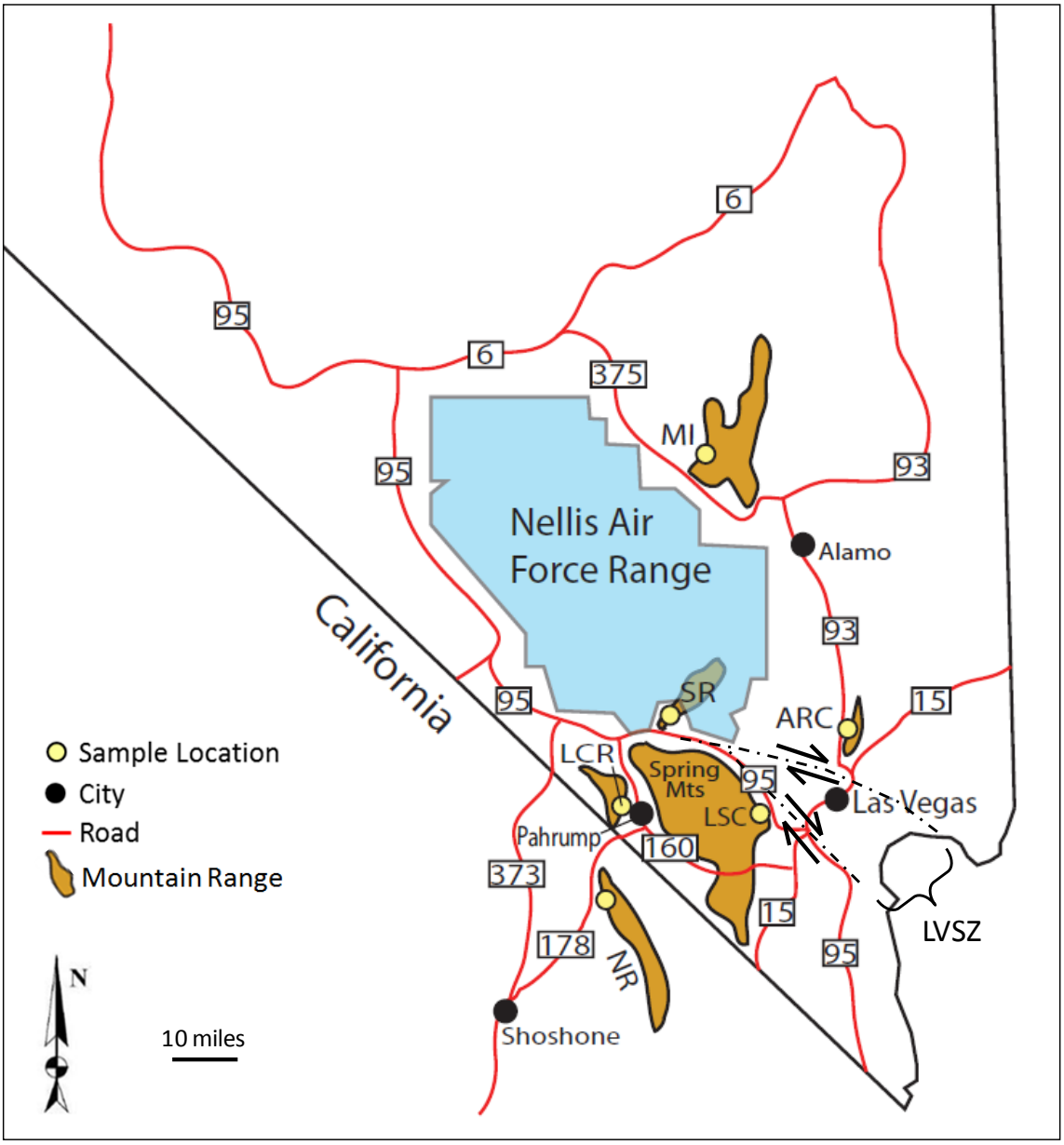

FIG. 3. - Map of study area in south-central Nevada and eastern California. ARC: Arrow Canyon Range; LCR: Last Chance Range: LSC: Lucky Strike Canyon; MI: Mount Irish Range; NR: Nopah Range; SR: Spotted Range; LVSZ: Las Vegas shear zone (indicated by dashed lines on map).

Spring Mountains, the Eureka Quartzite and the whole Ordovician section are much thinner than those north of the Las Vegas shear zone (Longwell and Mound, 1967).

Previous Provenance Studies

The Peace River Arch was suggested as the sole source of sediment for the Eureka Quartzite and its equivalents based on progressively younging ages of basal quartzite beds from north to south, a southerly decrease of thickness, and a southerly increase in textural maturity associated with a decrease in grain size (Ketner, 1966, 1968). Detrital zircon age populations also were interpreted to indicate a depositional model proposed for sourcing these quartz arenites that invokes southerly longshore currents carrying sediment more than 2000 km from the Peace River Arch (Gehrels et al., 1992; Gehrels et al., 1995; Gehrels and Dickinson, 1995; Gehrels, 2000). This model is referred to as the Long-Distance Transport Model (LDTM), and implies that little to no sediment was derived from exposed basement east of the passive margin or from recycling of underlying Precambrian or Lower Paleozoic siliciclastic rocks. More proximal sources of sediment such as the cratonal rocks to the north (Ross, 1964) or the cratonal basement to the east, rather than north (Wallin, 1990) were postulated to be the sediment sources for these units.

METHODS

Sampling Strategy

A 3-dimensional data set was developed to better understand regional and temporal variances within the provenance of the Eureka Quartzite in south-central Nevada and eastern California. Six sample locations (Fig. 3) were chosen along paleodepositional strike and dip.

Sample Locations and Collection

Samples of the Eureka Quartzite were collected at well exposed outcrops in the Arrow Canyon Range, Last Chance Range, Lucky Strike Canyon, Mount Irish, Nopah Range, and Spotted Range (Fig. 3). Stratigraphic sections were measured at each of these locations using a Jacob's staff and a Brunton compass. Each section was measured bed-by-bed at a resolution of 20 cm or less; descriptions included texture, facies, biotic assemblages, trace fossils, and sedimentary structures. Samples were taken for detrital zircons at the base and top of each section and from relevant zones based on changes in texture, sedimentary structures, and/or sequence stratigraphic position. Samples from basal and upper contacts were taken within 5 m or less of the contact.

Detrital zicon samples of ~5 kg were collected to ensure an adequate number of grains. Samples were first crushed at the sample site to reduce the risk of contamination, then sealed in a plastic sample bag and transported to the lab at Texas A&M.

Measured Sections

Sections of the Eureka Quartzite were measured at six locations (Fig. 3) in south-central Nevada and eastern California: Arrow Canyon Range (~49 m), Last Chance Range (~75m), Lucky Strike Canyon (~10 m), Mount Irish (~173 m), Nopah Range (~68 m), and Spotted Range (~107 m). Lucky Strike Canyon (Fig. 4) is the thinnest section and was deposited much further landward; this unit was juxtaposed with dramatically thicker basinward deposits by the right-lateral Las Vegas shear zone (Fig. 3) (Stewart et al., 1968; Fleck, 1970; Miller and Zilinsky, 1981; Longwell and Mound, 1967). In basinward (Mount Irish and Spotted Range) sections, a ~30-50 m thick brown quartz arenite occurs at the base of the Eureka Quartzite, unconformably overlying the Pogonip Group. This brown quartz arenite does not occur in further landward sections to the east. The bulk of the Eureka Quartzite is composed of grey-white, very-fine to fine, well sorted, well-rounded, and silica cemented grains. It is generally thin to medium bedded near the base and top, and may be thickly bedded in the middle. Sedimentary structures occur throughout each section, but some beds are massive. Ten distinct sedimentary facies (Table 1) are identified within the Eureka Quartzite: sandy dolomite (or dolomitic sand), massive quartz arenite, hematitic quartz arenite (red-beds), brown quartz arenite beds, bioturbated quartz arenite, stromatolitic quartz arenite, cross-bedded quartz arenite, hummocky cross-bedded quartz arenite, planar laminated quartz arenite, and shale. Each facies has its own distinct characteristics and not all facies were observed at every location.

FIG. 4. - Cross-section of measured sections from northwest to southeast. SB-0 represents the sequence boundary between Pogonip Group and Eureka Quartzite; SB-1 represent the sequence boundary between Ely Springs Dolomite and Eureka Quartzite. Black triangles represent smaller parasequences; blue triangles represent ~2-4 m.y. sequences within the Eureka Quarzite. Red circles are samples discussed in this paper, black circles are other samples taken.

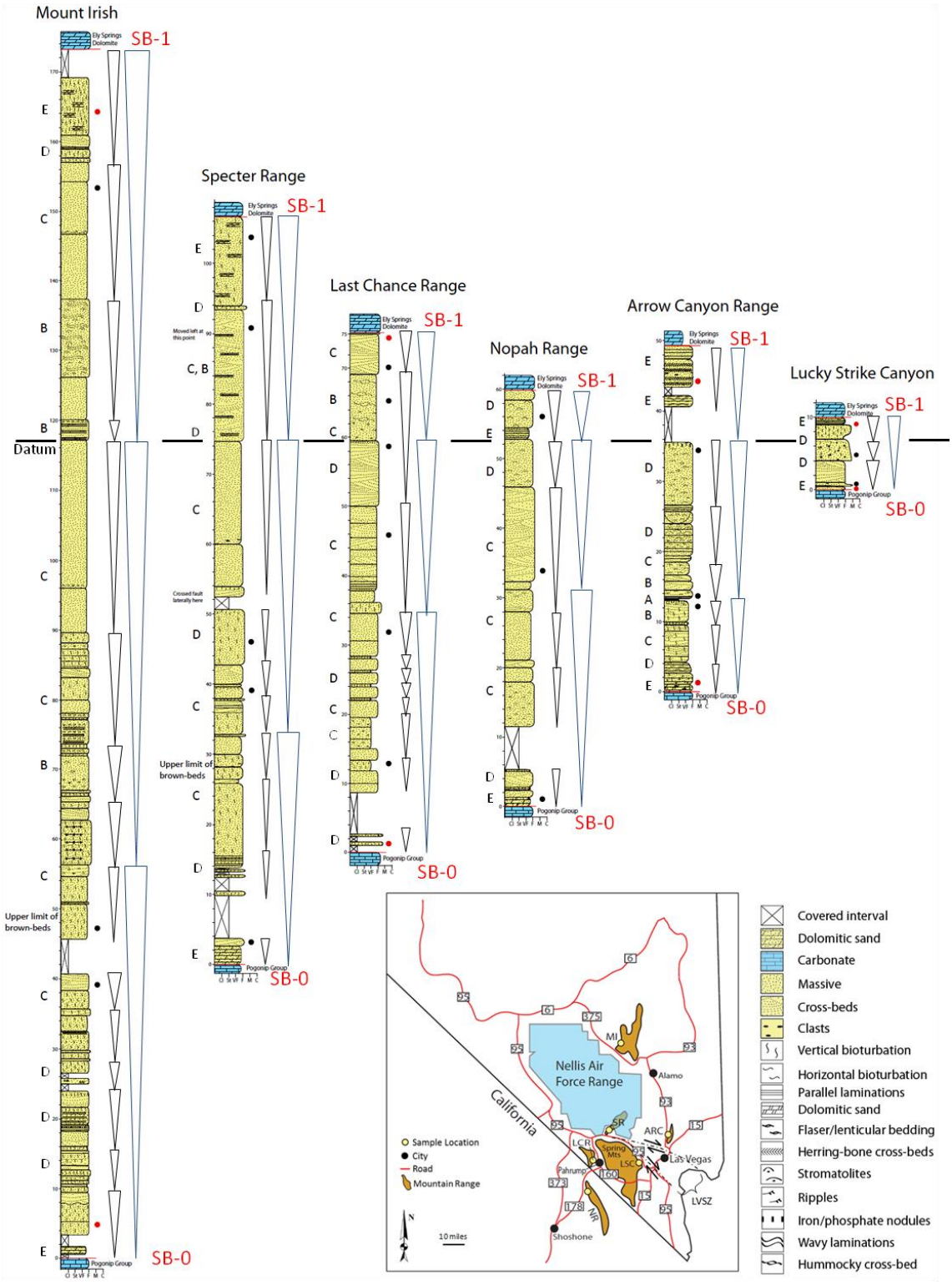
Mount Irish
Specter Range
Last Chance Range
Nopah Range
Arrow Canyon Range
Lucky Strike Canyon
Datum
SB-1
SB-0
Ely Springs Dolomite
Pogonip Group
Upper limit of brown-beds
Crossed fault laterally here
Moved left at this point
Nellis Air Force Range
California
Las Vegas
Alamo
Pahrump
Shoshone
LVSZ
Sample Location
City
Road
Mountain Range
10 miles
Covered interval
Dolomitic sand
Carbonate
Massive
Cross-beds
Clasts
Vertical bioturbation
Horizontal bioturbation
Parallel laminations
Dolomitic sand
Flaser/lenticular bedding
Herring-bone cross-beds
Stromatolites
Ripples
Iron/phosphate nodules
Wavy laminations
Hummocky cross-bed

TABLE 1. - Sedimentary facies

Facies Association	Facies Name	Description	Depositional Environment	Locations observed
A, E	Shale	Generally dark grey-brown and very thin-bedded. Commonly occurs as interbeds in quartz arenite. Typically occurs only near base of section.	Offshore, Tidal Flat	Lucky Strike Canyon
A, E	Laminated	Typically white-grey, fine-grained, well-sorted, well-rounded, and may be vitreous. Commonly occur as wavy or parallel laminations, may include flaser or lenticular bedding. Typically not associated with bioturbation. May be unclear if they have biological influence or a mechanical origin. Typically occur higher up section and common in sandy dolomite.	Offshore, Tidal Flat	Arrow Canyon Range Lucky Strike Canyon Mount Irish Nopah Range Spotted Range
B	Hummocky cross-bedded (HCS)	Typically white, fine- to medium-grained, well-sorted, and well-rounded. Hummocks are commonly more silicified and may include pockets or larger unsorted grains. May include stromatolitic facies near base and cross-bedding is truncated by hummocks. Observed near top of section.	Lower shoreface	Last Chance Range Mount Irish
B, C, D, E	Bioturbated	Typically dark grey-brown or white, fine-grained, well-sorted, and well-rounded. Generally thin-medium (< 30 cm) thick. Most commonly vertical but some horizontal Skolithos burrows; bed surfaces may include borings and other trace fossils (*Chondrites* and *Planolites*).	Offshore, Lower, Middle, Upper Shorefaces, and Tidal Flat	Arrow Canyon Range Last Chance Range Lucky Strike Canyon Mount Irish Nopah Range Spotted Range
B, C, D, E	Cross-bedded	Typically fine-grained, moderately well-sorted, well-rounded. May be thin (<30 cm) to several meters thick. Includes thin-thick low- to high-angle cross-beds, bimodal, trough, tangential, and herringbone cross-beds. Commonly occur with stromatolites, laminations, or bioturbation. Observed throughout entire section.	Lower, Middle, and Upper Shorefaces, and Tidal Flat	Arrow Canyon Range Last Chance Range Lucky Strike Canyon Mount Irish Nopah Range Spotted Range
B, C, D	Stromatolitic	Typically fine-grained, well-sortred, well-rounded, medium-set beds. Stromatolite morphology varies in height and width. Diversity and density vary greatly in and between beds. Typically occur further up section. Commonly are cross-bedded, with no bioturbation.	Lower, Middle, and Upper Shorefaces	Arrow Canyon Range Last Chance Range Mount Irish Nopah Range
B, C, D	Massive	Typically fine-grained, well-sorted, well-rounded, commonly vitreous and highly fractured. May be medium- to thick-bedded with no visible structures. More abundant higher up section	Offshore, Lower, Middle, and Upper Shorefaces	Last Chance Range Mount Irish Nopah Range Spotted Range
B, C, D	Sandy dolomite (Dolomitic sand)	Generally < ~5m thick. Sand grains are fine-lower to fine-upper, well-rounded, white. Commonly cross-bedded, bioturbated, may include carbonate clasts, sand-filled cracks, and quartz veins. Commonly associated with a crust with iron and phosphate nodules.	Middle to Upper Shoreface	Arrow Canyon Range Lucky Strike Canyon Mount Irish Spotted Range
B, C	Brown-bed	Generally dark tan-brown, fine-grained, well sorted, well-rounded. Typically are silica cemented but may be dolomite cemented. Commonly are bioturbated or cross-bedded. Occurs only lower in section.	Upper Shoreface	Mount Irish Spotted Range
B, C	Red-bed	Typically fine-grained, moderately well-sorted, well-rounded, iron-stained. Generally medium-set beds, may be massive but commonly are bioturbated. Hematite veins are common. More common lower in section.	Upper shoreface	Last Chance Range Spotted Range

Sample Preparation

Sample preparation was completed at Texas A&M. Surfaces of each sample were cleaned to remove any surface contamination, and then crushed and milled using a Jaw Crusher and Disc Mill. Milled samples were then separated by density using a Wilfley table set at an angle of 30^{o}. Collected light minerals (mostly quartz) were dried and saved. Collected heavy minerals were washed three times in acetone and then dried. Metal shavings and magnetic grains were removed using a neodymium-boron hand magnet. All remaining heavy minerals were separated under a vacuum hood using the heavy liquid Methylene Iodide (MEI). Following MEI separation, samples were rinsed six times with acetone, three times with ethanol, dried, and separated once more using a neodymium-boron hand magnet.

Detrital zircons were transferred into a Petri dish containing ethanol and were examined under a binocular microscope. A dental pick was used to separate apatite and other heavy minerals from the zircons. Double sided tape was adhered to a piece of glass and a one-inch internal diameter circle was etched into it. Tips of seven disposable pipettes were cut off, attached to the tape inside the one inch circle, and covered with tape to avoid contamination. In consecutive order, the tape from one pipette tip was removed and a random subset of separated zircons from each sample was pipetted into it wet until all the samples were on the tape. Four detrital zircon samples were placed on each circle of tape along with the three standards: PEIXE, magnetic FC-1, and non-magnetic FC-1.

After all of the samples and standards were placed on the double-sided tape, a plastic ring with a one inch internal diameter was placed on the tape around the samples and epoxy was poured into the ring and allowed to cure overnight. A lathe was used to reduce the cured puck to about 5-6 mm thick. The puck was fine polished using 6 μm, 1 μm, and 1/4 μm diamond plates, then carbon coated and imaged on a Cameca SVX50 microprobe using backscattered electrons (BSE) and Cathodoluminescence (CL). The BSE and CL images showed cores and inclusions within single zircon grains. These images were used to determine the best location to analyze individual grains and to record spot locations on grains during analysis.

Sample Analysis

Imaged pucks were transported to the Geoanalytical Laboratory at Washington State University (WSU) for U-Pb analysis following standard methods and procedures of the WSU Geoanalytical Lab (Chang et al., 2006). Laser ablation inductively coupled plasma mass spectrometry (LA-ICP-MS) was performed using the New Age™ UP-213 (Nd-YAG 213 nm) Laser Ablation System coupled with the Thermo Finnigan Element 2™ inductively coupled plasma mass spectrometer (ICP-MS). Pits ~30 μm in diameter were ablated into single zircon grains and the intensity of the measured signals was used to calculate the $^{207}Pb/^{206}Pb$ and $^{206}Pb/^{238}U$ ratios, these ratios were then used to calculate the $^{207}Pb/^{235}U$ ratio. LA-ICP-MS data was recorded and ratio calculations were performed using an Excel-based program (Chang et al., 2006). Standard grains were run at the beginning of every day and between sets of 10-15 zircons.

Sample Size

In a "worst-case" scenario, a total of 60 grains must be analyzed per sample to reduce the probability to <5% of missing an age population in a sample (Dodson et al., 1988); however, 117 grains per sample must be analyzed to ensure a 95% confidence of dating at least one grain of an age range that represents ≥5% of the total population (Vermeesch, 2004). In this study, a minimum of 92 detrital zircons were analyzed per sample, with a total of 791 zircon analyses.

Data Reduction

Collected data were first statistically cleaned by removing all values outside a 98% confidence interval (Chang et al., 2006). Once cleaned, fractionation factors were calculated from the analyses of each standard run before and after a set of 10-15 zircons. The calculated fractionation factors were then applied to the corresponding set of 10-15 zircons (Chang et al., 2006). After calculating fractionation values for all zircons, the data was compiled into two Excel spreadsheets per sample, one for fractionation factors using FC-1 standards and one for PEIXE standards. Zircon data for each spreadsheet was sorted, and values >10% discordant were culled and not reported in the results. The remaining data was plotted on Probability-Density Plots, Concordia diagrams, and Wetherill diagrams using Isoplot 3.00 (Ludwig, 2003). In general, data calculated using PEIXE fractionation factors were more consistent for the majority of the samples. To keep all data consistent, only values calculated from PEIXE fractionation factors are reported.

RESULTS

Depositional Environments

Based on the sedimentary facies (Table 1) observed in the six measured sections, the Eureka Quartzite is interpreted to have been deposited in a shallow marine environment (Ketner, 1968, Wallin, 1990; Druschke et al., 2009). These sedimentary facies are combined into five facies associations (Table 2) that represent deposition along a marine shelf and shoreface profile (Fig. 5).

TABLE 2. - Facies associations

Facies Association	Indicative Sedimentary Facies	Depositional Environment
A	Shale, laminated quartz arenite, bioturbation (horizontal)	Offshore
B	Hummocky cross-stratification, bioturbation (horizontal and vertical), sparse and small domal stromatolites, low-angle cross-bedding, possibly massive bedding	Lower Shoreface
C	Bioturbation (vertical and *Skolithos*), trough cross-bedding, tangential cross-bedding, increase in size and abundance of stromatolites, massive beds, possible sandy dolomite	Middle Shoreface
D	Bioturbation (intense *Skolithos*), tangential and high-angle planar cross-bedding, abundant stromatolites, massive beds, dolomitic sand, brown-beds, red-beds	Upper Shoreface
E	Bioturbation (vertical and horizontal), herringbone cross-bedding, lenticular and flaser bedding, laminated quartz arenite	Tidal Flat

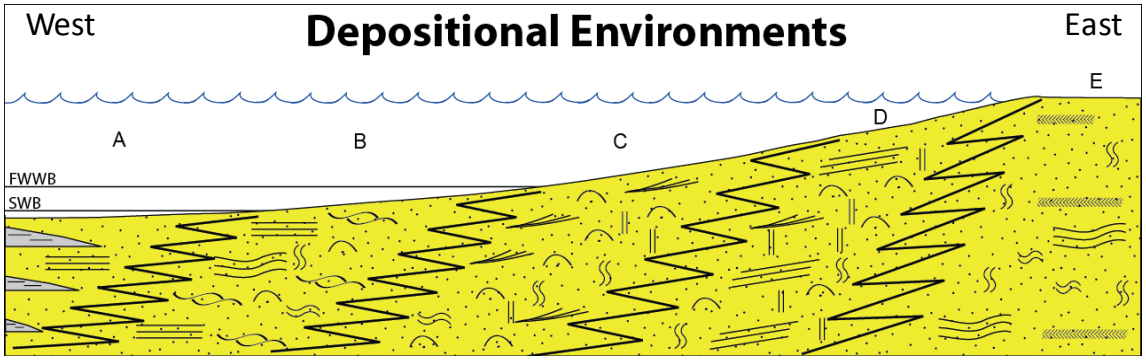

FIG. 5. - Depositional profile across the Eureka quartz arenite. Facies on this siliciclastic ramp show an offshore to onshore transition, with interbedded shale and quartz arenite beds occurring offshore. Further shoreward, hummocky cross-stratified (HCS) quartz arenite pass into trough cross-bedded and planar cross-bedded quartz arenite. Stromatolite and *Skolithos* abundance increases into the middle and upper shoreface, and locally produces massive quartz arenite. Facies Associations on diagram are: A) Offshore; B) Lower Shoreface; C) Middle Shoreface; D) Upper Shoreface; E) Subtidal and Tidal Flat.

Facies Association A (Fig. 6) represents deposition in an offshore environment, indicated by shale facies, laminated quartz arenite, and horizontal bioturbation. Shale facies represent deposition in an offshore, deeper water environment, and commonly are interbedded with fine-grained quartz arenite. Thin parallel-laminated quartz arenites commonly are bioturbated, and laminae may be indiscernible due to the degree of bioturbation (Miller, 1977).

Facies Association B (Fig. 7) represents deposition in a lower shoreface environment, indicated by hummocky cross-stratification, horizontal and vertical bioturbation, few domal stromatolites, low-angle cross-bedding and massive bedding (Miller, 1977; Druschke et al., 2009). Hummocky cross-stratified quartz arenites indicate deposition in an environment below fair-weather wave-base (FWWB) but

within storm wave-base (SWB), such as offshore to lower shoreface environments (Zimmerman and Cooper, 1999). Massive beds in lower to middle shoreface environments accumulated during storm events (Druschke et al., 2009). Small domal stromatolites are interpreted to form in lower to middle shoreface environments (Druschke et al., 2009) and increase in size and density landward in middle to upper shoreface environments.

Facies Association C (Fig. 8) represents deposition in a middle shoreface environment, indicated by trough cross-beds, tangential cross-beds, an increase in stromatolite size and abundance, and massive quartz arenite. Trough cross-beds are interpreted to represent deposition in a relatively high-energy environment above the FWWB and indicate deposition in middle to upper shoreface environments (Clifton, 2006; Miller, 1977).

Facies Association D (Fig. 9) represents deposition in an upper shoreface environment, indicated by intense *Skolithos* bioturbation, tangential, trough, and high-angle planar cross-beds, abundant and diverse stromatolites, massive beds, and dolomitic quartz arenite. Small- to large-scale planar cross-beds and intense bioturbation also are common, and indicate deposition in a higher energy environment such as an upper shoreface (Miller, 1977). Fluctuations in current and energy within this environment led to diverse bedding types (Miller, 1977). Low-angle cross bedding is interpreted to form near the center of sand bars or sand ridges (Drushke et al., 2008) in an upper shoreface environment.

Facies Association E (Fig. 10) represents deposition in a subtidal to tidal environment, indicated by laminated quartz arenite, vertical and horizontal bioturbation, herringbone cross-bedding, lenticular and flaser bedding, low-angle planar cross-beds, possible trough cross-beds, brown-beds, and red-beds. Thin parallel to wavy laminated siltstone, shale, and fine-grained quartz arenite are also interpreted to be deposited in low-energy tidal to subtidal environments (Druschke et al., 2009; Zimmerman and Cooper, 1999). Abundant trace fossils, including *Planolites* and *Chondrites*, local stromatolites, and microbial laminations associated with vertical burrows are interpreted to form in a low energy environment (Druschke et al., 2009). Tidally influenced lenticular or flaser bedding (Langenheim, 1978) may be associated with microbial laminations and bioturbation. Brown-beds and dolomitic sand or sandy dolomite commonly are bioturbated, and are interpreted to be associated with a tidally influenced transgression (Zimmerman and Cooper, 1999). They represent deposition in a lower-energy tidal flat (Druschke et al., 2009). At some locations, dolomitic sand may be capped by a regional condensed hardground or karst surface that includes quartz arenite enriched with iron oxide and possible grikes, dissolution fissures, filled with quartz sand (Keller and Lehnert, 2010) that also indicate a transgressive surface (Drushke et al., 2008). Herringbone cross-laminations indicate fluctuations in energy levels and are deposited in tidally influenced areas (Miller, 1977; Langenheim, 1978). Trough cross-beds also may form in or near tidal channels (Druschke et al., 2008).

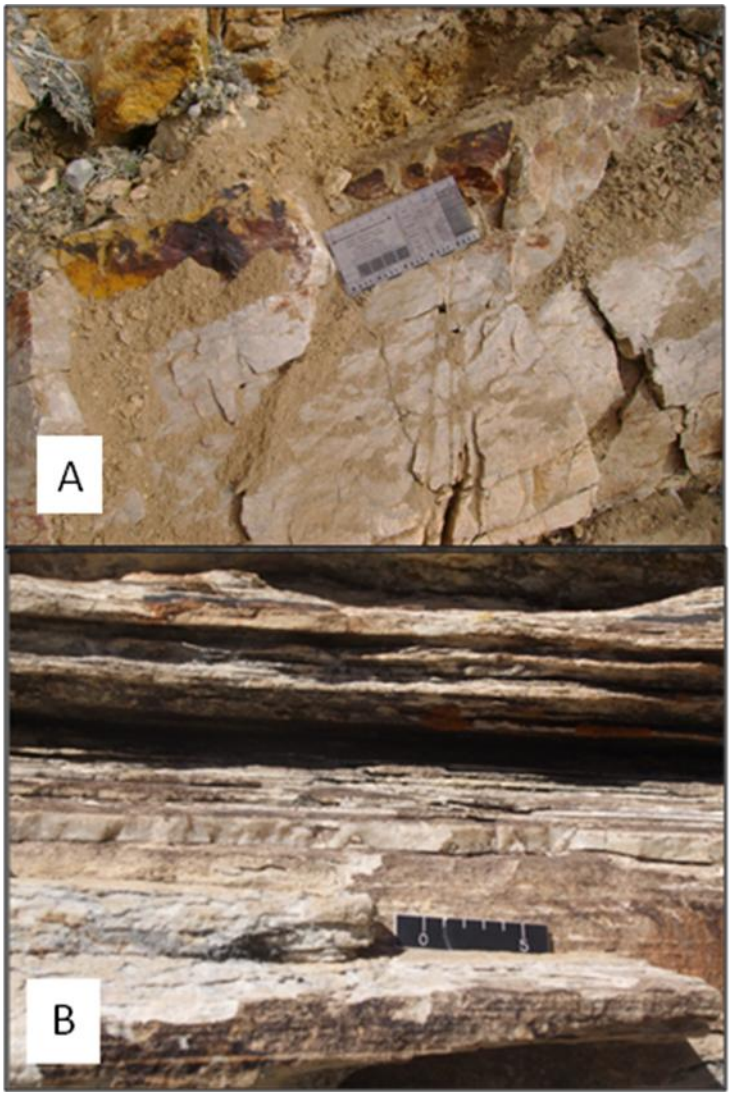

FIG. 6. - Pictures of offshore environment. A) interbedded shale; B) thinly laminated quartz arenite.

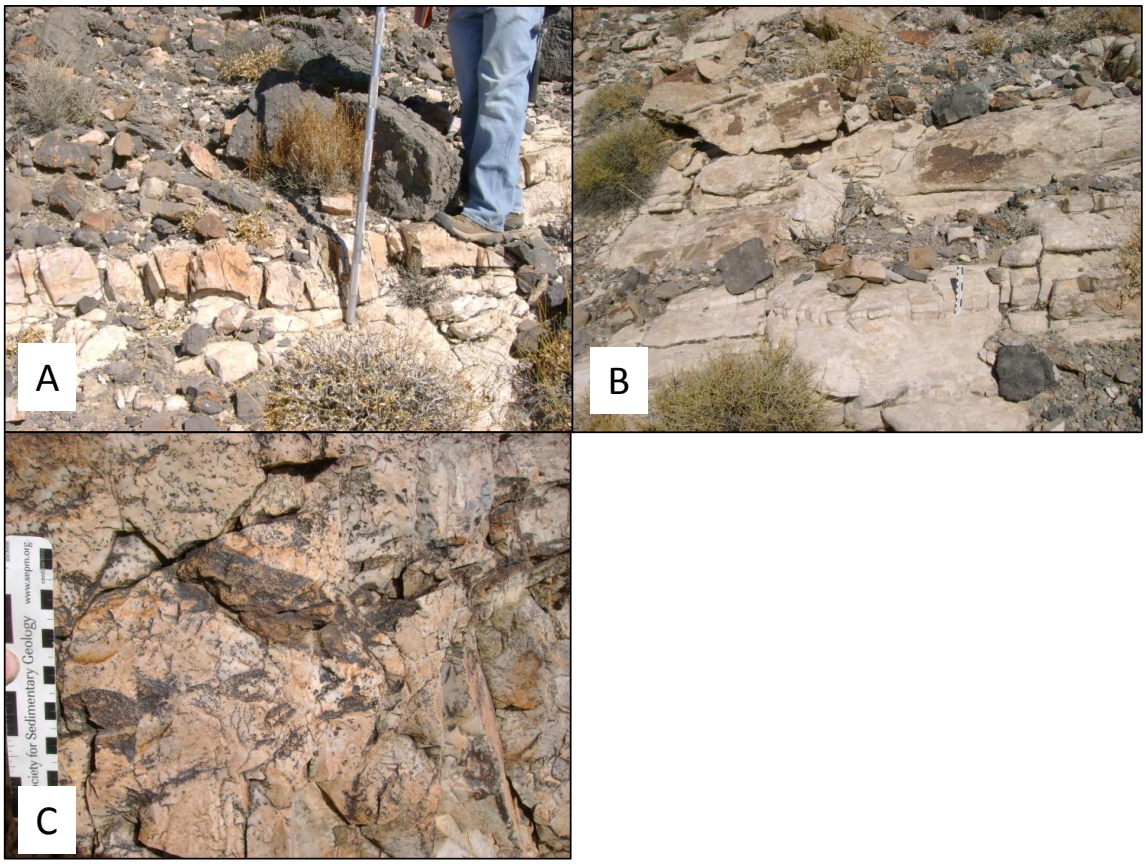

FIG. 7. - Pictures of lower shoreface environment. A) hummocky cross-stratification; B) hummocky cross-stratification; C) small domal stromatolites. Scale is in centimeters, Jacob's Staff is divided into 10 cm increments.

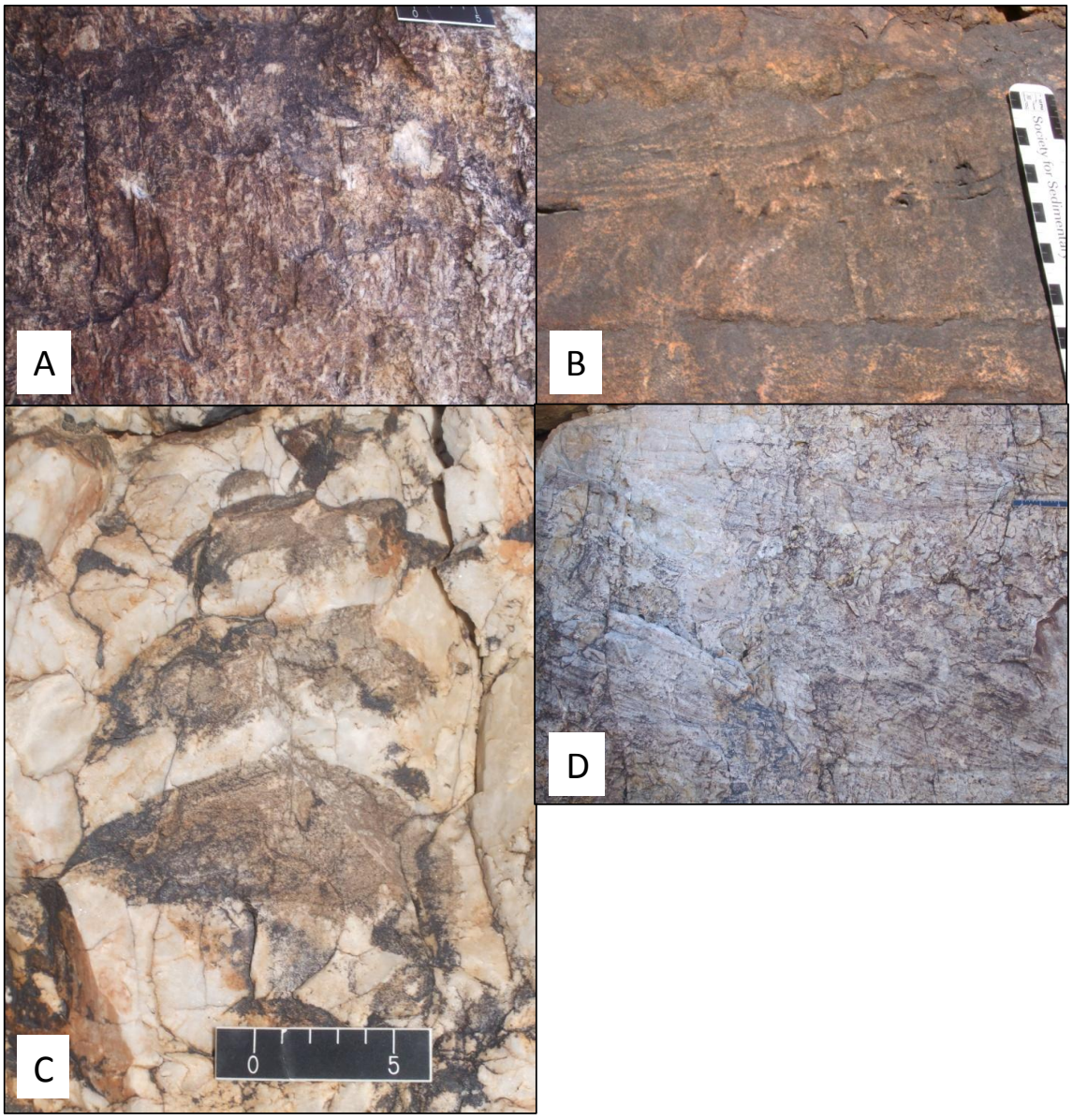

FIG. 8. - Pictures of middle shoreface environment. A) intense bioturbation; B) trough cross-beds; C) stromatolites; D) tangential cross-beds

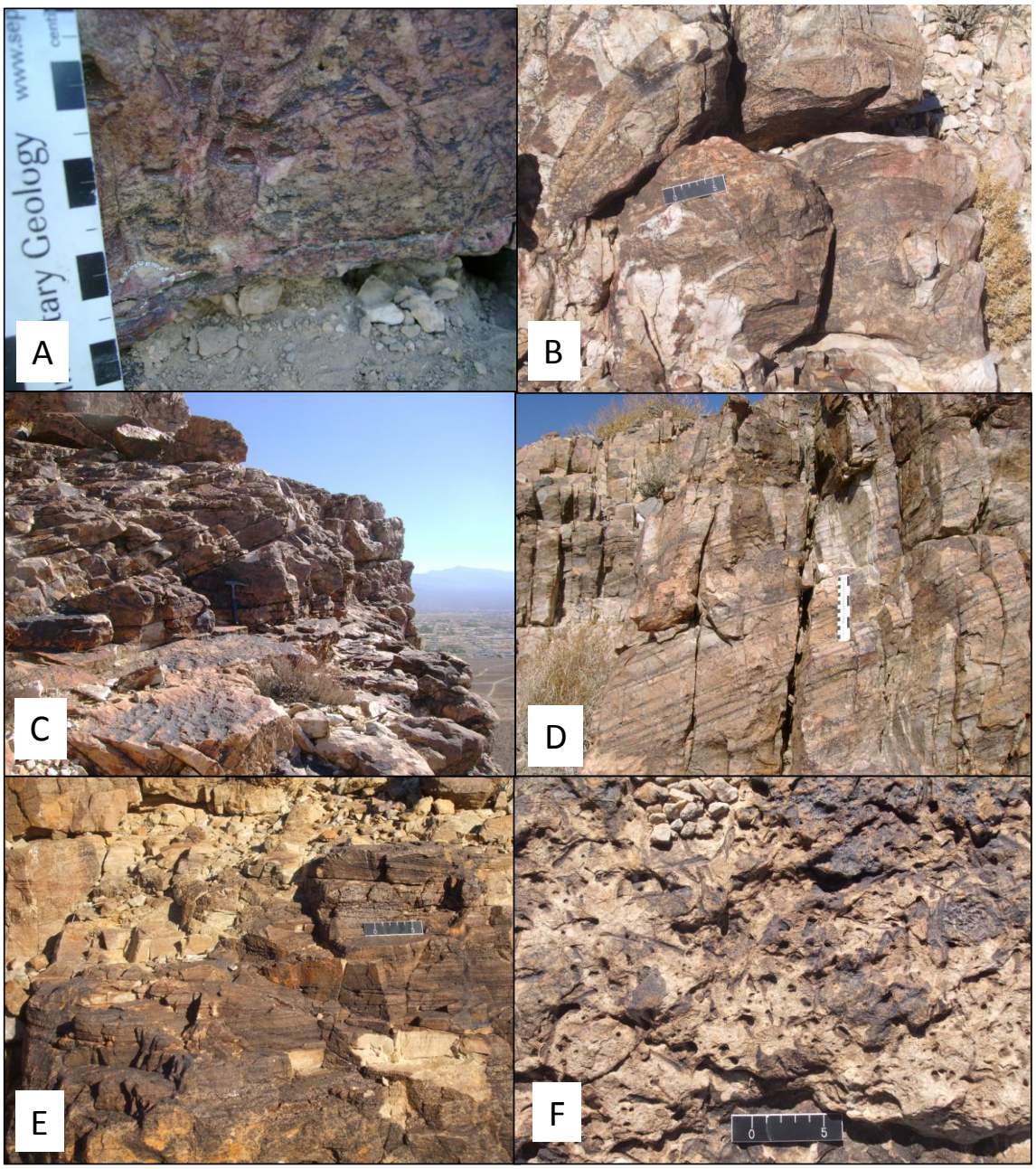

FIG. 9. - Pictures of upper shoreface environment. A) vertical *Skolithos* in red-bed; B) large stromatolite; C) thick high-angle cross-beds; D) thin high-angle cross-beds; E) brown-beds; F) bioturbation at surface of brown-bed.

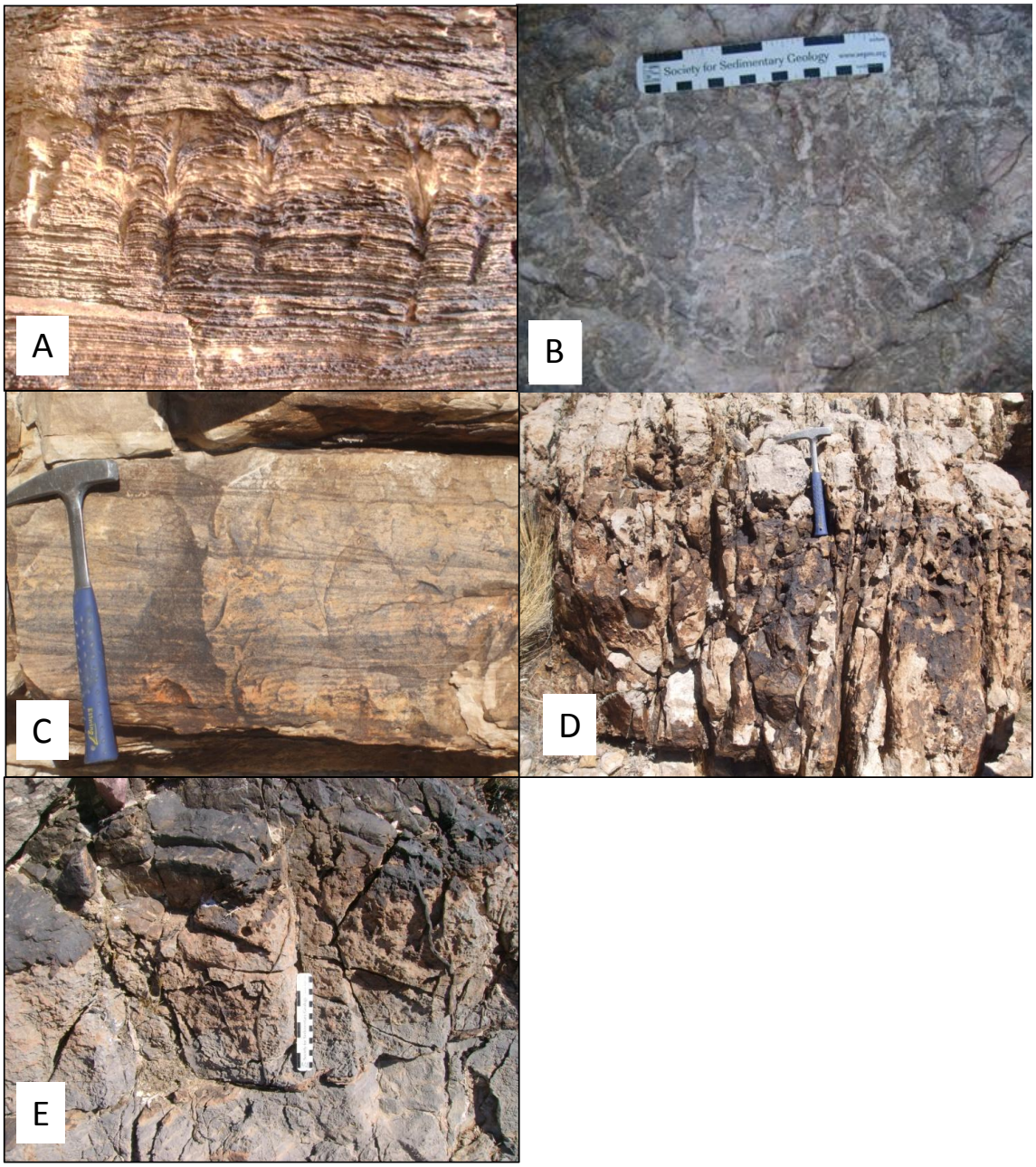

FIG. 10. - Pictures of subtidal and tidal flat environment. A) laminations and burrows in dolomitic quartz arenite; B) horizontal burrows; C) low-angle tangential cross-beds; D) dolomitic quartz arenite; E) quartz filled grikes in dolomitic sand.

Sequence Stratigraphy

Vertical stacking patterns of facies and facies associations in the measured sections record both parasequences and sequences within the stratigraphic framework for the Eureka Quartzite (Fig. 4). Parasequences are the smallest scale units, and when systematically arranged they form larger sequences (Christie-Blick et al., 1995). Sequences form when base level or sediment supply changes, and are defined as genetically related, relatively conformable successions bounded by unconformities or their correlative conformities (Christie-Blick et al., 1988; and references therein). In each section, an abrupt change in facies associated with a transition from shallow to deeper water environments was interpreted as a sequence boundary (Fig. 4). The Eureka Quartzite is a transgressive deposit interpreted to represent a complete 3rd-order sequence (Zimmerman and Cooper, 1999) including the late high-stand systems tract at the top of the Sauk Sequence (Keller and Lehnert, 2010 and references therein). The first sequence boundary (SB-0) is located at the contact between the base of the Eureka Quartzite and the underlying Pogonip Group; the second major sequence boundary (SB-1) is located at the contact between the Eureka Quartzite and the overlying Ely Springs Dolomite. This sequence boundary is interpreted to represent the boundary between the Sauk and Tippecanoe Sequences (Keller and Lehnert, 2010), but it most likely represents the top of the 2nd-order Sauk Sequence (Zimmerman and Cooper, 1999 and references therein) and Based on biostratigraphy and chemostratigraphy the interval between the two sequence boundaries represents ~10 m.y. (Fig. 2). Due to geographic location and imprecise biostratigraphic control, the sequence boundary at the base of the Eureka

Quartzite is difficult to precisely date, but it likely lies within the late Whiterockian or Chatfieldian (middle Mohawkian), and the upper sequence boundary occurs in the late Edenian Stage (Early Cincinnatian) (Druschke et al., 2008; Zimmerman and Cooper, 1999; Sweet, 2000; Saltzman et al., 2003). The lower to middle section of the Eureka Quartzite is interpreted to represent a Transgressive Systems Tract (TST) (Zimmerman and Cooper, 1999). These deposits record a deepening in water depth until a Maximum Flooding Zone (MFZ) is reached, and the remainder of the Eureka Quartzite is interpreted to represent a Highstand Systems Tract (HST) (Zimmerman and Cooper, 1999). The HST represents deposition in shallower water as sediment was deposited during sea-level fall or as sediment input caused a basinward shift in the shoreline. Confined within the 3rd-order sequence of the Eureka Quartzite are three ~2-4 m.y. sequences. Several small-scale parasequences that represent minor shallowing or deepening events also are recorded within each sequence.

Detrital Zircon Results

Detrital zircon age spectra were determined for both basal and upper samples (Fig. 11) from Arrow Canyon Range, Last Chance Range, Lucky Strike Canyon, and Mount Irish. A summary and description of the number of concordant grains and age populations for each sample is given in Table 3. Physical characteristics of zircon grains varied greatly from sample to sample in size, shape, color, and internal zoning. Analyzed zircons were generally clear, light tan or light pink in color, and typically were well rounded with fewer elliptical grains. Analyzed grains were ~100-250 μm in diameter, un-zoned to minor-zoned, and lacked inclusions. If an analyzed zircon was

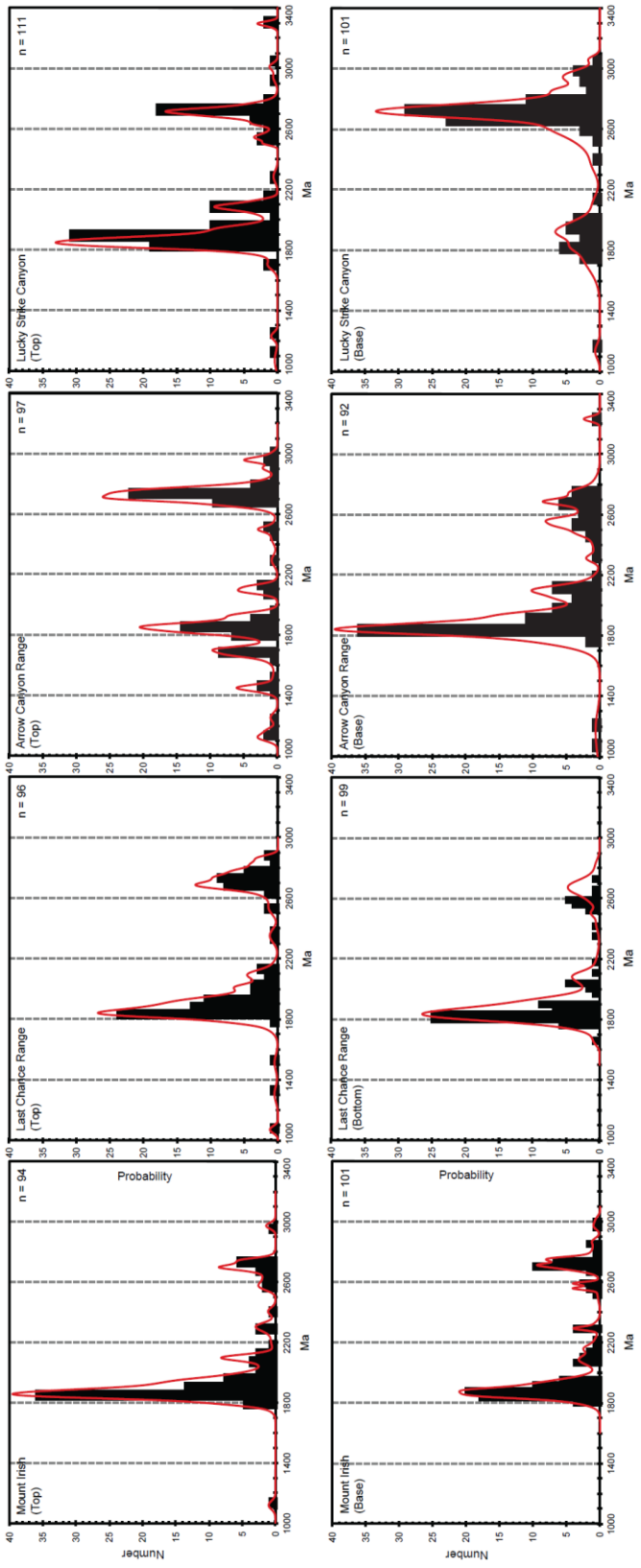

FIG. 11. - Probability-density plots and histogram. All histograms have been scaled from 1000-3400 Ma on the x-axis and 0-40 on the y-axis.

TABLE 3. - Description of analyzed samples.

Sample	Location	# of Grains	Description of Grains	Major Peak(s)	Minor Peak(s)
ACW-1	Arrow Canyon Range - Base	93	Majority were clear-light tan and light pink, rounded, sub-spherical and elliptical, and ~100-250 µm in diameter	~1800-1850 Ma	~1900 Ma ~1950-2000 Ma ~2100 Ma ~2650-2700 Ma
ACW-5	Arrow Canyon Range - Top	97	Clear-light tan, rounded, sub-spherical to spherical, and ~100-200 µm in diameter	~1700 Ma ~1800-1900 Ma ~2650-2750 Ma	~1450-1500 Ma ~2050-2150 Ma ~2900-3000 Ma
LSC-1	Lucky Strike Canyon - Base	101	Clear-light tan, rounded, sub-spherical to spherical, and ~100-200 µm in diameter	~2650-2750 Ma	~1750-2000 Ma
LSC-3	Lucky Strike Canyon - Top	111	Clear-light tan and light pink, rounded, sub-spherical to spherical, and ~150-250 µm in diameter	~1800-1950 Ma ~2700-2750 Ma	~2050-2100 Ma
MI-1	Mount Irish - Base	104	Clear-light tan, rounded, sub-spherical to elliptical, and ~100-200 µm in diameter	~1850-1950 Ma ~2700-2750 Ma	~2050-2100 Ma ~2300 Ma ~2550-2600 Ma
MI-5	Mount Irish - Top	94	Clear-light tan, rounded, sub-spherical to spherical, and ~100-200 µm in diameter	~1850-1900 Ma	~2050-2150 Ma ~2650-2750 Ma
PRMP-11	Last Chance Range - Base	99	white-light tan and light pink, ruonded, sub-spherical to spherical, and ~100-200 µm in diamter	~1800-1900 Ma	~2650-2700 Ma
PRMP-10	Last Chance Range - Top	96	clear-light pink, rounded, sub-spherical to spherical, and ~150-300 µm in diameter	~1800-1950 Ma ~2650-2750 Ma	

zoned, care was taken to place the laser spot in the center of the core, and not to cross into surrounding zones. To prevent errors in U/Pb age calculations, heavily zoned zircons and zircons with unavoidable inclusions were not analyzed.

U-Pb ages for detrital zircons >10% discordant were culled from the data set. U-Pb ages <10% discordant are displayed on probability-density plots (Fig. 11) and Wetherill Concordia diagrams (Fig. 12). Probability-density plots provide a convenient way to visualize data obtained by randomly sampling detrital zircons (Anderson, 2005)

and help to identify the most prevalent ages in a sample. These plots provide a quick, efficient, analytical comparison of each sample (Fedo et al., 2003; Sircombe, 2000; Vermeesch, 2004). A caveat of Probability-Density plots is that if sample size is too small, they may not adequately represent the zircon populations of a sample (Anderson, 2005). In these cases, invalid peaks should be removed or smoothed out, but since there is no way of knowing whether the peaks are invalid, this may result in the loss of significant data (Anderson, 2005). No peaks were removed or smoothed in the data presented.

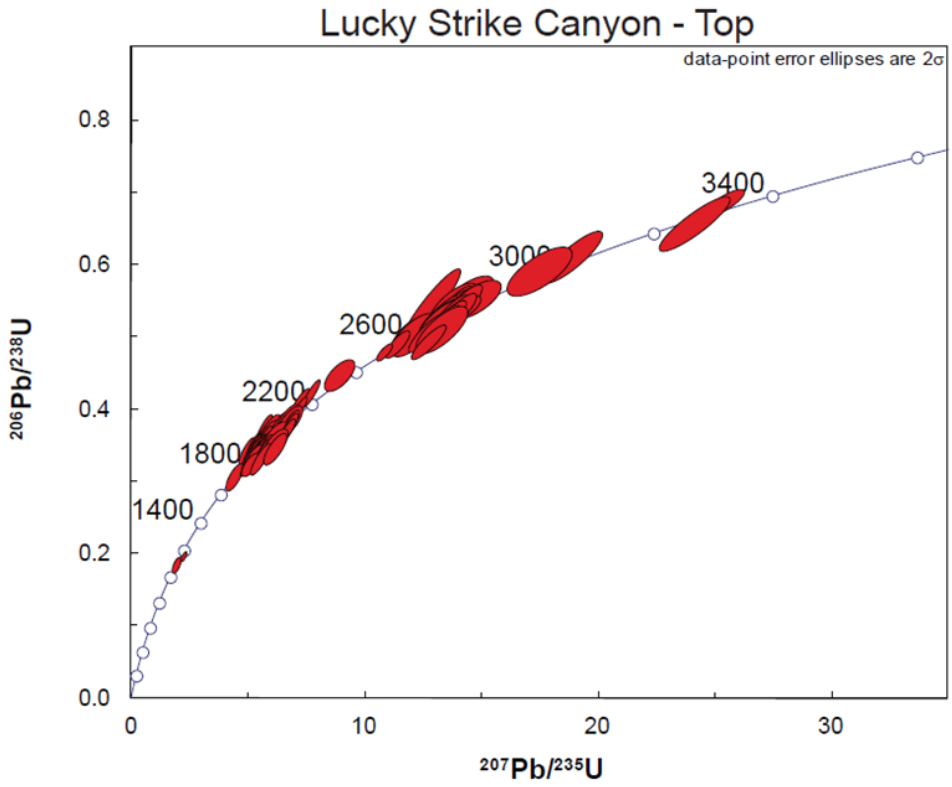

FIG. 12. - Example Wetherill Concordia plot. Sample is from the top of the Lucky Strike Canyon section.

Detrital Zircon Interpretation

Detrital zircon signatures of the Eureka Quartzite and its equivalents are distinct from other Paleozoic quartzites in the western Cordillera (Gehrels, 2000; Gehrels et al., 1995; Gehrels and Dickenson, 1995). Analysis of the eight detrital zircons samples indicates there is both spatial and temporal variance between each sample of the Eureka Quartzite. A visual comparison of the probability-density plots and histograms (Fig. 11) from base to base and top to top shows that the corresponding samples have similar age populations, but they differ in abundance. Variability in the height (probability) of peaks, the appearance and disappearance of other peaks, and the slight to noticeable variability within age populations likely indicate sourcing from different regions during deposition.

Temporal Variability

Mount Irish: The two samples from Mount Irish have similar detrital zircon populations; ~1.8-1.9 Ga zircons predominate in both the basal and upper sample, but it has a slightly higher relative probability at the top. A minor peak at ~2.65-2.7 Ga also exists in both samples, but this peak is diminished slightly in the top. At the base, three minor peaks occur at ~2.1 Ga, 2.3 Ga, and ~2.5-2.6 Ga, and a very small peak occurs at ~3.0 Ga. At the top, a minor peak occurs at ~2.1 Ga, a small peak occurs at ~2.3 Ga, and a very small peak occurs at ~3.0 Ga. A single ~1.1 Ga grain occurs in the upper sample, but none occur in the base.

Last Chance Range: The two samples from Last Chance Range have similar detrital zircon signatures, but vary in abundance. One prominent peak occurs at ~1.8-1.9

Ga in the base; while two prominent peaks occur at ~1.8-1.9 Ga and ~2.6-2.7 Ga in the top. In both samples, the most prominent peak occurs at ~1.8-1.9 Ga with similar relative probabilities; while, the minor peak at ~2.6-2.7 Ga nearly doubles in the top. Individual grains occur at ~1.0-1.1 Ga, ~1.3 Ga, ~1.5 Ga, and ~2.3-2.4 Ga in the base but are absent in the upper sample. A small peak occurs at ~2.1 Ga in both samples.

Arrow Canyon Range: The two samples from Arrow Canyon have very different detrital zircon signatures. At the base of the section a very prominent peak occurs at ~1.8-1.9 Ga, with smaller peaks at 2.05-2.2 Ga and two peaks between 2.5-2.8 Ga; whereas at the top of the section, prominent peaks occur at ~2.6-2.8 Ga, ~2.05-2.1, ~1.8-1.9 Ga, ~1.7-1.75 Ga, and 1.4 Ga. Prominent peaks in each sample also vary widely in relative probability. While probability of the ~1.8-1.9 Ga peak is reduced to half from the base to the top, the probability of the ~2.65-2.7 Ga peak more than tripled. There is also significant variation in the minor peaks moving up-section. Three minor peaks at the base occur at ~2.05-2.1 Ga, ~2.5-2.55 Ga, and ~2.65-2.7 Ga. At the top of Arrow Canyon, these peaks are greatly reduced or disappear completely, but several minor peaks occur at ~1.45 Ga, ~1.65-1.7 Ga, ~2.1 Ga, and ~2.95-3.0 Ga.

Lucky Strike Canyon: The two samples from Lucky Strike Canyon have two similar main peaks but they vary greatly in abundance. At the base, the prominent peak occurs at ~2.7 Ga and a minor peak occurs at ~1.8-1.9 Ga; whereas at the top, the prominent peak occurs at ~1.8-1.9 Ga. In the upper sample, the ~1.8-1.9 Ga peak is more than five times greater than at the base, but the ~2.7 Ga peak is much smaller than at the base. A minor peak at ~2.05-2.1 Ga and a small peak at ~3.3 Ga are present in the

top, but are absent in the basal sample. A very small peak ~1.1-1.2 Ga occurs in both samples.

Spatial Variability and Significance

Detrital zircon signatures in the Eureka Quartzite vary stratigraphically within, and between, each section (Fig. 11), indicating temporal and spatial changes in provenance. 1.8-1.9 Ga zircons are common in all samples, but are the most prominent population in six of the eight samples. This indicates the Trans-Hudson Orogeny is the most common zircon source for all locations. 2.6-2.7 Ga zircons also are common constituents of every sample, and is the most prominent population in the basal Lucky Strike Canyon and upper Arrow Canyon Range samples. At the onset of deposition, ~2.6-2.7 Ga rocks were the primary source of zircon with a lesser amount of ~1.8-1.9 basement available. Sediment at the base of Lucky Strike Canyon was deposited as sea level rose during a Transgressive Systems Tract. The ~1.8-1.9 Ga source for the base of other sections of the Eureka Quartzite may have been covered up; while a more proximal ~2.6-2.7 Ga source was subaerially exposed, eroded, and deposited at the base of this section. Therefore, this base may be equivalent to sediment deposited within sections further basinward. As sea level fell, ~1.8-1.9 Ga rocks were deposited at the top of Lucky Strike Canyon. As sea level rose, ~2.6-2.7 Ga rocks sourced fewer zircons, and provenance shifted to include more zircons from the ~1.8-1.9 Ga source. A very small to non-existent peak at ~1.0-1.1 Ga occurs in all basal samples and increases slightly at the top of the Eureka Quartzite. The exception to this is Lucky Strike Canyon, where an increase in the size of the ~1.0-1.1 Ga peak occurs upsection. The small amount of ~1.0-

1.3 Ga grains in almost all samples indicates a very small, but persistent, source of Grenville age sediment, possibly due to reworking.

A statistical method to study spatial differences in detrital zircon populations is to analyze the overlap and similarity of samples from the same unit but from different geographical locations (Gehrels, 2000). Overlap indicates the degree to which age populations in the sample overlap with the age populations in a standard; similarity measures how similar the overlapping age proportions are by summing the square root of the product of each pair of probabilities for an age over the time period of interest (Gehrels, 2000). Using this method, overlap and similarity are both measured on a scale from 1-0. A value of 1 represents perfect overlap or similar proportions of overlapping ages, and a value of 0 represents no overlap or very different proportions of overlapping ages (Gehrels, 2000). Overlap and similarity values were calculated for basal and upper samples, and are compared to LA-ICP-MS data provided by Gehrels (Table 4). Comparison of basal samples results in a range in overlap values from 0.708-0.884, and a range in similarity values from 0.687-0.920. This indicates that the ages in basal samples have a good overlap with Gehrel's data, and the same age peaks occur at each location. Calculated similarity values indicate a close similarity in most age probabilities for each sample. Lucky Strike Canyon records the lowest similarity value (0.687) in the base of the Eureka Quartzite. This is expected because this section was deposited much further inboard than the other sections. Comparison of upper samples results in a range in overlap values from 0.701-0.862, and a range in similarity values from 0.727-0.889. This indicates that the ages in upper samples also have a good

overlap with Gehrel's data, and roughly the same age peaks occur in each sample. Calculated similarity values indicate a close similarity in most age probabilities for each sample. Arrow Canyon Range records the lowest similarity value in the top of the Eureka Quartzite and has a unique detrital zircon signature not observed in the other sections.

TABLE 4. - Overlap and similarity values

Overlap - Top					
Gehrel's Data	Gehrel's Data				
Arrow Canyon Range	0.753	Arrow Canyon Range			
Lucky Strike Canyon	0.766	0.802	Lucky Strike Canyon		
Mount Irish	0.701	0.743	0.752	Mount Irish	
Last Chance Range	0.778	0.862	0.717	0.721	Last Chance Range
Similarity - Top					
Gehrel's Data	Gehrel's Data				
Arrow Canyon Range	0.752	Arrow Canyon Range			
Lucky Strike Canyon	0.879	0.820	Lucky Strike Canyon		
Mount Irish	0.893	0.727	0.889	Mount Irish	
Last Chance Range	0.911	0.807	0.885	0.873	Last Chance Range
Overlap - Base					
Gehrel's Data	Gehrel's Data				
Arrow Canyon Range	0.798	Arrow Canyon Range			
Lucky Strike Canyon	0.837	0.803	Lucky Strike Canyon		
Mount Irish	0.731	0.708	0.849	Mount Irish	
Last Chance Range	0.808	0.802	0.846	0.884	Last Chance Range
Similarity - Base					
Gehrel's Data	Gehrel's Data				
Arrow Canyon Range	0.903	Arrow Canyon Range			
Lucky Strike Canyon	0.716	0.711	Lucky Strike Canyon		
Mount Irish	0.876	0.854	0.766	Mount Irish	
Last Chance Range	0.904	0.920	0.687	0.852	Last Chance Range

Provenance Change and Sequence Stratigraphy

Geographic position is not the only determining factor for different detrital zircon signatures; sea-level change is extremely important as well. Long term sea-level changes can cover available sediment sources and uncover others, causing provenance areas to shift. These long term changes and their effects can be characterized by sequence stratigraphic systems tracts (Fig. 13). During a Lowstand Systems Tract, the previously deposited shelf becomes subaerially exposed, which leads to erosion and development of incised valleys that ultimately develops from local sediment sources. During a Lowstand, extensive portions of Basement #1 and Basement #2 (Fig. 12) are exposed and eroded, and provide several other possible sediment sources for deposition along coastal plains or deltas. A relative sea-level rise, or Transgressive Systems Tract, will subsequently cover the shelf and most of the proximal provenance sources. These areas will then be covered by sediment derived from Basement #2. This scenario does not rule out the reworking of previously deposited sediment or newly derived sediment, but it does greatly reduce the likelihood and abundance of shelf and Basement #1 sediment input. As sea-level remains high during a Highstand Systems Tract, or begins to fall during a Falling Stage Systems Tract, Basement #1 may become partially uncovered. During this stage the majority of sediment will be sourced by Basement #2, but an influx of Basement #1 and reworked sediment may also be deposited from incised valleys. Comparison of probability-density plots and histograms (Fig. 11) of calculated U/Pb ages indicates that the Trans-Hudson Orogen and Archean basement were the

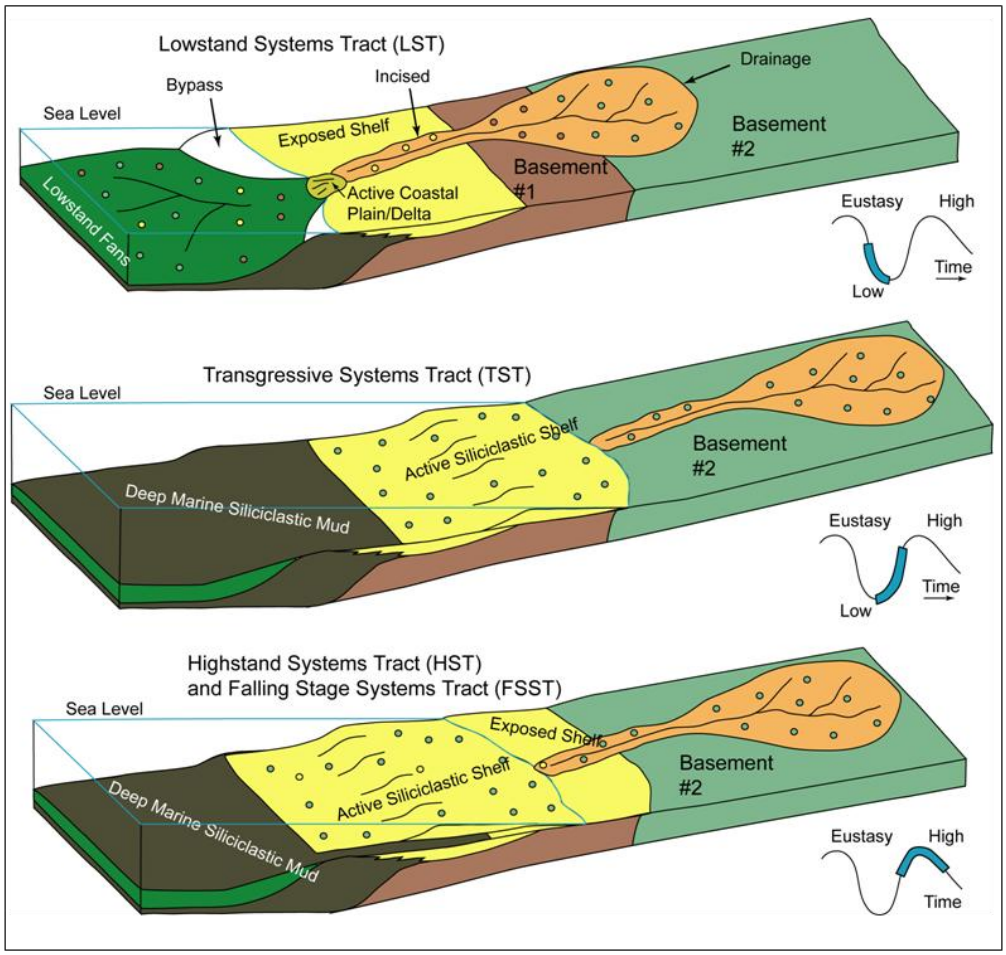

FIG. 13. - Provenance change and systems tracts. The colored dots represent different sediment sources: yellow-siliciclastic shelf, brown-basement #1, and green-basement #2. During the LST (top) when the sea level is low, both basement sources and the exposed siliciclastic shelf will be subaerially exposed and eroded to supply sediment for coastal plains, deltas, or lowstand fans. During the TST (middle) when the sea level is rising, the siliciclastic shelf and local basement rocks will be covered by sediment from remote basement rocks. During the HST or FSST (bottom) when sea level begins to fall, sediment from the previously constructed siliciclastic shelf and remote basement rocks will prograde into the basin.

primary zircon sources at the onset of deposition with minor input from Grenville age and Paleoproterozoic sources. Upper samples record the same primary sources, but the Archean peak (except for Arrow Canyon Range and Lucky Strike Canyon) and Paleoproterozoic peak is reduced. This indicates that as sea level rose, zircons from proximal Archean and Paleoproterozoic sources were less prominent and likely covered.

Potential Sources and Provenance

Possible source regions for the detrital grains in the Eureka Quartzite were derived from tectonic models and composite basement maps (e.g. Ross and Villeneuve, 2003; Whitemeyer and Karlstrom, 2007; Hammer et al., 2011). Detrital zircon ages between ~1.0-1.3 Ga correlate with a Grenville Orogen source related to tectonism that occurred between ~1.3-1.0 Ga and included magmatism, metamorphism, and accretion with Laurentia extending from Labrador to Mexico during the amalgamation of Rodinia (Hoffman, 1989; Karlstrom et al., 1999). This age population may also represent the reworking and recycling of sediments originally transported and deposited by large fluvial systems carrying sediment westward from the Grenville Orogen in eastern or southern Laurentia (Rainbird et al., 1992, 1997; Gehrels et al., 1995 and references therein; Druschke et al., 2011). A Grenville source is suggested by the similarity of detrital zircon population distributions in western North America and the Grenville Province (Stewart et al., 2001).

Detrital zircon ages between ~1.6-1.7 Ga in the Eureka Quartzite are most likely sourced from nearby Yavapai (1.7-1.8 Ga) and Mazatzal (1.65-1.8 Ga) Provinces located proximal to the Cordilleran margin (Druschke et al., 2011; Stewart et al., 2001).

Recycling of the Mesoproterozoic Belt Supergroup is another possible source as it also contains large populations of ~1.6-1.8 Ga grains (Ross and Villeneuve, 2003).

A prominent ~1.8-2.0 Ga population in all of the Eureka Quartzite samples suggests sediment was sourced from the Trans-Hudson Orogen (THO), in the center of the Transcontinental Arch. The THO represents amalgamation of the Hearne, Wyoming, and Superior cratons with Laurentia between ~1.95-1.8 Ga (Whitmeyer and Karlstrom, 2007; Hammer et al., 2010). During the Middle-Late Ordovician, the THO was exposed and available for erosion (Witzke, 1980).

A prominent ~2600-2800 Ma peak, and minor peaks ranging from~2.0-2.2 Ga and ~2.4-3.3 Ga in the Eureka Quartzite, are most likely sourced by erosion of Paleoproterozoic-Archean basement rocks proximal to the Cordilleran margin, and/or those amalgamated by the THO. Paleoproterozoic-Archean provinces include the Slave, Hearne, Wyoming, and Sask Provinces, as well as the Medicine Hat Block (MHB) between the Hearne and Wyoming Provinces (Whitmeyer and Karlstrom, 2007). In northwest Canada, the Slave Province contains a well-defined division within the craton. The Mesoarchean western Slave basement contains grains ~2.9-4.0 Ga and the juvenile Slave basement contains grains <2.85 Ga (Hammer et al., 2010). Rocks ~2.5-3.5 Ga of the Hearne Province and the MHB lie between the Slave and Superior Provinces; although the MHB is composed primarily of ~2.6-2.7 Ga gneisses, ages up to 3.3 Ga are recorded (Hammer et al., 2010 and references therein). These rocks form the western edge of the Trans-Hudson Orogen, and were heavily reworked and likely severely deformed during the Tran-Hudson Orogeny (Hammer et al., 2010). Plutonic rocks

~2.55-2.8 Ga dominate the Wyoming Province (Ross and Villeneuve, 2003), but the Wyoming craton also has an older core with gneisses ranging from ~3.0-3.6 Ga. In the southernmost Wyoming craton, basement older than ~2.5-2.7 Ga is overlain by ~2.1-2.4 Ga rocks of the Snowy Pass Supergroup (Whitmeyer and Karlstrom, 2007). Based on similarities of ~2.1 Ga and ~2.4 Ga mafic dikes (Whitmeyer and Karlstrom, 2007), the Wyoming Province was interpreted to be a complex extension of the Hearne Province, or a fragment rifted off the Superior Province. The Sask craton was uplifted by the Trans-Hudson orogen and contains ~2.4-3.1 Ga rocks. It was subaerially exposed to erosion during the Ordovician (Chiarenzelli et al., 1998; Bickford et al., 2005).

DISCUSSION OF RESULTS

Basal samples of the Eureka Quartzite at Arrow Canyon Range, Last Chance Range, and Mount Irish record similar ages with a prominent peak at ~1.8-1.9 Ga and a smaller yet significant peak at ~2.6-2.8 Ga. The data from the base of Lucky Strike Canyon records the opposite with a prominent peak at ~2.6-2.8 Ga, and a smaller peak at ~1.8-1.9 Ga. A very small Grenville-age peak was identified in only two samples from the base of the Eureka Quartzite. Upper samples of the Eureka Quartzite at Last Chance Range, Lucky Strike Canyon, and Mount Irish record similar ages with a prominent peak at ~1.8-2.0 Ga and a smaller peak at ~2.6-2.8 Ga. These peaks also are recorded in the sample from the top of Arrow Canyon, but they are less significant, and many smaller peaks occur at ~1.45 Ga, ~1.65-1.7 Ga, ~2.1 Ga, and ~2.95-3.0 Ga. A small Grenville-age peak exists in all samples from the top of the Eureka Quartzite. Comparison of detrital zircon analyses from basal and upper samples of the Eureka Quartzite indicates three primary sediment sources: 1) the Trans-Hudson Orogeny, 2) Paleoproterozoic-Archean basement, and 3) the Grenville Orogeny.

Trans-Hudson Orogeny (THO): At the onset of Eureka Quartzite deposition, sea level was relatively low in a Transgressive Systems Tract, and more sources were available for erosion and deposition at the base of the Eureka Quartzite. A prominent ~1.8-2.0 Ga peak indicates, however, that the THO was the primary sediment source for both the lower and upper Eureka Quartzite. Sediment eroded from the THO was likely transported by fluvial systems across the Transcontinental Arch and its exposed

basement rocks before being deposited. This likely increased the sediment eroded from local or proximal sources. A ~1.6-1.7 Ga population of zircons occurs in three basal samples and all four upper samples of the Eureka Quartzite. This population indicates erosion and minor deposition from the Yavapai and Mazatzal Provinces proximal to the Cordilleran margin (Druschke et al., 2011; Stewart et al., 2001).

Paleoproterozoic to Archean basement: Because sea-level was lower at the onset of its deposition, a larger Paleoproterozoic to Archean influence was expected in basal samples of the Eureka Quartzite, but in both Arrow Canyon and Last Chance Range, Paleoproterozoic to Archean abundance increases upsection. Many Paleoproterozoic to Archean basement rocks were amalgamated with Laurentia during the Trans-Hudson Orogeny, and include the Slave, Hearne, Wyoming, and Sask Provinces as well as the Medicine Hat Block (Whitmeyer and Karlstrom, 2007). Fluvial systems draining from the THO would have further eroded and transported sediment from available Paleoproterozoic-Archean sources. The increase in significance of ~2.6-2.8 Ga grains in the top of the Eureka Quartzite (except at Mount Irish) following the transgression indicates that erosion or reworking of Archean sources, especially the proximal Wyoming Province, was still occurring during Late Ordovician. This likely occurred during a highstand or falling stage systems tract. Sediment eroded from ~2.0-2.3 Ga Paleoproterozoic crust was still in moderate supply or likely being reworked, although it is much more abundant in the inboard Lucky Strike Canyon section than the other sections.

A Paleoproterozoic and Archean peak occurs in the base of Lucky Strike Canyon, but the Archean peak is much more prominent. This section was deposited much further inboard from the other sections, and the detrital zircon signatures indicate that proximal Archean sources played a much larger role in early deposition of the Lucky Strike Canyon section.

Grenville Orogeny: Each sample from the top of the Eureka Quartzite records Grenville-age peaks, but only two samples from the base record this population: Arrow Canyon Range and Lucky Strike Canyon. Detrital zircons of this age likely resulted from sediment eroded off the Grenville orogeny in eastern or southern Laurentia and transported westward by a vast and intense fluvial system (Rainbird et al., 1992, 1997; Gehrels et al., 1995 and references therein; Druschke et al., 2011). Grains of this age are distributed relatively evenly throughout the samples, except for the top of the Arrow Canyon Range section, which has twice as many, though it is still a small number of grains.

The sample from the top of Arrow Canyon Range has a much different signature than all other Eureka Quartzite samples, with prominent peaks at ~2.6-2.8 Ga, and ~1.8-1.9 Ga, and several smaller peaks at ~1.1-1.2 Ga, ~1.4-1.5 Ga, ~1.7 Ga, ~2.1-2.2 Ga, ~2.5 Ga, and ~2.9 Ga. The prominent Archean peak indicates that at this location, the primary source was Archean and indicates there must have been a local high within the Archean crust near the Arrow Canyon section to source Archean sediment. This sample also contains more Grenville-age peaks than the others. It may have a similar provenance as the other three samples, or it may indicate the source of Grenville-age

sediment was more proximal to this location. A relatively large ~1.6-1.7 Ga peak, corresponding to a Yavapai/Mazatzal source, occurs in this sample that is virtually absent from the others. The mixture of ages indicates possible reworking of sediment or erosion of locally exposed basement, or a combination of both. Exposed arches along the Cordilleran margin to the north include the Lemhi Arch and Salmon River Arch, and contain Belt metasedimentary rocks of this age (Link, 2009).

CONCLUSIONS

Ten sedimentary facies were identified within the Eureka Quartzite based on the detailed descriptions of six measured sections. These facies are grouped into five facies associations, and represent deposition in a shallow marine environment and their relative positions are identified across a marine siliciclastic shelf model. Stacking patterns of these facies indicate that the Eureka Quartzite was deposited in a transgressive system and represent a single 3rd-order sequence. Facies stacking patterns indicate three ~2-4 m.y. sequences, and numerous parasequences recording smaller sea-level fluctuations are recorded within the Eureka Quartzite.

U/Pb ages of detrital zircon grains in the Eureka Quartzite indicate provenance areas of ~1.6-1.7 Ga, ~1.8-1.9 Ga, ~2.0-2.3 Ga and ~2.6-2.8 Ga basement rocks. These ages represent an eastern source, likely from the Yavapai and Mazatzal Provinces (~1.6-1.7 Ga), the Trans-Hudson Orogen (~1.8-1.9 Ga), Paleoproterozoic crust (~2.0-2.3 Ga), and proximal Archean (~2.6-2.8 Ga) sources such as the Wyoming Province. Sediments likely were transported by rivers draining off the Transcontinental Arch to the passive margin. Long-shore currents also played an important role in deposition and likely account for the similarity of Middle to Late Ordovician supermature quartz arenite deposits of western Laurentia. Although the Peace River Arch, along with local and proximal sources, likely sourced some sediment, it is apparent Eureka Quartzite provenance was dominated by the Trans-Hudson Orogen.

Comparison of detrital zircon analyses indicates temporal and spatial changes in provenance. Temporal change can be explained by long term sea level fluctuations. During a relative sea level low, proximal sources were subaerially exposed and weathered; as the continent flooded and relative sea-level rose, proximal sources were covered and sediment was transported from further inboard sources. Comparison of analyses from location to location indicates minimal spatial change in provenance. Two locations are different, Lucky Strike Canyon and Arrow Canyon Range. Spatial changes observed within the Lucky Strike Canyon are caused by deposition further inboard relative to the other locations, and later, its juxtaposition with basinward deposits along the Las Vegas shear zone. Spatial change observed within the top sample from the Arrow Canyon Range section must be caused by a local and proximal Archean high that was subaerially exposed during the transgression, but the nearest known Archean basement is the Wyoming Province.

REFERENCES

ALGEO, T., AND SESLAVINSKY, K., 1995, The Paleozoic World: Continental flooding, Hyposemetry, and Sea Level: American Journal of Science, v. 295, p. 787-822.

ANDERSON, T., 2005, Detrital zircons as tracers of sedimentary provenance: limiting conditions from statistics and numerical simulation: Chemical Geology, v. 216, p. 249-270.

BICKFORD, M.E., MOCK, T.D., COLLERSON, K.D., LEWRY, J.F., AND STEINHART III, W.E., 2005, Origin of the Archean Sask craton and its extent within the Trans-Hudson Orogen: evidence from Pb and Nd isotopic compositions of basement rocks and post-orogenic intrusions: Canadian Journal of Earth Sciences, v. 42, n. 4, p. 659-684.

CHANG, Z., VERVOORT, J.D., KNAACK, C., AND MCCLELLAND, W.C., 2006, U-Pb dating of zircon by LA-ICPMS: Geochemistry, Geophysics, Geosystems, v. 7, no. 5, p. 1-14.

CHIARENZELLI, J., ASPLER, L., VILLENEUVE, M., AND LEWRY, J., 1998, Early Proterozoic Evolution of the Saskatchewan Craton and its Allochthonous Cover, Trans-Hudson Orogen: Journal of Geology, v. 106, p. 247-267.

CHRISTIE-BLICK, N., GROTZINGER, J.P., AND VON DER BORCH, C.C., 1988, Sequence stratigraphy in Proterozoic successions: Geology, v. 16, p. 100-104.

CHRISTIE-BLICK, N., DYSON, I.A., AND VON DER BORCH, C.C., 1995, Sequence stratigraphy and the interpretation of Neoproterozoic earth history: Precambrian Research, v. 73, p. 3-26.

CLIFTON, H.E., 2006, A reexamination of facies models for clastic shorelines, *in* Posamentier, R.G., and Walker, R.G., eds., Facies models revisited: SEPM Special Publications, v. 84, p. 237-292.

COOPER , J.D., AND KELLER, M., 2001, Paleokars in the Ordovician of the southern Great Basin, USA: implications for sea-level history: Sedimentology, v. 48, p. 855-873.

DAPPLES, E. C., 1955, General lithofacies relationship of St. Peter Sandstone and Simpson Group: American Association of Petroleum Geologists Bulletin, v. 39, p. 444-467.

DODSON, M.H., COMPSTON, W., WILLIAMS, I.S., AND WILSON, J.F., 1988, A search for ancient detrital zircons in Zimbabwean sediments: Journal of the Geological Society of London, v. 145, p. 977-983.

DOTT, R. H. JR., BYERS, C. W., FIELDER, G. W., STENZEL, S. R., AND WINFREE, K. E., 1986, Aeolian to marine transition in Cambro-Ordovician cratonic sheet sandstones of the northern Mississippi valley U.S.A.: Sedimentology, v. 33, p. 345-367.

DRUSCHKE, P.A., JIANG, G., ANDERSON, T.B., AND HANSON, A.D., 2009, Stromatolites in the Late Ordovician Eureka Quartzite: implications for microbial growth and preservation in siliciclastic settings: Sedimentology, v. 56, p. 1275-1291.

DRUSCHKE, P., HANSON, A.D., WELLS, M.L., GEHRELS, G.E., AND STOCKLI, D., 2011, Paleogeographic isolation of the Cretaceous to Eocene Sevier hinterland, east-central Nevada: Insights from U-Pb and (U-Th)/He detrital zircon ages of hinterland strata: Geological Society of America Bulletin, v.123, p. 1141-1160.

FEDO, C.M., SIRCOMBE, K.N., AND RAINBIRD, R.H., 2003, Detrital zircon analysis of the sedimentary record, *in* Hanchar, J.M., and Hoskin, P.W.O., eds., Zircon: Reviews in Mineralogy and Geochemistry, v. 53, p. 277-303.

FLECK, R.J., 1970, Tectonic style, magnitude, and age of deformation in the Sevier Orogenic belt in southern Nevada and eastern California: Geological Society of America Bulletin, v.81, p. 1705-1720.

GEHRELS, G.E., 2000, Introduction to detrital zircon studies of Paleozoic and Triassic strata in western Nevada and northern California, *in* Soreghan, M.J., and Gehrels, G.E., eds., Paleozoic and Triassic paleogeography and tectonics of western Nevada and northern California: Geological Society of America Special Paper 347, p. 1-17.

GEHRELS, G.E., AND DICKINSON, W.R., 1995, Detrital zircon provenance of Cambrian to Triassic miogeoclinal and eugeoclinal strata in Nevada: American Journal of Science, v. 295, p. 18-48.

GEHRELS, G.E., DICKINSON, W.R., ROSS, G.M., STEWART, J.H., AND HOWELL, D.G., 1995, Detrital zircon reference for Cambrian to Triassic miogeoclinal strata of western North America: Geology, v. 23, p. 831-834.

HALL, C.D., 1989, Storm bedding in the Middle Ordovician Kinnikinic Quartzite, Beaverhead Range, east central Idaho: Geological Society of America Abstracts with Programs, v. 21, p. 88-89.

HAMMER, P.T.C., CLOWES, R.M., COOK. F.A., VAN DER VELDEN, A.J., AND VASUDEVAN, K., 2010, The Lithoprobe trans-continental lithospheric cross sections: imaging the internal structure of the North American continent: Canadian Journal of Earth Science, v. 47, p. 821-857.

HARRIS, M. T., SEXTON, L. A., AND SHEEHAN, P. M., 1995, Depositional facies and sequences of upper Ordovician shelf and shallow ramp carbonates of the eastern great basin (Utah and Nevada) U.S.A.: Ordovician Odyssey: Short papers for the seventh International Symposium on the Ordovician System, p.265-266.

HOFFMAN, P.F., 1989, Precambrian geology and tectonic history of North America, *in* Bally, A.W., and Palmer, A.R., eds., The Geology of North America - An Overview: Boulder Colorado, Geological Society of America, Geology of North America 1989, v. A, p. 447-512.

KARLSTROM, K.E., HARLAN, S.S., WILLIAMS, M.L., MCLELLAND, J., GEISSMAN, J.W., AND AHALL, K., 1999, Refining Rodinia: Geologica Evidence for the Australia-Western U.S. connection in the Proterozoic: GSA Today, v. 9, p. 1-7.

KELLER, M., AND LEHNERT, O., 2010, Ordovician paleokarst and quartz sand: Evidence of volcanically triggered extreme climates: Palaeogeography, Palaeoclimatology, Palaeoecology, v. 296, p. 297-309.

KETNER, K.B., 1966, Comparison of Ordovician Eugeosynclinal and Miogeosynclinal Quartzites of the Cordilleran Geosyncline: United States Geological Survey Professional Paper 550-C, p. C54-C60.

KETNER, K.B., 1968, Origin of Ordovician Quartzite in the Cordilleran Miogeosyncline: United States Geological Survey Professional Paper 600-B, p. B169-B177.

LANGHENHEIM, JR, R.L., CARSS, B.W., KENNERNLY, B.J., MCCUTCHEON, V.A., AND WAINES, R.H., 1964, Paleozoic Section in Arrow Canyon Range, Clark County, Nevada: American Association of Petroleum Geologists Bulletin, v. 46, p. 592-609.

LANGHENHEIM, JR, R.L., 1978, Stratigraphy and paleoenvironments of Middle Ordovician arenites, southeastern Nevada: Geological Society of America Abstracts with Programs, v. 10, p. 113.

LEATHAM, W.B., 1985, Ages of the Fish Haven and lowermost Laketown dolomites in the Bear River Range, Utah, *in* Kerns, G.J., and Kerns, R.L., eds., Orogenic patterns and stratigraphy of north central Utah and southeastern Idaho, p. 29-38.

LINK, P.K., 2009, Mantle drip from the rising Lemhi Arch: 500 ma plutons and detrital zircons in Upper Cambrian sandstones, Eastern Idaho: Geological Society of America Abstracts with Programs, v. 41, p. 181

LONGWELL, C.R. AND MOUND, M.C., 1967, A New Ordovician Formation in Nevada Dated by Conodonts: Geological Society of America Bulletin, v. 78, p. 405-412.

LUDWIG, K.R., 2003, User's Manual for Isoplot 3.00. A Geochronological toolkit for Microsoft Excel: Berkeley Geochronology Center, Special Publication No. 4.a, Berkeley, CA.

MEASURES, E.A., 1992, Stratigraphy, carbonate lithologies, and depositional environments of Upper Ordovician Fish Haven Dolomite and Saturday Mountain Formation, east-central and central Idaho, and implications for platform development and margin tectonics: Unpublished Ph.D. Dissertation, University of Idaho, Moscow, Idaho, 535 p.

MILLER, M.F., 1977, Middle and Upper Ordovician biogenic structures and paleoenvironments, southern Nevada: Journal of Sedimentary Petrology, v. 47, p. 1328-1338.

MILLER, R.H., AND ZILINSKY, G.A., 1981, Lower Ordovician through Lower Devonian Cratonic margin rocks of the southern Great Basin: Geological Society of America Bulletin, v. 92, p. 255-261.

RAINBIRD, R.H., HEAMAN, L.M., AND YOUNG, G., 1992, Sampling Laurentia: Detrital zircon geochronology offers evidence for an extensive Neoproterozoic river system originating from the Grenville orogen: Geology, v. 20, p. 351-354.

RAINBIRD, R.H., MCNICOLl, V.J., THERIAULT, R.J., HEAMAN, L.M., ABBOTT, J.G., LONG, D.G.F., AND THORKELSON, D.J., 1997, Pan-continental River System Draining Grenville Orogen Recorded by U-Pb and Sm-Nd Geochronology of Neoproeterozoic Quartzarenites and Mudrocks, Northwestern Canada: Geology, v. 105, p. 1-17.

ROSS, R.J., 1964, Relations of Middle Ordovician Time and Rock Units in Basin Ranges, Western United States: American Association of Petroleum Geologists Bulletin, v. 48, p. 1526-1554.

SALTZMAN, M.R., YOUNG, S., BERGSTROM, S.M., HOLMDEN, C., AND PATTERSON, W.P., 2003, Age and significance of the sequence boundary at the base of the Eureka Quartzite in central Nevada: Geological Society of America Abstracts with Programs, v. 35, p. 473.

STEWART, J.H., ALBERS, J.P., AND POOLE, F.G., 1968, Summary of evidence for right lateral displacement in the western Great Basin: Geological Society of America Bulletin, v. 79, p. 1407-1414

STEWART, J.H., GEHRELS, G.E., BARTH, A.P., LINK, P.K., CHRISTIE-BLICK, N., AND WRUCKE, C.T., 2001, Detrital zircon provenance of Mesoproterozoic to Cambrian arenites in the western United States and northwestern Mexico: Geological Society of America Bulletin, v. 113, p. 1343-1356.

SWEET, W.C., 2000, Conodonts and biostratigraphy of Upper Ordovician strata along a shelf to basin transect in Central Nevada: Journal of Paleontology, v. 74, p. 1148-1160.

VERMEESCH, P., 2004, How many grains are needed for a provenance study?: Earth and Planetary Science Letters, v. 224, p. 441-451.

WALLIN, E.T., 1990, Provenance of selected lower Paleozoic siliciclastic rocks in the Roberts Mountains allochthon, Nevada: Geological Society of America Special Paper 255, p. 17-32.

WEBB, G.W., 1956, Middle Ordovician detailed stratigraphic sections for western Utah and eastern Nevada: Utah Geological and Mineralogical Survey Bulletin, v. 57, p. 1-77.

WEBB, G.W., 1958, Middle Ordovician stratigraphy in eastern Nevada and western Utah: American Association of Petroleum Geologists Bulletin, v. 42, no. 10, p. 2335-2377.

WHITMEYER, S.J., AND KARLSTROM, K.E., 2007, Tectonic model for the Proterozoic growth of North America: Geosphere, v. 3, p. 220-259.

WITZKE, B.J., 1980, Paleoclimatic constraints for Paleozoic paleolatitudes of Laurentia and Euramerica, *in* Mckerrow, W.S., and Scotese, C.R., eds., Paleozoic paleogeography and biogeography; Geological Society [London] Memoir 12, p. 57-73.

ZIMMERMAN, M.K., AND COOPER, J.D., 1999, Sequence stratigraphy of the Eureka Quartzite, southeastern California and southern Nevada: Acta Universitatis Carolinae, Geologica, v.43, p. 147-150.

ZIMMERMAN, M.K., AND COOPER, J.D., 1999, Conodont biostratigraphy of Eureka Quartzite (Middle Ordovician) sequence boundaries, southwestern Nevada: Acta Universitatis Carolinae, Geologica, v. 43, p. 41-42.

APPENDIX A

COORDINATES OF LOCATIONS

Location	Latitude	Longitude	UTM Zone	Easting	Northing
Arrow Canyon Range	36° 43' 45"	-114° 53' 32"	11S	688206	4066927
Last Chance Range	36° 17' 3"	-116° 5' 23"	11S	581734	4015867
Lucky Strike Canyon	36° 23' 57"	-115° 27' 42"	11S	637936	4029352
Mount Irish	37° 29' 1"	-115° 28' 20"	11S	635071	4149629
Nopah Range	36° 6' 24"	-116° 10' 1"	11S	574979	3996108
Spotted Range	36° 37' 15"	-115° 57' 50"	11S	592634	4053336

APPENDIX B

LEGEND FOR MEASURED SECTIONS

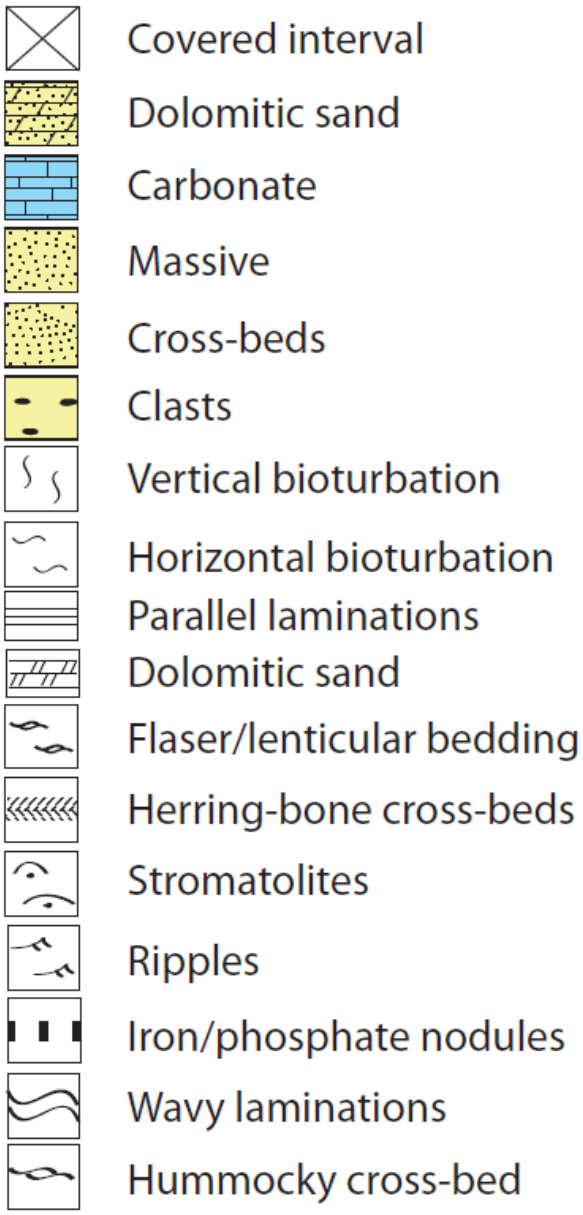

APPENDIX C

ARROW CANYON RANGE

DATA TABLES

Sample ACW-1 (Arrow Canyon Range – Base)								
Sample	**238U/ 206Pb**	**1σ (%)**	**207Pb/ 206Pb**	**1σ (%)**	**238U/ 206Pb Age (Ma)**	**1σ**	**207Pb/ 206Pb Age (Ma)**	**1σ**
< 10% Discordant								
ACW1_501a	2.51	0.0316	0.1257	0.0491	2158	58	2039	84
ACW1_279a	1.80	0.0212	0.1836	0.0472	2844	48	2686	76
ACW1_320a	2.48	0.0161	0.1281	0.0488	2185	30	2071	84
ACW1_10a	2.93	0.0197	0.1115	0.0110	1893	32	1825	20
ACW_32a	2.91	0.0226	0.1122	0.0145	1904	37	1836	26
ACW1_171a	1.86	0.0179	0.1838	0.0308	2775	40	2688	50
AWC1_433a	2.94	0.0175	0.1127	0.0346	1888	29	1843	61
ACW1_400a	2.01	0.0180	0.1689	0.0469	2602	38	2547	77
ACW1_340a	2.90	0.0175	0.1148	0.0469	1911	29	1876	82
ACW1_144a	2.97	0.0275	0.1125	0.0174	1872	45	1840	31
ACW1_16a	1.90	0.0196	0.1837	0.0103	2730	44	2686	17
ACW_78a	2.09	0.0241	0.1624	0.0145	2517	50	2481	24
AWC1_380a	2.04	0.0133	0.1679	0.0338	2569	28	2537	56
ACW1_58a	2.91	0.0214	0.1150	0.0110	1903	35	1880	20
ACW_104a	3.01	0.0230	0.1118	0.0147	1850	37	1828	26
ACW1_210a	2.01	0.0203	0.1710	0.0106	2598	43	2568	18
ACW1_431a	3.05	0.0185	0.1106	0.0469	1830	29	1809	83
AWC1_446a	3.09	0.0176	0.1093	0.0340	1809	28	1788	61
ACW1_15a	2.06	0.0217	0.1669	0.0117	2555	46	2527	19
ACW1_301a	2.89	0.0180	0.1158	0.0469	1913	30	1893	82
ACW1_456a	2.95	0.0195	0.1138	0.0469	1881	32	1861	82
ACW1_377a	3.15	0.0221	0.1077	0.0490	1779	34	1761	87
ACW_103a	2.83	0.0230	0.1185	0.0166	1953	39	1933	29

ACW1_412a	1.86	0.0170	0.1907	0.0489	2773	38	2748	78
ACW_93a	2.03	0.0233	0.1706	0.0143	2585	49	2563	24
ACW_100a	2.54	0.0250	0.1319	0.0155	2139	45	2123	27
AWC1_385a	3.04	0.0176	0.1115	0.0339	1835	28	1824	60
ACW1_312a	3.02	0.0188	0.1123	0.0470	1844	30	1837	83
ACW1_83a	2.93	0.0256	0.1154	0.0117	1891	42	1886	21
ACW1_219a	3.08	0.0148	0.1107	0.0306	1814	23	1811	55
ACW1_480a	2.66	0.0212	0.1270	0.0476	2059	37	2057	82
ACW1_243a	3.06	0.0186	0.1114	0.0308	1823	29	1822	55
ACW1_55a	2.80	0.0224	0.1205	0.0327	1966	38	1964	57
ACW1_363a	4.79	0.0189	0.0810	0.0476	1222	21	1222	91
AWC1_399a	2.66	0.0144	0.1269	0.0337	2056	25	2055	58
AWC1_537a	3.10	0.0153	0.1101	0.0342	1802	24	1801	61
AWC1_314a	3.09	0.0135	0.1108	0.0339	1810	21	1812	60
ACW1_214a	1.94	0.0222	0.1835	0.0113	2681	48	2684	19
ACW_94a	3.00	0.0236	0.1136	0.0149	1855	38	1858	27
ACW1_430a	3.10	0.0215	0.1104	0.0494	1802	34	1807	87
ACW1_40a	2.69	0.0232	0.1262	0.0118	2038	40	2046	21
ACW1_513a	2.96	0.0218	0.1156	0.0491	1879	36	1890	86
ACW1_164a	3.06	0.0204	0.1123	0.0108	1823	32	1836	19
ACW1_223a	3.07	0.0241	0.1119	0.0118	1817	38	1831	21
AWC1_493a	3.14	0.0168	0.1099	0.0346	1783	26	1798	62
ACW1_132a	3.09	0.0182	0.1115	0.0307	1806	29	1824	55
ACW1_28a	1.56	0.0222	0.2575	0.0107	3201	56	3232	17
AWC1_351a	3.14	0.0166	0.1100	0.0340	1781	26	1799	61
ACW1_54a	2.15	0.0158	0.1629	0.0306	2459	32	2486	51
ACW_89a	2.90	0.0228	0.1184	0.0145	1910	38	1932	26
ACW_77a	3.07	0.0248	0.1126	0.0149	1816	39	1841	27
ACW1_113a	3.06	0.0172	0.1130	0.0308	1821	27	1848	55
ACW_64a	2.68	0.0245	0.1286	0.0148	2047	43	2079	26
ACW_101a	3.12	0.0267	0.1115	0.0161	1795	42	1825	29
ACW1_17a	2.90	0.0272	0.1194	0.0156	1912	45	1948	28
ACW1_199a	3.08	0.0193	0.1129	0.0147	1812	30	1846	26
ACW_43a	3.06	0.0241	0.1137	0.0155	1824	38	1859	28
ACW_53a	2.12	0.0230	0.1682	0.0145	2492	47	2540	24
ACW1_408a	5.65	0.0331	0.0752	0.0528	1050	32	1074	103
ACW1_302a	2.94	0.0171	0.1183	0.0138	1886	28	1930	25
ACW1_170a	3.12	0.0174	0.1123	0.0138	1794	27	1836	25
ACW1_42a	2.70	0.0190	0.1287	0.0313	2032	33	2080	54

ACW1_466a	2.11	0.0194	0.1709	0.0488	2504	40	2566	79
ACW1_244a	2.68	0.0165	0.1299	0.0138	2044	29	2096	24
ACW1_235a	3.08	0.0178	0.1139	0.0139	1813	28	1863	25
AWC1_348a	3.16	0.0178	0.1113	0.0344	1772	28	1820	61
AWC1_352a	3.18	0.0258	0.1107	0.0350	1762	40	1811	62
AWC1_315a	3.16	0.0154	0.1114	0.0343	1772	24	1822	61
AWC1_423a	3.15	0.0156	0.1123	0.0343	1776	24	1837	61
ACW1_151a	3.12	0.0289	0.1133	0.0163	1791	45	1853	29
ACW1_176a	3.09	0.0186	0.1144	0.0150	1807	29	1871	27
ACW1_269a	2.42	0.0179	0.1468	0.0138	2228	34	2309	24
ACW1_204a	1.97	0.0226	0.1908	0.0146	2651	49	2749	24
ACW_67a	3.19	0.0276	0.1115	0.0187	1758	42	1824	34
ACW1_278a	2.06	0.0178	0.1808	0.0468	2554	37	2660	76
ACW1_277a	2.73	0.0164	0.1304	0.0136	2013	28	2104	24
ACW1_114a	3.14	0.0181	0.1139	0.0146	1782	28	1863	26
AWC1_539a	3.25	0.0177	0.1107	0.0342	1732	27	1810	61
ACW1_451a	2.03	0.0306	0.1864	0.0492	2585	65	2711	79
ACW1_182a	3.18	0.0181	0.1129	0.0312	1761	28	1847	55
ACW1_237a	3.13	0.0239	0.1152	0.0336	1789	37	1884	59
ACW1_134a	2.72	0.0214	0.1334	0.0258	2021	37	2143	44
ACW1_362a	3.22	0.0240	0.1131	0.0497	1741	37	1850	87
ACW1_273a	3.08	0.0247	0.1182	0.0333	1814	39	1929	59
ACW1_76a	3.23	0.0215	0.1137	0.0316	1737	33	1859	56
ACW1_450a	3.29	0.0183	0.1122	0.0490	1711	27	1835	86
ACW1_318a	3.08	0.0211	0.1194	0.0473	1810	33	1948	82
ACW1_115a	2.83	0.0216	0.1302	0.0161	1950	36	2101	28
ACW1_394a	2.12	0.0190	0.1840	0.0489	2494	39	2690	79
ACW1_106a	3.13	0.0182	0.1184	0.0141	1789	28	1932	25
ACW1_411a	2.11	0.0226	0.1859	0.0490	2497	47	2706	79
ACW1_81a	2.49	0.0167	0.1532	0.0308	2179	31	2382	52
> 10% Discordant								
ACW1_47a	2.80	0.0211	0.1384	0.0310	1969	36	2207	52.8
ACW1_390a	3.36	0.0188	0.1153	0.0489	1678	28	1885	85.5
ACW_30a	3.55	0.0246	0.1141	0.0146	1600	35	1866	26.2
ACW1_167a	3.44	0.0193	0.1207	0.0138	1646	28	1967	24.4
ACW1_159a	2.64	0.0216	0.1771	0.0160	2073	38	2626	26.4
AWC1_479a	3.83	0.0211	0.1163	0.0341	1495	28	1901	60
ACW1_69a	6.68	0.0215	0.1096	0.0306	899	18	1793	54.8
ACW1_345a	9.20	0.0224	0.1444	0.0469	665	14	2281	78.6

ACW1_209a	10.92	0.0178	0.1374	0.0307	565	10	2194	52.4
ACW1_334a	13.46	0.0181	0.1355	0.0468	462	8	2170	79.4
ACW1_344a	13.60	0.0174	0.1369	0.0490	457	8	2188	82.9

Sample ACW-5 (Arrow Canyon Range – Top)								
Sample	**238U/ 206Pb**	**1σ (%)**	**207Pb/ 206Pb**	**1σ (%)**	**238U/ 206Pb Age (Ma)**	**1σ**	**207Pb/ 206Pb Age (Ma)**	**1σ**
< 10% Discordant								
ACW5_395a	2.77	0.0210	0.1152	0.0224	1986	36	1884	40
ACW5_226a	1.79	0.0236	0.1870	0.0261	2856	54	2716	42
ACW5_105a	1.66	0.0186	0.2097	0.0115	3040	45	2904	19
ACW5_436a	2.87	0.0305	0.1129	0.0165	1929	51	1847	30
ACW5_114a	3.24	0.0257	0.1025	0.0081	1736	39	1671	15
ACW5_100a	1.76	0.0213	0.1965	0.0253	2895	49	2797	41
ACW5_336a	2.91	0.0205	0.1126	0.0236	1905	34	1842	42
ACW5_24a	3.27	0.0262	0.1022	0.0117	1722	39	1665	22
ACW5_333a	2.99	0.0171	0.1102	0.0253	1860	28	1803	45
ACW5_304a	2.95	0.0160	0.1115	0.0247	1880	26	1824	44
ACW5_228a	2.86	0.0205	0.1149	0.0224	1931	34	1878	40
ACW5_461a	2.98	0.0234	0.1112	0.0236	1866	38	1820	42
ACW5_86a	2.90	0.0145	0.1138	0.0091	1907	24	1860	16
ACW5_147a	2.96	0.0255	0.1124	0.0089	1878	41	1838	16
ACW5_472a	1.90	0.0196	0.1818	0.0221	2727	44	2669	36
ACW5_372a	2.28	0.0204	0.1455	0.0222	2342	40	2293	38
ACW5_383a	3.29	0.0345	0.1029	0.0178	1712	52	1677	33
ACW5_175a	3.01	0.0281	0.1107	0.0117	1849	45	1812	21
ACW5_207a	1.86	0.0212	0.1869	0.0222	2770	48	2715	36
ACW5_45a	1.68	0.0151	0.2159	0.0092	3009	36	2950	15
ACW5_320a	1.81	0.0308	0.1942	0.0165	2833	70	2778	27
ACW5_161a	1.88	0.0263	0.1849	0.0081	2748	59	2698	13
ACW5_137a	1.84	0.0203	0.1901	0.0248	2793	46	2743	40
ACW5_137a	1.84	0.0203	0.1901	0.0248	2793	46	2743	40
ACW5_426a	1.88	0.0310	0.1858	0.0167	2751	69	2706	27
ACW5_35a	2.95	0.0162	0.1130	0.0110	1879	26	1848	20
ACW5_460a	1.92	0.0204	0.1811	0.0223	2706	45	2663	36
ACW5_197a	1.87	0.0196	0.1877	0.0250	2766	44	2722	41
ACW5_108a	3.26	0.0133	0.1044	0.0096	1723	20	1704	18
ACW5_298a	1.86	0.0310	0.1898	0.0165	2770	69	2740	27
ACW5_201a	2.07	0.0170	0.1654	0.0246	2537	36	2511	41
ACW5_134a	1.88	0.0193	0.1871	0.0247	2744	43	2717	40
ACW5_300a	1.87	0.0306	0.1893	0.0165	2764	68	2736	27

ACW5_453a	3.73	0.0417	0.0944	0.0267	1531	57	1516	50
ACW5_390a	1.89	0.0318	0.1864	0.0170	2736	70	2711	28
ACW5_81a	1.90	0.0301	0.1856	0.0103	2728	67	2704	17
ACW5_33a	3.93	0.0159	0.0911	0.0105	1461	21	1448	20
ACW5_79a	2.85	0.0163	0.1177	0.0109	1938	27	1922	19
ACW5_184a	3.92	0.0267	0.0913	0.0086	1465	35	1452	16
ACW5_65a	2.59	0.0280	0.1291	0.0087	2102	50	2086	15
ACW5_38a	1.87	0.0186	0.1893	0.0110	2756	41	2736	18
ACW5_267a	1.88	0.0317	0.1889	0.0167	2751	71	2733	27
ACW5_22a	3.98	0.0187	0.0906	0.0134	1445	24	1437	25
ACW5_151a	1.92	0.0143	0.1844	0.0090	2708	32	2693	15
ACW5_39a	2.94	0.0197	0.1147	0.0161	1885	32	1875	29
ACW5_189a	1.86	0.0162	0.1929	0.0095	2779	37	2767	16
ACW5_143a	3.29	0.0132	0.1044	0.0092	1711	20	1704	17
ACW5_83a	1.88	0.0172	0.1904	0.0121	2755	38	2745	20
ACW5_60a	1.84	0.0200	0.1954	0.0158	2798	45	2788	26
ACW5_446a	1.95	0.0201	0.1814	0.0221	2674	44	2666	36
ACW5_349a	3.32	0.0174	0.1038	0.0252	1698	26	1694	46
ACW5_401a	3.04	0.0311	0.1116	0.0166	1831	49	1826	30
ACW5_234a	3.07	0.0262	0.1110	0.0084	1820	41	1815	15
ACW5_51a	1.71	0.0312	0.2174	0.0099	2967	74	2961	16
ACW5_125a	2.99	0.0176	0.1137	0.0153	1861	28	1860	27
ACW5_354a	1.93	0.0203	0.1845	0.0222	2691	44	2693	36
ACW5_405a	1.93	0.0173	0.1848	0.0247	2691	38	2696	40
ACW5_66a	1.79	0.0260	0.2049	0.0446	2857	60	2865	71
ACW5_101a	2.97	0.0136	0.1149	0.0095	1871	22	1879	17
ACW5_130a	3.00	0.0192	0.1138	0.0123	1853	31	1861	22
ACW5_340a	1.89	0.0335	0.1915	0.0173	2742	74	2755	28
ACW5_178a	1.97	0.0177	0.1810	0.0100	2648	38	2662	16
ACW5_91a	3.05	0.0267	0.1122	0.0106	1826	42	1836	19
ACW5_165a	1.91	0.0188	0.1890	0.0156	2718	41	2734	25
ACW5_37a	1.71	0.0226	0.2203	0.0163	2965	54	2983	26
ACW5_70a	3.33	0.0140	0.1046	0.0106	1694	21	1706	19
ACW5_445a	1.95	0.0210	0.1841	0.0223	2670	46	2691	36
ACW5_299a	3.13	0.0202	0.1102	0.0223	1789	32	1804	40
ACW5_148a	2.62	0.0299	0.1305	0.0195	2085	53	2105	34
ACW5_150a	3.03	0.0145	0.1135	0.0089	1837	23	1857	16
ACW5_170a	2.21	0.0162	0.1581	0.0246	2410	32	2435	41
ACW5_164a	3.36	0.0183	0.1040	0.0251	1679	27	1697	46

ACW5_411a	1.90	0.0320	0.1920	0.0168	2727	71	2760	27
ACW5_76a	1.90	0.0195	0.1920	0.0158	2726	43	2760	26
ACW5_67a	1.94	0.0231	0.1876	0.0171	2684	51	2721	28
ACW5_392a	3.13	0.0346	0.1108	0.0171	1786	54	1813	31
ACW5_200a	2.63	0.0191	0.1306	0.0157	2075	34	2107	27
ACW5_404a	3.07	0.0324	0.1134	0.0197	1820	51	1854	35
ACW5_378a	1.94	0.0184	0.1882	0.0248	2675	40	2727	40
ACW5_241a	1.95	0.0169	0.1883	0.0247	2670	37	2727	40
ACW5_64a	2.64	0.0145	0.1316	0.0093	2073	26	2119	16
ACW5_74a	2.93	0.0140	0.1186	0.0109	1893	23	1936	19
ACW5_30a	1.93	0.0193	0.1909	0.0157	2687	42	2750	26
ACW5_439a	1.97	0.0231	0.1863	0.0227	2647	50	2709	37
ACW5_459a	2.97	0.0307	0.1176	0.0167	1870	50	1919	30
ACW5_106a	4.11	0.0191	0.0910	0.0163	1405	24	1446	31
ACW5_47a	1.98	0.0139	0.1864	0.0090	2631	30	2711	15
ACW5_78a	4.82	0.0207	0.0823	0.0160	1214	23	1252	31
ACW5_57a	2.97	0.0228	0.1184	0.0132	1873	37	1932	24
ACW5_179a	5.22	0.0149	0.0788	0.0111	1130	15	1166	22
ACW5_61a	5.50	0.0154	0.0767	0.0127	1078	15	1114	25
ACW5_92a	5.50	0.0146	0.0771	0.0107	1076	14	1123	21
ACW5_177a	3.13	0.0190	0.1143	0.0161	1786	30	1868	29
ACW5_48a	2.24	0.0211	0.1641	0.0102	2382	42	2498	17
ACW5_75a	3.51	0.0193	0.1043	0.0162	1618	28	1701	30
ACW5_110a	2.88	0.0505	0.1295	0.0131	1919	83	2091	23
ACW5_397a	3.83	0.0196	0.1006	0.0220	1496	26	1635	40
> 10% Discordant								
ACW5_111a	3.92	0.0271	0.1030	0.0252	1463	35	1679	46
ACW5_259a	4.40	0.0224	0.1059	0.0226	1321	27	1729	41
ACW5_72a	2.78	0.0164	0.2006	0.0100	1980	28	2831	16
ACW5_18a	19.89	0.0144	0.1468	0.0150	316	4	2309	26

WETHERIL PLOTS

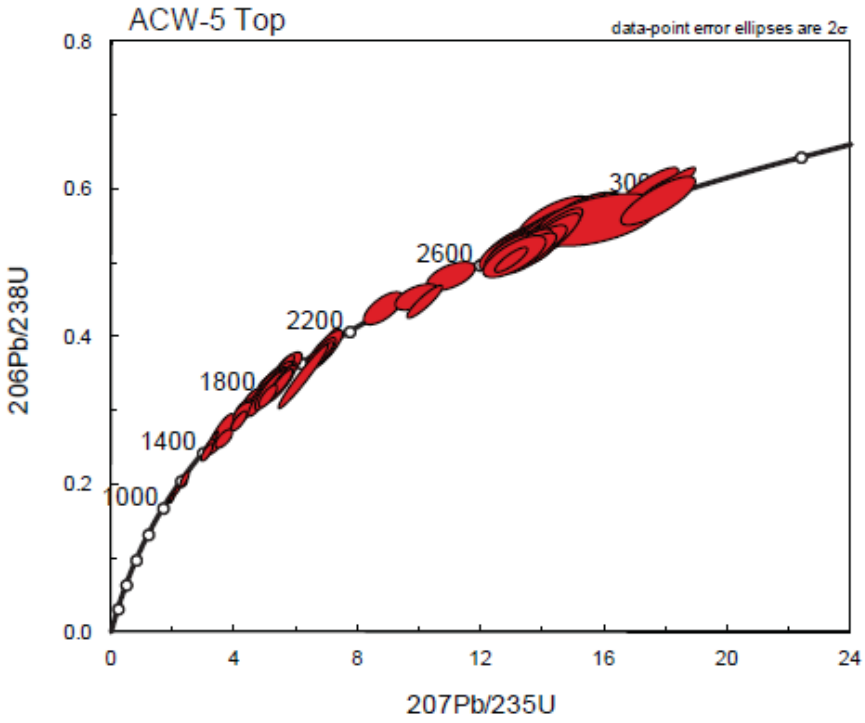

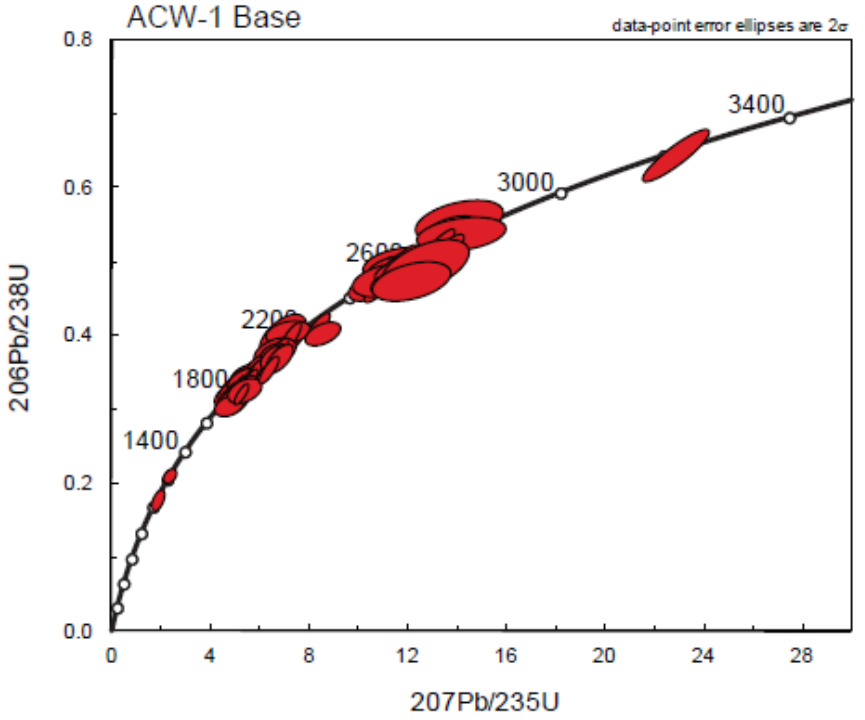

STRATIGRAPHIC SECTION

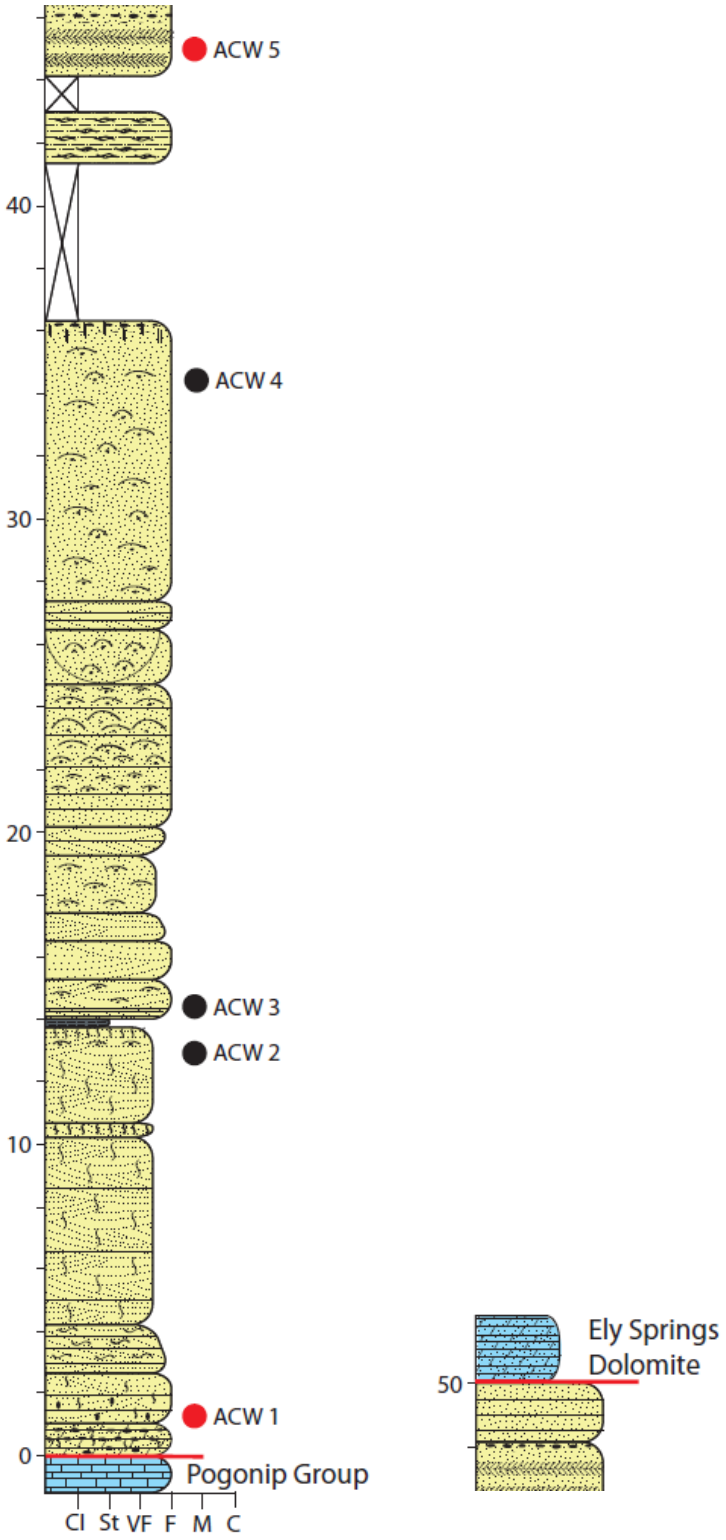

APPENDIX D

LUCKY STRIKE CANYON

DATA TABLES

Sample LSC-1 (Lucky Strike Canyon - Base)								
Sample	**238U/ 206Pb**	**1σ (%)**	**207Pb/ 206Pb**	**1σ (%)**	**238U/ 206Pb Age (Ma)**	**1σ**	**207Pb/ 206Pb Age (Ma)**	**1σ**
< 10% Discordant								
LSC1_84a	1.47	0.0201	0.2208	0.0239	3349	52	2987	38
LSC1_29a	1.79	0.0263	0.1765	0.1074	2856	60	2620	168
LSC1_136a	1.80	0.0247	0.1795	0.0601	2847	57	2648	96
LSC1_25a	1.78	0.0251	0.1828	0.0600	2870	58	2678	96
LSC1_32a	1.79	0.0252	0.1825	0.0670	2862	58	2675	107
LSC1_9a	1.96	0.0265	0.1640	0.1074	2655	57	2497	170
LSC1_22a	1.84	0.0318	0.1782	0.1076	2801	72	2637	168
LSC1_23a	1.84	0.0281	0.1783	0.1076	2798	63	2637	168
LSC1_59a	1.81	0.0279	0.1824	0.0670	2837	64	2674	107
LSC1_108a	1.80	0.0267	0.1847	0.0150	2848	61	2696	25
LSC1_27a	1.85	0.0272	0.1785	0.1074	2780	61	2639	168
LSC1_115a	1.84	0.0267	0.1809	0.0604	2801	60	2661	97
LSC1_239a	1.65	0.0245	0.2108	0.0332	3058	59	2912	53
LSC1_6a	1.84	0.0258	0.1825	0.0670	2800	58	2676	107
LSC1_58a	1.78	0.0266	0.1902	0.1074	2869	61	2744	166
LSC1_13a	2.58	0.0229	0.1244	0.0599	2110	41	2020	103
LSC1_31a	1.90	0.0249	0.1757	0.0670	2726	55	2612	107
LSC1_94a	2.96	0.0228	0.1099	0.0607	1874	37	1798	106
LSC1_192a	2.66	0.0580	0.1213	0.0335	2059	101	1976	58
LSC1_7a	1.88	0.0251	0.1780	0.1074	2744	56	2634	168
LSC1_88a	1.87	0.0234	0.1792	0.0600	2756	52	2646	96
LSC1_97a	1.84	0.0179	0.1852	0.0134	2801	40	2700	22
LSC1_1a	3.05	0.0247	0.1080	0.0673	1830	39	1766	118

LSC1_104a	1.84	0.0251	0.1848	0.0671	2792	57	2697	107
LSC1_18a	1.91	0.0242	0.1768	0.0669	2715	53	2623	107
LSC1_91a	1.86	0.0201	0.1836	0.0165	2778	45	2686	27
LSC1_85a	1.80	0.0228	0.1911	0.0169	2842	52	2751	27
LSC1_20a	3.01	0.0217	0.1095	0.0601	1847	35	1791	106
LSC1_33a	1.91	0.0276	0.1781	0.1075	2716	61	2635	168
LSC1_16a	1.88	0.0245	0.1811	0.0600	2745	55	2663	96
LSC1_65a	3.02	0.0209	0.1095	0.0602	1842	33	1791	106
LSC1_106a	1.87	0.0187	0.1837	0.0138	2763	42	2687	23
LSC1_129a	1.92	0.0251	0.1776	0.0600	2704	55	2630	96
LSC1_46a	1.90	0.0293	0.1793	0.1075	2721	65	2647	168
LSC1_105a	1.83	0.0183	0.1891	0.0163	2808	42	2734	27
LSC1_50a	1.96	0.0199	0.1749	0.0231	2662	43	2605	38
LSC1_60a	1.81	0.0247	0.1940	0.0240	2833	56	2777	39
LSC1_83a	1.79	0.0214	0.1982	0.0288	2866	49	2812	46
LSC1_246a	1.83	0.0235	0.1927	0.0307	2813	53	2766	50
LSC1_130a	1.84	0.0227	0.1910	0.0599	2795	51	2751	95
LSC1_11a	2.75	0.0253	0.1209	0.0672	1997	43	1970	115
LSC1_102a	1.85	0.0188	0.1901	0.0164	2780	42	2743	27
LSC1_240a	1.87	0.0276	0.1879	0.0309	2760	62	2724	50
LSC1_164a	1.82	0.0213	0.1954	0.0305	2822	49	2788	49
LSC1_47a	2.99	0.0246	0.1124	0.0670	1858	40	1839	117
LSC1_49a	2.95	0.0221	0.1138	0.0603	1880	36	1861	105
LSC1_79a	1.96	0.0243	0.1780	0.0669	2656	53	2634	107
LSC1_100a	1.88	0.0221	0.1882	0.0136	2748	49	2727	22
LSC1_57a	1.73	0.0189	0.2122	0.0232	2943	44	2923	37
LSC1_14a	1.93	0.0238	0.1825	0.0669	2694	52	2675	107
LSC1_4a	2.99	0.0247	0.1128	0.0671	1858	40	1846	117
LSC1_93a	1.88	0.0221	0.1888	0.0138	2748	49	2732	23
LSC1_80a	3.13	0.0250	0.1087	0.0671	1788	39	1778	118
LSC1_34a	2.00	0.0230	0.1742	0.0669	2612	49	2598	107
LSC1_162a	1.87	0.0223	0.1906	0.0304	2759	50	2747	49
LSC1_53a	1.87	0.0211	0.1911	0.0232	2760	47	2751	38
LSC1_43a	1.88	0.0192	0.1903	0.0232	2753	43	2744	38
LSC1_26a	1.98	0.0238	0.1777	0.0669	2638	51	2631	107
LSC1_15a	1.86	0.0212	0.1926	0.0600	2771	48	2764	95
LSC1_51a	1.79	0.0227	0.2042	0.0138	2866	52	2860	22
LSC1_182a	1.88	0.0218	0.1904	0.0305	2750	49	2746	49
LSC1_103a	2.89	0.0188	0.1172	0.0169	1915	31	1913	30

LSC1_78a	1.65	0.0258	0.2314	0.0145	3057	63	3062	23
LSC1_107a	1.93	0.0195	0.1852	0.0135	2691	43	2700	22
LSC1_137a	1.94	0.0190	0.1837	0.0164	2676	42	2686	27
LSC1_134a	1.92	0.0186	0.1868	0.0168	2699	41	2714	27
LSC1_64a	1.91	0.0289	0.1892	0.0236	2718	64	2735	38
LSC1_144a	1.92	0.0241	0.1871	0.0168	2700	53	2717	27
LSC1_70a	1.73	0.0192	0.2165	0.0233	2936	45	2955	37
LSC1_76a	1.74	0.0191	0.2155	0.0233	2926	45	2947	37
LSC1_44a	2.91	0.0235	0.1177	0.0248	1906	39	1921	44
LSC1_77a	1.73	0.0197	0.2180	0.0234	2943	46	2966	37
LSC1_119a	1.92	0.0232	0.1887	0.0177	2704	51	2731	29
LSC1_63a	1.96	0.0221	0.1839	0.0138	2658	48	2688	23
LSC1_61a	1.93	0.0222	0.1880	0.0237	2690	49	2725	38
LSC1_92a	2.86	0.0206	0.1203	0.0240	1934	34	1961	42
LSC1_36a	2.02	0.0304	0.1776	0.1075	2591	65	2630	168
LSC1_126a	1.90	0.0220	0.1933	0.0167	2727	49	2770	27
LSC1_145a	1.94	0.0215	0.1882	0.0170	2684	47	2727	28
LSC1_87a	1.95	0.0184	0.1860	0.0231	2663	40	2707	38
LSC1_123a	1.99	0.0212	0.1822	0.0167	2628	46	2673	27
LSC1_132a	3.13	0.0188	0.1114	0.0168	1789	29	1823	30
LSC1_253a	2.86	0.0249	0.1210	0.0311	1933	41	1970	54
LSC1_139a	1.95	0.0188	0.1873	0.0164	2667	41	2719	27
LSC1_236a	3.03	0.0213	0.1151	0.0308	1841	34	1881	54
LSC1_207a	1.93	0.0245	0.1919	0.0304	2697	54	2758	49
LSC1_184a	2.90	0.0209	0.1199	0.0305	1908	34	1955	54
LSC1_156a	2.96	0.0209	0.1183	0.0304	1878	34	1930	53
LSC1_66a	1.86	0.0222	0.2034	0.0135	2776	50	2854	22
LSC1_96a	5.37	0.0187	0.0775	0.0234	1101	19	1134	46
LSC1_201a	2.67	0.0205	0.1313	0.0303	2052	36	2115	52
LSC1_116a	1.98	0.0209	0.1874	0.0168	2637	45	2719	27
LSC1_90a	2.05	0.0237	0.1795	0.0669	2560	50	2648	107
LSC1_157a	1.99	0.0228	0.1876	0.0307	2629	49	2721	50
LSC1_217a	1.99	0.0209	0.1901	0.0303	2628	45	2743	49
LSC1_225a	2.00	0.0305	0.1902	0.0309	2611	65	2744	50
LSC1_5a	3.43	0.0199	0.1085	0.0599	1648	29	1774	106
LSC1_238a	2.06	0.0301	0.1917	0.0309	2550	63	2757	50
LSC1_142a	1.93	0.0249	0.2128	0.0254	2695	55	2927	41
LSC1_178a	2.54	0.0253	0.1515	0.0333	2142	46	2362	56
LSC1_74a	3.69	0.0207	0.1052	0.0600	1547	28	1718	106

> 10% Discordant								
LSC1_111a	1.96	0.0225	0.2278	0.0237	2660	49	3037	38
LSC1_56a	2.56	0.0494	0.1618	0.0601	2129	89	2474	98
LSC1_247a	3.04	0.0317	0.1775	0.0305	1831	50	2629	50

Sample LSC-3 (Lucky Strike Canyon - Top)								
Sample	**238U/ 206Pb**	**1σ (%)**	**207Pb/ 206Pb**	**1σ (%)**	**238U/ 206Pb Age (Ma)**	**1σ**	**207Pb/ 206Pb Age (Ma)**	**1σ**
< 10% Discordant								
LSC3_132a	2.70	0.0247	0.1099	0.0141	2030	43	1797	25
LSC3_117a	2.93	0.0231	0.1042	0.0155	1895	38	1701	28
LSC3_163a	1.84	0.0370	0.1706	0.0151	2801	84	2564	25
LSC3_125a	2.77	0.0234	0.1130	0.0137	1989	40	1849	25
LSC3_14a	2.72	0.0138	0.1148	0.0087	2019	24	1877	16
LSC3_164a	2.45	0.0207	0.1276	0.0127	2204	38	2065	22
LSC3_36a	2.85	0.0219	0.1112	0.0237	1940	37	1820	42
LSC3_7a	2.38	0.0183	0.1321	0.0092	2263	35	2126	16
LSC3_149a	2.86	0.0206	0.1115	0.0226	1932	34	1823	40
LSC3_9a	2.89	0.0153	0.1107	0.0103	1913	25	1812	19
LSC3_5a	2.76	0.0193	0.1159	0.0133	1991	33	1895	24
LSC3_42a	2.89	0.0205	0.1114	0.0229	1913	34	1822	41
LSC3_177a	2.77	0.0359	0.1157	0.0271	1984	61	1891	48
LSC3_184a	2.86	0.0247	0.1126	0.0233	1931	41	1842	42
LSC3_51a	1.88	0.0112	0.1775	0.0081	2755	25	2630	13
LSC3_98a	2.75	0.0227	0.1169	0.0232	1998	39	1909	41
LSC3_103a	2.69	0.0243	0.1195	0.0127	2039	42	1949	22
LSC3_1a	2.90	0.0145	0.1116	0.0124	1908	24	1825	22
LSC3_99a	1.80	0.0214	0.1878	0.0228	2845	49	2723	37
LSC3_209a	2.89	0.0225	0.1123	0.0127	1918	37	1837	23
LSC3_102a	2.24	0.0199	0.1447	0.0228	2381	39	2284	39
LSC3_211a	1.84	0.0230	0.1835	0.0227	2798	52	2685	37
LSC3_18a	1.98	0.0152	0.1680	0.0106	2638	33	2538	18
LSC3_175a	1.84	0.0207	0.1840	0.0123	2795	47	2690	20
LSC3_137a	2.97	0.0222	0.1100	0.0227	1870	36	1800	41
LSC3_83a	2.88	0.0236	0.1131	0.0123	1922	39	1850	22
LSC3_115a	2.81	0.0223	0.1155	0.0137	1962	38	1888	24
LSC3_49a	2.49	0.0155	0.1297	0.0091	2175	29	2094	16
LSC3_180a	2.90	0.0219	0.1129	0.0136	1912	36	1847	24
LSC3_109a	2.93	0.0201	0.1120	0.0227	1895	33	1832	41
LSC3_48a	2.86	0.0135	0.1145	0.0122	1931	22	1872	22
LSC3_195a	2.97	0.0266	0.1112	0.0234	1873	43	1820	42
LSC3_32a	1.87	0.0143	0.1835	0.0087	2764	32	2685	14

LSC3_23a	2.55	0.0137	0.1281	0.0121	2131	25	2072	21
LSC3_155a	2.61	0.0237	0.1255	0.0229	2093	42	2036	40
LSC3_55a	2.95	0.0159	0.1123	0.0125	1884	26	1836	22
LSC3_76a	2.94	0.0197	0.1126	0.0150	1889	32	1843	27
LSC3_182a	2.93	0.0203	0.1131	0.0126	1891	33	1849	23
LSC3_87a	1.86	0.0224	0.1876	0.0208	2779	50	2721	34
LSC3_111a	1.81	0.0207	0.1934	0.0227	2830	47	2772	37
LSC3_205a	2.91	0.0223	0.1142	0.0133	1906	37	1867	24
LSC3_150a	1.85	0.0231	0.1885	0.0137	2787	52	2730	22
LSC3_2a	1.46	0.0114	0.2683	0.0083	3365	30	3296	13
LSC3_181a	2.93	0.0237	0.1132	0.0230	1891	39	1852	41
LSC3_8a	1.86	0.0102	0.1867	0.0082	2769	23	2713	13
LSC3_188a	1.64	0.0237	0.2243	0.0136	3069	58	3012	22
LSC3_107a	1.93	0.0296	0.1799	0.0136	2696	65	2652	22
LSC3_194a	2.98	0.0230	0.1123	0.0136	1865	37	1836	24
LSC3_91a	5.46	0.0227	0.0750	0.0283	1085	23	1069	56
LSC3_120a	1.70	0.0234	0.2148	0.0227	2986	56	2942	36
LSC3_151a	2.97	0.0211	0.1126	0.0129	1869	34	1842	23
LSC3_168a	1.89	0.0203	0.1856	0.0122	2741	45	2703	20
LSC3_63a	3.01	0.0111	0.1114	0.0081	1849	18	1823	15
LSC3_57a	2.97	0.0131	0.1127	0.0097	1868	21	1844	17
LSC3_142a	2.90	0.0197	0.1156	0.0121	1912	33	1889	22
LSC3_133a	2.61	0.0240	0.1276	0.0226	2090	43	2065	39
LSC3_3a	2.95	0.0118	0.1137	0.0089	1880	19	1860	16
LSC3_123a	3.04	0.0210	0.1109	0.0229	1833	33	1814	41
LSC3_80a	2.98	0.0246	0.1127	0.0134	1863	40	1843	24
LSC3_128a	1.99	0.0238	0.1739	0.0229	2622	51	2596	38
LSC3_153a	2.95	0.0198	0.1141	0.0126	1884	32	1866	23
LSC3_15a	2.04	0.0153	0.1685	0.0111	2568	32	2543	19
LSC3_214a	3.28	0.0255	0.1041	0.0229	1714	38	1698	42
LSC3_169a	2.95	0.0214	0.1138	0.0134	1879	35	1861	24
LSC3_64a	2.59	0.0128	0.1292	0.0120	2105	23	2087	21
LSC3_19a	2.92	0.0158	0.1151	0.0120	1896	26	1881	22
LSC3_186a	1.91	0.0234	0.1851	0.0226	2716	52	2699	37
LSC3_183a	1.91	0.0236	0.1847	0.0225	2712	52	2696	37
LSC3_22a	2.09	0.0103	0.1644	0.0079	2517	21	2502	13
LSC3_97a	1.90	0.0245	0.1861	0.0125	2724	54	2708	20
LSC3_67a	2.88	0.0244	0.1169	0.0131	1919	40	1910	23
LSC3_52a	1.86	0.0130	0.1926	0.0117	2778	29	2765	19

LSC3_196a	3.01	0.0264	0.1126	0.0238	1847	42	1841	43
LSC3_58a	2.89	0.0244	0.1168	0.0127	1913	40	1908	23
LSC3_45a	2.62	0.0116	0.1288	0.0089	2087	21	2082	16
LSC3_31a	2.99	0.0216	0.1136	0.0137	1859	35	1857	25
LSC3_16a	1.90	0.0197	0.1879	0.0112	2725	44	2724	18
LSC3_140a	1.89	0.0219	0.1899	0.0134	2743	49	2742	22
LSC3_78a	3.04	0.0219	0.1121	0.0120	1832	35	1833	22
LSC3_10a	3.00	0.0161	0.1135	0.0135	1855	26	1857	24
LSC3_179a	2.88	0.0214	0.1180	0.0134	1922	36	1926	24
LSC3_156a	2.85	0.0228	0.1190	0.0132	1937	38	1942	23
LSC3_85a	2.95	0.0284	0.1154	0.0130	1880	46	1886	23
LSC3_46a	3.09	0.0223	0.1108	0.0121	1806	35	1812	22
LSC3_62a	3.08	0.0137	0.1113	0.0123	1811	22	1820	22
LSC3_187a	1.92	0.0219	0.1877	0.0133	2704	48	2722	22
LSC3_69a	1.94	0.0223	0.1858	0.0119	2677	49	2705	19
LSC3_88a	1.98	0.0220	0.1813	0.0124	2637	47	2664	20
LSC3_141a	3.02	0.0255	0.1139	0.0150	1842	41	1863	27
LSC3_126a	1.53	0.0235	0.2668	0.0120	3249	60	3287	19
LSC3_161a	2.78	0.0247	0.1235	0.0265	1981	42	2008	46
LSC3_166a	3.04	0.0251	0.1138	0.0240	1835	40	1861	43
LSC3_26a	1.94	0.0114	0.1879	0.0083	2678	25	2724	14
LSC3_189a	2.91	0.0203	0.1189	0.0125	1905	33	1939	22
LSC3_93a	2.90	0.0225	0.1192	0.0119	1909	37	1945	21
LSC3_40a	3.02	0.0116	0.1150	0.0089	1843	19	1879	16
LSC3_24a	2.92	0.0199	0.1188	0.0127	1901	33	1939	23
LSC3_199a	2.67	0.0217	0.1297	0.0135	2051	38	2093	24
LSC3_50a	1.97	0.0136	0.1848	0.0117	2642	29	2696	19
LSC3_13a	3.10	0.0155	0.1124	0.0126	1802	24	1839	23
LSC3_61a	3.13	0.0137	0.1120	0.0097	1788	21	1832	17
LSC3_144a	1.96	0.0262	0.1886	0.0229	2654	57	2730	37
LSC3_30a	3.10	0.0152	0.1134	0.0109	1800	24	1854	20
LSC3_29a	3.12	0.0148	0.1130	0.0125	1792	23	1848	22
LSC3_35a	3.10	0.0211	0.1140	0.0227	1801	33	1863	40
LSC3_192a	2.71	0.0209	0.1302	0.0129	2022	36	2100	23
LSC3_4a	2.03	0.0201	0.1870	0.0109	2583	43	2716	18
LSC3_114a	2.83	0.0227	0.1264	0.0252	1948	38	2049	44
LSC3_20a	5.10	0.0151	0.0813	0.0131	1155	16	1230	25
LSC3_131a	3.03	0.0265	0.1207	0.0159	1840	42	1967	28
LSC3_38a	2.90	0.0257	0.1283	0.0211	1911	42	2075	37

> 10% Discordant								
LSC3_124a	2.42	0.0220	0.1757	0.0133	2233	41	2613	22
LSC3_116a	3.66	0.0228	0.1245	0.0122	1557	31	2022	21
LSC3_11a	3.52	0.0812	0.1363	0.0152	1612	115	2181	26
LSC3_28a	3.33	0.0277	0.1542	0.0286	1692	41	2393	48
LSC3_41a	5.49	0.1070	0.1201	0.0411	1078	105	1958	72
LSC3_71a	5.65	0.1995	0.1217	0.0201	1050	191	1982	35
LSC3_239a	5.03	0.0409	0.2219	0.0282	1169	44	2994	45

WETHERIL PLOTS

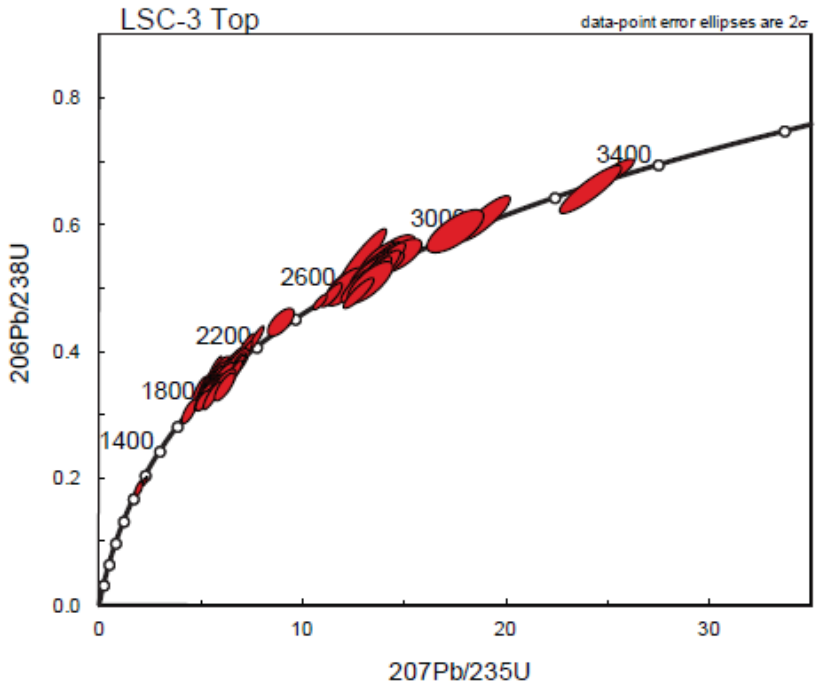

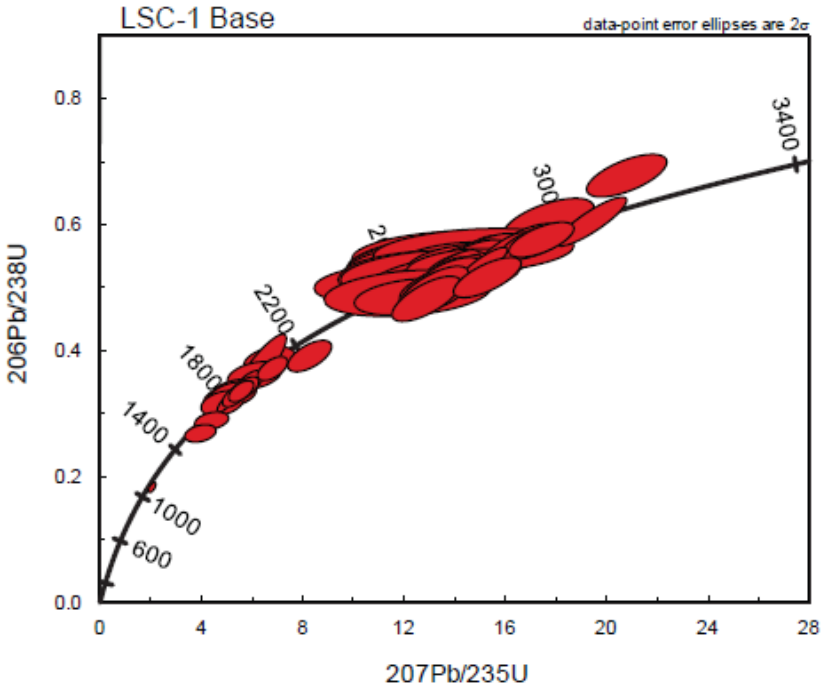

STRATIGRAPHIC SECTION

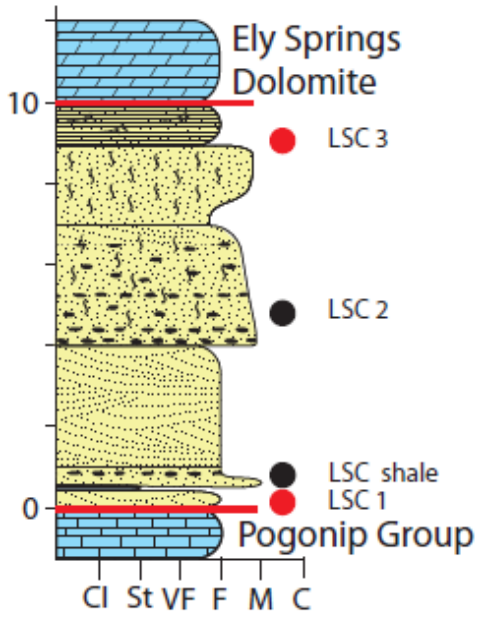

APPENDIX E

MOUNT IRISH

DATA TABLES

Sample MI-1 (Mount Irish - Top)								
Sample	**238U/ 206Pb**	**1σ (%)**	**207Pb/ 206Pb**	**1σ (%)**	**238U/ 206Pb Age (Ma)**	**1σ**	**207Pb/ 206Pb Age (Ma)**	**1σ**
< 10% Discordant								
MI1_322a	1.69	0.0329	0.2020	0.0309	3001	78	2842	49
MI1_15a	1.84	0.0100	0.1868	0.0164	2795	23	2715	27
MI1_319a	3.03	0.0172	0.1113	0.0274	1839	27	1821	49
MI1_284a	3.00	0.0156	0.1123	0.0133	1855	25	1837	24
MI1_34a	3.00	0.0132	0.1131	0.0180	1856	21	1849	32
MI1_274a	1.92	0.0157	0.1848	0.0271	2704	35	2696	44
MI1_9a	2.85	0.0158	0.1187	0.0172	1939	26	1937	30
MI1_262a	2.88	0.0165	0.1176	0.0135	1919	27	1919	24
MI1_97a	3.06	0.0184	0.1116	0.0161	1824	29	1826	29
MI1_154a	1.93	0.0170	0.1845	0.0127	2687	37	2694	21
MI1_108a	1.91	0.0131	0.1874	0.0141	2710	29	2720	23
MI1_361a	1.95	0.0171	0.1826	0.0133	2666	37	2677	22
MI1_42a	3.09	0.0157	0.1110	0.0161	1808	25	1817	29
MI1_32a	1.89	0.0201	0.1905	0.0176	2732	45	2746	29
MI1_237a	1.94	0.0263	0.1854	0.0109	2684	58	2702	18
MI1_237a	1.94	0.0263	0.1854	0.0109	2684	58	2702	18
MI1_349a	2.34	0.0159	0.1469	0.0136	2292	31	2310	23
MI1_4a	1.92	0.0126	0.1883	0.0159	2706	28	2727	26
MI1_363a	3.09	0.0199	0.1113	0.0284	1807	31	1821	51
MI1_246a	1.89	0.0127	0.1921	0.0065	2737	28	2760	11
MI1_246a	1.89	0.0127	0.1921	0.0065	2737	28	2760	11
MI1_126a	2.63	0.0167	0.1297	0.0152	2076	30	2094	27
MI1_270a	2.63	0.0170	0.1300	0.0277	2079	30	2098	48

MI1_265a	2.13	0.0156	0.1654	0.0274	2486	32	2512	45
MI1_63a	2.67	0.0147	0.1281	0.0167	2050	26	2071	29
MI1_333a	2.36	0.0170	0.1463	0.0278	2278	33	2303	47
MI1_394a	2.95	0.0226	0.1163	0.0156	1880	37	1900	28
MI1_251a	1.81	0.0145	0.2057	0.0124	2838	33	2872	20
MI1_19a	3.01	0.0167	0.1145	0.0176	1847	27	1872	31
MI1_186a	1.74	0.0201	0.2182	0.0131	2924	47	2968	21
MI1_1a	2.90	0.0152	0.1188	0.0164	1908	25	1938	29
MI1_85a	1.96	0.0191	0.1857	0.0161	2657	41	2705	26
MI1_396a	3.06	0.0203	0.1136	0.0169	1824	32	1858	30
MI1_131a	3.01	0.0185	0.1153	0.0135	1850	30	1885	24
MI1_64a	3.02	0.0135	0.1149	0.0146	1843	22	1879	26
MI1_217a	3.11	0.0150	0.1121	0.0129	1798	23	1834	23
MI1_212a	2.10	0.0142	0.1700	0.0059	2508	29	2558	10
MI1_212a	2.10	0.0142	0.1700	0.0059	2508	29	2558	10
MI1_292a	2.71	0.0185	0.1276	0.0277	2022	32	2065	48
MI1_220a	3.08	0.0189	0.1134	0.0094	1813	30	1854	17
MI1_220a	3.08	0.0189	0.1134	0.0094	1813	30	1854	17
MI1_17a	3.05	0.0103	0.1142	0.0169	1826	16	1868	30
MI1_122a	1.99	0.0122	0.1833	0.0140	2621	26	2683	23
MI1_419a	3.04	0.0116	0.1147	0.0138	1831	18	1875	25
MI1_38a	3.06	0.0208	0.1142	0.0170	1823	33	1868	30
MI1_36a	3.06	0.0247	0.1142	0.0170	1822	39	1867	30
MI1_222a	3.07	0.0170	0.1139	0.0134	1816	27	1862	24
MI1_401a	3.20	0.0118	0.1099	0.0132	1754	18	1799	24
MI1_37a	3.09	0.0147	0.1132	0.0146	1805	23	1852	26
MI1_416a	2.68	0.0275	0.1299	0.0185	2044	48	2097	32
MI1_135a	2.93	0.0129	0.1189	0.0145	1891	21	1940	26
MI1_45a	2.92	0.0119	0.1195	0.0161	1897	20	1948	28
MI1_40a	1.74	0.0134	0.2241	0.0160	2930	31	3010	26
MI1_410a	3.05	0.0198	0.1150	0.0146	1829	31	1881	26
MI1_3a	1.98	0.0120	0.1866	0.0160	2635	26	2712	26
MI1_128a	3.10	0.0165	0.1136	0.0150	1803	26	1857	27
MI1_258a	3.04	0.0180	0.1157	0.0274	1835	29	1891	49
MI1_88a	3.01	0.0224	0.1169	0.0178	1851	36	1909	32
MI1_12a	3.05	0.0099	0.1154	0.0172	1829	16	1886	31
MI1_203a	1.96	0.0162	0.1903	0.0066	2660	35	2745	11
MI1_203a	1.96	0.0162	0.1903	0.0066	2660	35	2745	11
MI1_300a	2.74	0.0182	0.1279	0.0275	2005	31	2069	48

MI1_44a	2.98	0.0138	0.1180	0.0171	1866	22	1926	30
MI1_55a	3.08	0.0185	0.1145	0.0172	1810	29	1872	31
MI1_280a	2.58	0.0173	0.1365	0.0276	2111	31	2184	47
MI1_393a	3.12	0.0085	0.1135	0.0130	1793	13	1856	23
MI1_112a	2.56	0.0239	0.1380	0.0186	2126	43	2202	32
MI1_21a	3.15	0.0142	0.1126	0.0163	1777	22	1843	29
MI1_137a	3.12	0.0166	0.1137	0.0161	1793	26	1860	29
MI1_290a	2.12	0.0131	0.1734	0.0059	2494	27	2591	10
MI1_290a	2.12	0.0131	0.1734	0.0059	2494	27	2591	10
MI1_295a	3.11	0.0140	0.1145	0.0100	1800	22	1872	18
MI1_295a	3.11	0.0140	0.1145	0.0100	1800	22	1872	18
MI1_11a	2.14	0.0120	0.1720	0.0162	2468	25	2577	27
MI1_378a	3.11	0.0138	0.1153	0.0144	1799	22	1884	26
MI1_105a	2.77	0.0198	0.1290	0.0169	1990	34	2085	29
MI1_72a	1.93	0.0199	0.1993	0.0149	2690	44	2821	24
MI1_331a	3.06	0.0246	0.1170	0.0153	1821	39	1911	27
MI1_331a	3.06	0.0246	0.1170	0.0153	1821	39	1911	27
MI1_87a	3.07	0.0225	0.1167	0.0163	1816	35	1906	29
MI1_408a	1.99	0.0125	0.1916	0.0145	2620	27	2756	24
MI1_279a	3.11	0.0158	0.1155	0.0070	1795	25	1888	13
MI1_279a	3.11	0.0158	0.1155	0.0070	1795	25	1888	13
MI1_248a	3.20	0.0351	0.1129	0.0291	1752	54	1847	52
MI1_205a	1.99	0.0167	0.1941	0.0128	2625	36	2777	21
MI1_285a	3.12	0.0202	0.1162	0.0276	1793	31	1899	49
MI1_425a	3.23	0.0166	0.1128	0.0157	1739	25	1844	28
MI1_266a	3.24	0.0137	0.1126	0.0070	1736	21	1842	13
MI1_266a	3.24	0.0137	0.1126	0.0070	1736	21	1842	13
MI1_374a	3.23	0.0153	0.1132	0.0145	1741	23	1851	26
MI1_67a	3.02	0.0250	0.1202	0.0195	1842	40	1959	34
MI1_39a	3.08	0.0141	0.1183	0.0170	1813	22	1930	30
MI1_46a	3.05	0.0169	0.1195	0.0172	1829	27	1949	30
MI1_211a	2.72	0.0194	0.1346	0.0123	2018	34	2159	21
MI1_211a	2.72	0.0194	0.1346	0.0123	2018	34	2159	21
MI1_307a	2.07	0.0141	0.1869	0.0070	2538	30	2715	11
MI1_307a	2.07	0.0141	0.1869	0.0070	2538	30	2715	11
MI1_255a	2.55	0.0136	0.1454	0.0064	2132	25	2292	11
MI1_255a	2.55	0.0136	0.1454	0.0064	2132	25	2292	11
MI1_50a	3.22	0.0166	0.1148	0.0178	1744	25	1877	32
MI1_31a	3.05	0.0214	0.1211	0.0205	1828	34	1973	36

MI1_30a	3.25	0.0275	0.1151	0.0195	1731	42	1881	35
MI1_421a	3.29	0.0187	0.1146	0.0144	1712	28	1874	26
MI1_71a	3.23	0.0181	0.1176	0.0175	1741	27	1919	31
> 10% Discordant								
MI1_371a	3.16	0.0115	0.1236	0.0129	1774	18	2009	23
MI1_305a	3.15	0.0225	0.1241	0.0984	1775	35	2016	165
MI1_305a	3.15	0.0225	0.1241	0.0984	1775	35	2016	165
MI1_223a	2.83	0.0156	0.1395	0.0097	1948	26	2221	17
MI1_223a	2.83	0.0156	0.1395	0.0097	1948	26	2221	17
MI1_48a	3.29	0.0154	0.1218	0.0166	1710	23	1982	29
MI1_61a	4.08	0.0204	0.1172	0.0143	1413	26	1914	26
MI1_41a	2.84	0.0228	0.1824	0.0157	1946	38	2675	26
MI1_35a	4.29	0.0175	0.1300	0.0147	1351	21	2099	26
MI1_196a	6.20	0.0225	0.0980	0.0257	964	20	1586	47
MI1_5a	6.73	0.0223	0.1297	0.0158	893	19	2094	28
MI1_341a	5.40	0.0656	0.1986	0.0272	1095	66	2815	44
MI1_110a	7.52	0.0163	0.1701	0.0141	805	12	2558	23
MI1_8a	12.11	0.0573	0.1463	0.0164	511	28	2303	28
MI1_99a	12.21	0.0437	0.1480	0.0150	507	21	2323	26

Sample MI-5 (Mount Irish - Top)								
Sample	**238U/ 206Pb**	**1σ (%)**	**207Pb/ 206Pb**	**1σ (%)**	**238U/ 206Pb Age (Ma)**	**1σ**	**207Pb/ 206Pb Age (Ma)**	**1σ**
< 10% Discordant								
MI5_276a	2.57	0.0211	0.1175	0.0149	2120	38	1918	27
MI5_31a	2.71	0.0197	0.1132	0.0162	2024	34	1851	29
MI5_3a	2.79	0.0226	0.1117	0.0168	1978	38	1827	30
MI5_6a	2.77	0.0329	0.1137	0.0191	1989	56	1860	34
MI5_74a	2.78	0.0237	0.1142	0.0214	1984	40	1867	38
MI_5_297a	2.56	0.0556	0.1233	0.0243	2129	100	2005	43
MI5_4a	2.81	0.0229	0.1130	0.0165	1960	39	1848	29
MI5_5a	1.79	0.0239	0.1844	0.0149	2855	55	2693	24
MI5_18a	2.75	0.0210	0.1154	0.0164	1999	36	1886	29
MI5_45a	2.80	0.0220	0.1135	0.0198	1967	37	1856	35
MI5_1a	2.78	0.0233	0.1142	0.0180	1978	40	1868	32
MI5_66a	2.87	0.0193	0.1115	0.0192	1925	32	1825	34
MI5_9a	2.70	0.0206	0.1187	0.0155	2033	36	1937	27
MI_5_130a_left	2.82	0.0261	0.1141	0.0103	1958	44	1866	18
MI5_13a	2.88	0.0228	0.1120	0.0161	1922	38	1833	29
MI5_52a	2.82	0.0158	0.1140	0.0168	1954	27	1864	30
MI5_157a	2.85	0.0165	0.1130	0.0134	1937	28	1849	24
MI5_58a	2.88	0.0203	0.1126	0.0202	1921	34	1842	36
MI5_272a	2.87	0.0218	0.1131	0.0140	1928	36	1850	25
MI_5_327a	2.47	0.0257	0.1304	0.0087	2192	48	2103	15
MI_5_402a	2.98	0.0264	0.1095	0.0088	1866	43	1791	16
MI_5_361a	2.89	0.0222	0.1128	0.0083	1915	37	1845	15
MI5_316a	1.85	0.0278	0.1830	0.0106	2780	62	2680	17
MI5_139a	2.49	0.0232	0.1307	0.0109	2180	43	2107	19
MI5_350a	2.23	0.0302	0.1470	0.0137	2390	60	2311	23
MI5_23a	1.97	0.0183	0.1699	0.0132	2642	39	2557	22
MI5_43a	2.88	0.0170	0.1136	0.0133	1920	28	1858	24
MI5_189a	2.89	0.0241	0.1132	0.0098	1913	40	1852	18
MI_5_147a	2.91	0.0221	0.1127	0.0086	1902	36	1843	16
MI5_128a	2.76	0.0150	0.1186	0.0136	1994	26	1935	24
MI5_132a	2.82	0.0220	0.1162	0.0099	1956	37	1898	18
MI5_182a	1.84	0.0211	0.1872	0.0170	2799	48	2718	28
MI5_194a	2.79	0.0237	0.1173	0.0205	1972	40	1916	36

MI5_253a	2.77	0.0277	0.1184	0.0121	1986	47	1932	22
MI_5_222a	2.93	0.0267	0.1125	0.0113	1892	44	1841	20
MI5_11a	2.91	0.0168	0.1134	0.0129	1906	28	1854	23
MI5_120a	1.83	0.0161	0.1887	0.0161	2806	36	2731	26
MI5_85a	2.93	0.0228	0.1125	0.0193	1891	37	1841	35
MI5_184a	2.94	0.0176	0.1125	0.0163	1886	29	1840	29
MI5_226a	2.91	0.0244	0.1135	0.0203	1902	40	1857	36
MI5_179a	2.80	0.0274	0.1176	0.0127	1966	46	1921	23
MI5_382a	1.98	0.0253	0.1724	0.0135	2641	55	2581	22
MI5_234a	1.84	0.0248	0.1888	0.0195	2793	56	2732	32
MI5_80a	3.00	0.0170	0.1108	0.0145	1852	27	1813	26
MI5_158a	2.89	0.0191	0.1148	0.0165	1918	32	1877	29
MI_5_326a	2.55	0.0221	0.1293	0.0084	2133	40	2088	15
MI5_8a	2.88	0.0208	0.1150	0.0151	1919	34	1879	27
MI5_94a	2.82	0.0215	0.1173	0.0193	1955	36	1916	34
MI5_306a	2.90	0.0253	0.1144	0.0150	1907	42	1870	27
MI5_293a	2.91	0.0321	0.1144	0.0104	1906	53	1871	19
MI5_354a	2.81	0.0267	0.1180	0.0151	1963	45	1926	27
MI5_190a	2.94	0.0228	0.1135	0.0143	1889	37	1857	26
MI_5_385a	2.72	0.0232	0.1218	0.0093	2015	40	1982	16
MI5_70a	2.93	0.0178	0.1138	0.0128	1891	29	1861	23
MI5_92a	2.94	0.0185	0.1135	0.0140	1886	30	1857	25
MI5_264a	2.96	0.0192	0.1131	0.0170	1879	31	1849	30
MI5_307a	2.29	0.0219	0.1457	0.0166	2333	43	2296	28
MI5_238a	3.06	0.0201	0.1099	0.0174	1824	32	1798	31
MI5_91a	3.01	0.0176	0.1116	0.0182	1850	28	1826	33
MI5_229a	2.91	0.0282	0.1150	0.0113	1904	46	1880	20
MI_5_174a	1.86	0.0223	0.1905	0.0081	2776	50	2746	13
MI5_171a	2.85	0.0245	0.1176	0.0114	1941	41	1920	20
MI5_41a	1.89	0.0188	0.1865	0.0130	2740	42	2711	21
MI5_69a	3.11	0.0192	0.1088	0.0196	1795	30	1780	35
MI5_396a	1.90	0.0268	0.1858	0.0165	2727	59	2706	27
MI5_169a	2.96	0.0230	0.1140	0.0208	1875	37	1864	37
MI5_302a	2.81	0.0235	0.1198	0.0175	1964	40	1953	31
MI5_246a	2.95	0.0243	0.1146	0.0100	1884	40	1874	18
MI5_389a	2.88	0.0282	0.1172	0.0169	1924	47	1914	30
MI5_280a	5.24	0.0212	0.0770	0.0140	1126	22	1120	28
MI_5_239a	1.92	0.0225	0.1847	0.0073	2707	49	2695	12
MI_5_256a	2.82	0.0236	0.1200	0.0087	1959	40	1956	15

MI5_201a	2.58	0.0267	0.1307	0.0118	2108	48	2107	21
MI_5_130a_right	3.01	0.0217	0.1131	0.0104	1847	35	1849	19
MI5_30a	2.22	0.0179	0.1552	0.0151	2398	36	2404	25
MI5_148a	2.65	0.0165	0.1282	0.0176	2067	29	2073	31
MI5_156a	2.75	0.0304	0.1233	0.0128	1998	52	2005	23
MI5_278a	2.93	0.0235	0.1162	0.0198	1892	38	1898	35
MI5_126a	2.65	0.0203	0.1283	0.0199	2064	36	2074	35
MI5_100a	2.00	0.0194	0.1777	0.0191	2610	41	2631	31
MI_5_112a	2.99	0.0202	0.1153	0.0087	1862	33	1884	16
MI5_242a	2.87	0.0257	0.1194	0.0153	1924	43	1948	27
MI5_98a	2.67	0.0176	0.1289	0.0165	2051	31	2083	29
MI5_323a	2.87	0.0270	0.1202	0.0156	1929	45	1960	28
MI5_275a	3.01	0.0261	0.1152	0.0111	1849	42	1882	20
MI5_114a	2.03	0.0245	0.1773	0.0204	2579	52	2627	34
MI5_355a	2.86	0.0283	0.1224	0.0185	1935	47	1991	33
MI5_54a	1.77	0.0176	0.2188	0.0127	2886	41	2972	20
MI5_300a	2.93	0.0313	0.1196	0.0125	1893	51	1951	22
MI5_386a	3.05	0.0275	0.1162	0.0169	1829	44	1899	30
MI5_145a	3.19	0.0206	0.1133	0.0200	1758	32	1853	36
MI5_2a	2.62	0.0228	0.1383	0.0257	2083	40	2206	44
MI5_84a	2.63	0.0191	0.1452	0.0191	2075	34	2290	32
MI_5_353a	3.41	0.0282	0.1121	0.0097	1657	41	1835	17
> 10% Discordant								
MI5_330a	1.96	0.0333	0.2263	0.0105	2659	72	3026	17
MI5_384a	3.11	0.0247	0.1265	0.0137	1798	39	2049	24
MI5_351a	2.49	0.0306	0.1625	0.0115	2175	56	2482	19
MI5_115a	2.30	0.0418	0.1827	0.0436	2328	81	2677	70
MI_5_103a	3.13	0.0190	0.1560	0.0081	1789	30	2412	14
MI5_312a	4.78	0.0332	0.1272	0.0148	1224	37	2059	26
MI5_56a	5.42	0.0200	0.1769	0.0190	1092	20	2624	31

WETHERIL PLOTS

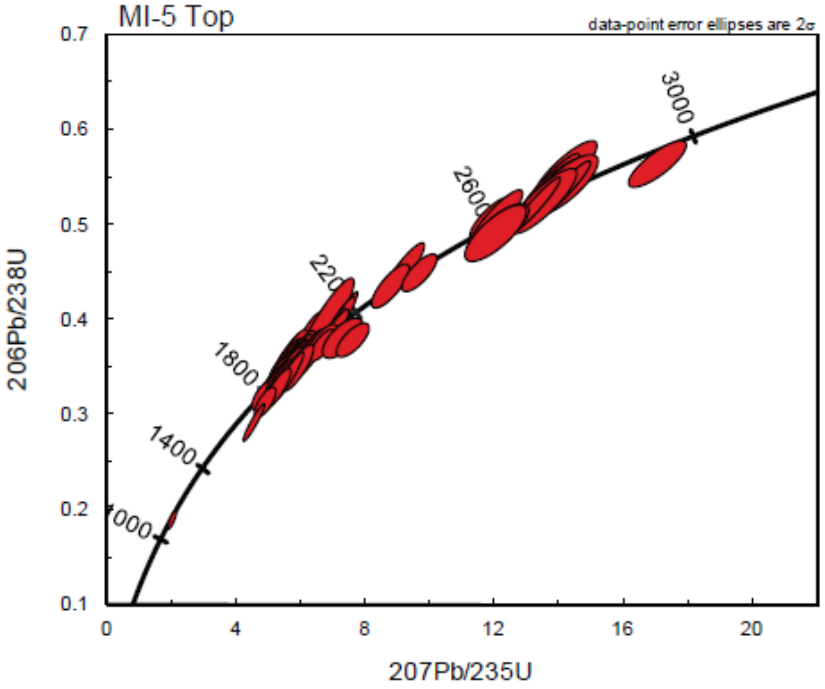

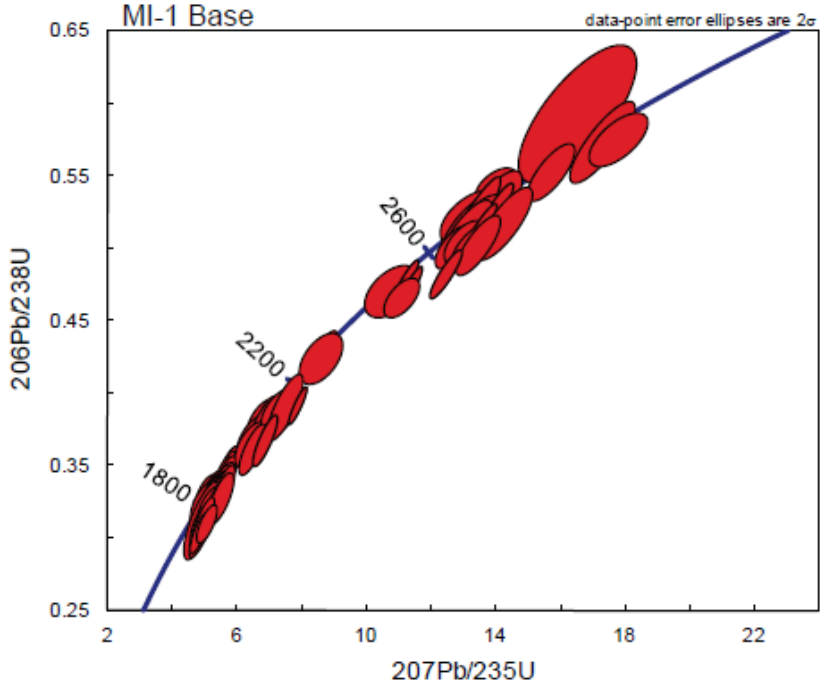

STRATIGRAPHIC SECTION

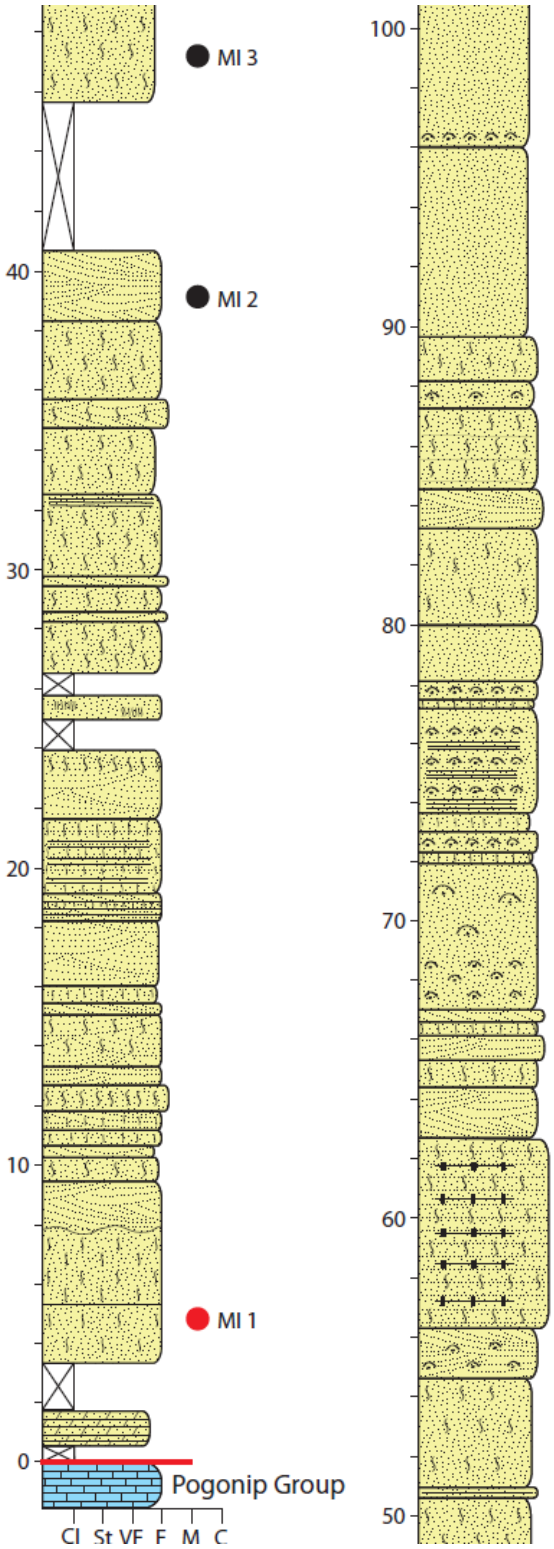

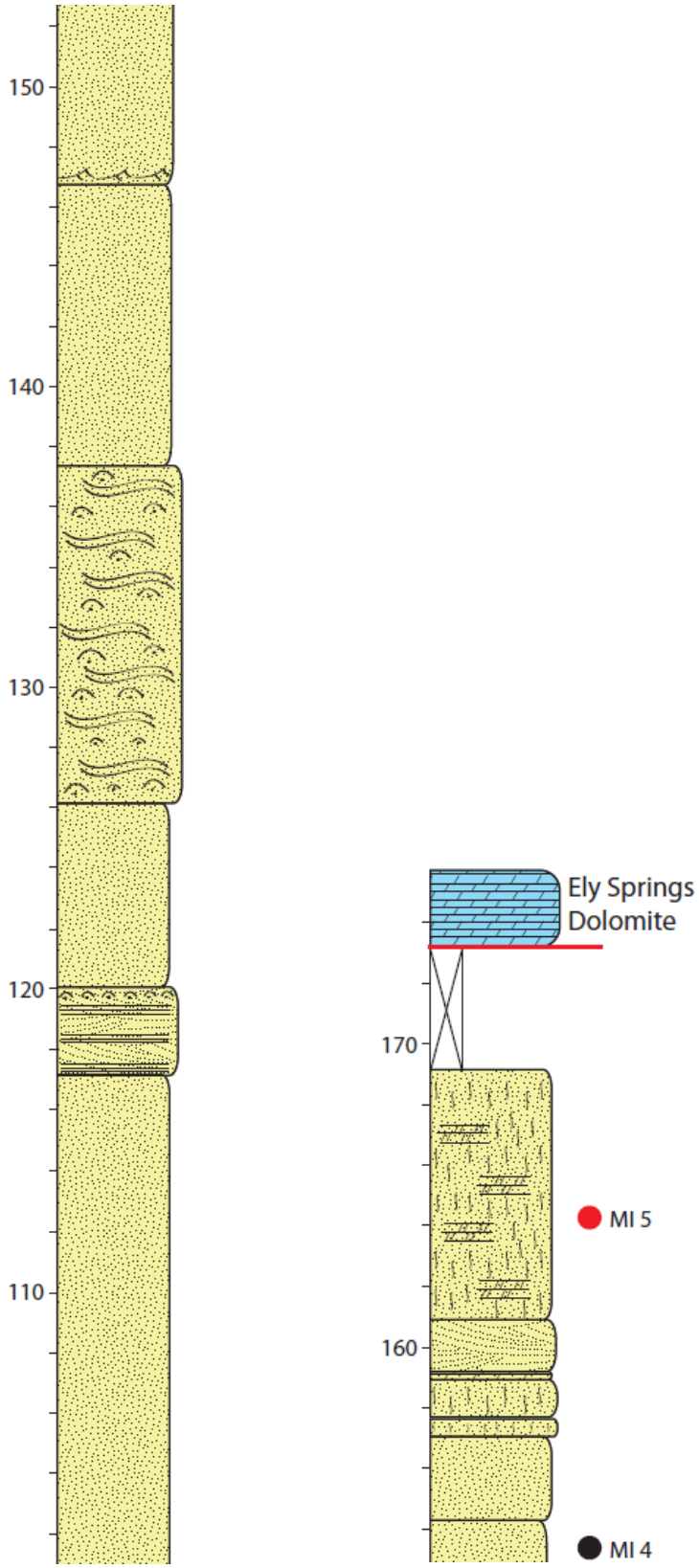
150
140
130
120
110
Ely Springs
Dolomite
170
MI 5
160
MI 4

APPENDIX F

LAST CHANCE RANGE

DATA TABLES

Sample PRMP-11 (Last Chance Range - Base)								
Sample	**238U/ 206Pb**	**1σ (%)**	**207Pb/ 206Pb**	**1σ (%)**	**238U/ 206Pb Age (Ma)**	**1σ**	**207Pb/ 206Pb Age (Ma)**	**1σ**
< 10% Discordant								
PRMP11_85a	2.92	0.0210	0.1080	0.0301	1898	34	1765	54
PRMP11_384a	2.85	0.0364	0.1107	0.0141	1938	61	1811	25
PRMP11_9a	1.84	0.0263	0.1799	0.0357	2801	59	2652	58
PRMP11_113a	1.87	0.0170	0.1775	0.0300	2759	38	2629	49
PRMP11_50a	2.57	0.0180	0.1246	0.0304	2118	32	2024	53
PRMP11_298a	2.93	0.0217	0.1107	0.0264	1893	35	1811	47
PRMP11_44a	2.92	0.0178	0.1109	0.0304	1896	29	1814	54
PRMP11_49a	2.79	0.0322	0.1158	0.0326	1973	55	1893	58
PRMP11_387a	2.94	0.0384	0.1107	0.0149	1886	62	1812	27
PRMP11_151a	2.86	0.0210	0.1141	0.0281	1930	35	1865	50
PRMP11_66a	2.96	0.0167	0.1111	0.0303	1876	27	1818	54
PRMP11_146a	2.10	0.0187	0.1582	0.0267	2513	39	2436	45
PRMP11_311a	2.88	0.0378	0.1141	0.0148	1920	62	1866	26
PRMP11_458a	2.94	0.0388	0.1121	0.0156	1886	63	1834	28
PRMP11_6a	2.93	0.0209	0.1126	0.0361	1893	34	1842	64
PRMP11_68a	3.02	0.0168	0.1097	0.0305	1842	27	1794	54
PRMP11_103a	2.84	0.0174	0.1162	0.0304	1946	29	1898	54
PRMP11_431a	2.99	0.0381	0.1112	0.0155	1860	61	1819	28
PRMP11_83a	3.00	0.0175	0.1110	0.0305	1857	28	1816	54
PRMP11_222a	2.91	0.0195	0.1139	0.0270	1905	32	1863	48
PRMP11_63a	2.96	0.0267	0.1124	0.0325	1877	43	1839	58
PRMP11_19a	2.94	0.0192	0.1130	0.0358	1885	31	1848	63
PRMP11_394a	2.61	0.0372	0.1268	0.0149	2091	66	2055	26

PRMP11_69a	3.05	0.0223	0.1098	0.0308	1827	35	1796	55
PRMP11_38a	1.86	0.0232	0.1895	0.0363	2778	52	2738	58
PRMP11_326a	1.89	0.0303	0.1851	0.0258	2737	67	2699	42
PRMP11_37a	1.91	0.0192	0.1824	0.0358	2712	42	2675	58
PRMP11_173a	1.90	0.0136	0.1846	0.0260	2731	30	2695	42
PRMP11_99a	3.01	0.0176	0.1117	0.0307	1851	28	1826	55
PRMP11_174a	2.97	0.0162	0.1131	0.0260	1870	26	1849	46
PRMP11_227a	3.12	0.0159	0.1085	0.0171	1794	25	1775	31
PRMP11_143a	1.80	0.0178	0.1993	0.0264	2851	41	2821	42
PRMP11_309a	2.98	0.0181	0.1127	0.0160	1863	29	1844	29
PRMP11_61a	3.07	0.0187	0.1102	0.0359	1820	30	1802	64
PRMP11_342a	2.08	0.0369	0.1646	0.0136	2527	77	2503	23
PRMP11_430a	2.84	0.0382	0.1182	0.0142	1945	64	1929	25
PRMP11_81a	2.99	0.0203	0.1129	0.0263	1861	33	1847	47
PRMP11_137a	2.86	0.0170	0.1174	0.0263	1931	28	1917	46
PRMP11_22a	3.05	0.0187	0.1111	0.0360	1830	30	1817	64
PRMP11_308a	2.98	0.0363	0.1134	0.0143	1864	59	1854	26
PRMP11_212a	3.01	0.0130	0.1124	0.0160	1848	21	1839	29
PRMP11_130a	3.05	0.0204	0.1111	0.0364	1826	32	1817	65
PRMP11_451a	3.07	0.0387	0.1108	0.0160	1816	61	1813	29
PRMP11_283a	3.05	0.0318	0.1115	0.0276	1827	50	1824	49
PRMP11_100a	2.89	0.0196	0.1174	0.0361	1918	32	1916	63
PRMP11_187a	2.87	0.0285	0.1181	0.0260	1928	47	1928	46
PRMP11_132a	3.02	0.0144	0.1128	0.0262	1845	23	1845	47
PRMP11_8a	2.91	0.0247	0.1166	0.0374	1904	41	1905	66
PRMP11_89a	3.04	0.0184	0.1121	0.0262	1833	29	1834	47
PRMP11_97a	3.07	0.0188	0.1114	0.0360	1816	30	1822	64
PRMP11_313a	3.11	0.0168	0.1103	0.0156	1798	26	1804	28
PRMP11_317a	3.08	0.0267	0.1113	0.0256	1814	42	1821	46
PRMP11_292a	1.98	0.0374	0.1793	0.0146	2635	80	2647	24
PRMP11_250a	3.07	0.0171	0.1117	0.0159	1817	27	1827	29
PRMP11_356a	3.10	0.0383	0.1110	0.0147	1802	60	1816	26
PRMP11_253a	3.01	0.0129	0.1141	0.0157	1851	21	1866	28
PRMP11_240a	2.99	0.0268	0.1148	0.0257	1861	43	1876	46
PRMP11_10a	1.99	0.0199	0.1791	0.0358	2620	43	2644	58
PRMP11_282a	3.07	0.0184	0.1122	0.0157	1818	29	1836	28
PRMP11_88a	2.53	0.0179	0.1358	0.0313	2150	33	2174	53
PRMP11_170a	3.02	0.0200	0.1140	0.0279	1843	32	1864	49
PRMP11_204a	3.07	0.0274	0.1124	0.0263	1816	43	1838	47

PRMP11_120a	3.13	0.0190	0.1105	0.0369	1786	30	1807	66
PRMP11_223a	3.12	0.0280	0.1109	0.0263	1791	44	1814	47
PRMP11_375a	2.91	0.0375	0.1182	0.0148	1902	62	1929	26
PRMP11_115a	3.07	0.0487	0.1128	0.0248	1819	77	1846	44
PRMP11_228a	3.05	0.0275	0.1135	0.0262	1829	44	1856	47
PRMP11_219a	3.05	0.0285	0.1136	0.0269	1830	45	1858	48
PRMP11_278a	3.08	0.0153	0.1127	0.0264	1815	24	1843	47
PRMP11_225a	2.66	0.0277	0.1296	0.0260	2060	49	2092	45
PRMP11_274a	2.65	0.0167	0.1299	0.0155	2063	29	2097	27
PRMP11_248a	3.01	0.0181	0.1153	0.0265	1849	29	1884	47
PRMP11_166a	3.11	0.0497	0.1119	0.0257	1797	78	1831	46
PRMP11_105a	2.09	0.0229	0.1739	0.0359	2525	48	2596	59
PRMP11_304a	2.70	0.0116	0.1291	0.0153	2029	20	2086	27
PRMP11_339a	3.17	0.0130	0.1112	0.0162	1768	20	1820	29
PRMP11_127a	3.11	0.0185	0.1133	0.0269	1799	29	1853	48
PRMP11_149a	1.98	0.0477	0.1871	0.0239	2631	102	2717	39
PRMP11_239a	3.09	0.0288	0.1140	0.0265	1805	45	1864	47
PRMP11_243a	2.02	0.0171	0.1836	0.0158	2592	36	2686	26
PRMP11_165a	3.12	0.0479	0.1135	0.0241	1791	75	1856	43
PRMP11_320a	2.73	0.0155	0.1294	0.0185	2013	27	2090	32
PRMP11_112a	3.13	0.0477	0.1138	0.0241	1788	74	1860	43
PRMP11_293a	3.10	0.0303	0.1148	0.0281	1803	47	1877	50
PRMP11_80a	2.04	0.0484	0.1831	0.0241	2574	102	2681	39
PRMP11_161a	3.04	0.0481	0.1177	0.0244	1835	76	1922	43
PRMP11_119a	3.06	0.0495	0.1169	0.0252	1823	78	1910	44
PRMP11_102a	3.31	0.0161	0.1094	0.0302	1702	24	1790	54
PRMP11_193a	2.14	0.0300	0.1743	0.0261	2469	61	2600	43
PRMP11_128a	2.76	0.0477	0.1299	0.0242	1991	81	2096	42
PRMP11_272a	3.62	0.0152	0.1018	0.0168	1572	21	1657	31
PRMP11_96a	3.08	0.0485	0.1183	0.0253	1814	76	1931	45
PRMP11_154a	3.06	0.0502	0.1193	0.0252	1825	79	1946	44
PRMP11_157a	3.19	0.0478	0.1146	0.0242	1756	73	1874	43
PRMP11_74a	3.23	0.0483	0.1143	0.0241	1739	73	1869	43
PRMP11_141a	3.09	0.0503	0.1194	0.0254	1810	79	1947	45
PRMP11_416a	2.96	0.0398	0.1249	0.0171	1877	65	2027	30
PRMP11_472a	2.64	0.0391	0.1410	0.1025	2073	69	2239	167
PRMP11_86a	3.47	0.0187	0.1096	0.0357	1632	27	1792	64
> 10% Discordant								

PRMP11_114a	3.63	0.0208	0.1099	0.0304	1567	29	1797	54
PRMP11_205a	2.87	0.0309	0.1525	0.0290	1930	51	2374	49
PRMP11_163a	7.35	0.0533	0.1068	0.0255	822	41	1745	46
PRMP11_232a	4.51	0.0873	0.2981	0.0359	1291	101	3460	55
PRMP11_254a	11.62	0.0221	0.1071	0.0151	532	11	1751	27

Sample PRMP-10 (Last Chance Range - Top)								
Sample	**238U/ 206Pb**	**1σ (%)**	**207Pb/ 206Pb**	**1σ (%)**	**238U/ 206Pb Age (Ma)**	**1σ**	**207Pb/206Pb Age (Ma)**	**1σ**
< 10% Discordant								
PRMP10_147a	2.52	0.0352	0.1175	0.0111	2155	64	1918	20
PRMP10_9a	2.74	0.0323	0.1123	0.0170	2003	55	1837	30
PRMP10_174a	1.63	0.0243	0.2043	0.0125	3083	59	2861	20
PRMP10_161a	2.66	0.0319	0.1174	0.0126	2056	56	1917	22
PRMP10_14a	2.40	0.0356	0.1295	0.0168	2242	67	2092	29
PRMP10_192a	1.79	0.0260	0.1835	0.0123	2862	60	2685	20
PRMP10_123a	2.86	0.0213	0.1116	0.0122	1932	35	1826	22
PRMP10_190a	1.67	0.0206	0.2048	0.0124	3019	49	2865	20
PRMP10_66a	2.56	0.0232	0.1242	0.0102	2124	42	2017	18
PRMP10_104a	2.90	0.0161	0.1109	0.0291	1908	27	1815	52
PRMP10_146b	2.89	0.0237	0.1115	0.0132	1913	39	1823	24
PRMP10_61a	4.23	0.0106	0.0846	0.0282	1369	13	1305	54
PRMP10_150a	1.80	0.0212	0.1878	0.0259	2854	49	2723	42
PRMP10_8a	2.88	0.0308	0.1123	0.0175	1923	51	1836	31
PRMP10_18a	2.47	0.0333	0.1295	0.0170	2188	61	2091	30
PRMP10_135a	2.78	0.0334	0.1158	0.0116	1980	57	1893	21
PRMP10_89a	3.00	0.0218	0.1089	0.0096	1854	35	1782	17
PRMP10_51a	2.94	0.0423	0.1110	0.0365	1886	69	1815	65
PRMP10_98a	2.90	0.0176	0.1125	0.0298	1912	29	1841	53
PRMP10_15a	2.56	0.0382	0.1263	0.0175	2127	69	2047	31
PRMP10_211a	2.92	0.0214	0.1118	0.0116	1899	35	1829	21
PRMP10_97a	1.85	0.0306	0.1832	0.0102	2781	69	2682	17
PRMP10_80a	2.87	0.0273	0.1138	0.0120	1929	45	1861	22
PRMP10_229a	2.91	0.0207	0.1126	0.0124	1904	34	1841	22
PRMP10_215a	1.89	0.0122	0.1804	0.0253	2743	27	2657	41
PRMP10_152a	1.87	0.0164	0.1823	0.0280	2760	37	2674	46
PRMP10_184a	2.01	0.0116	0.1671	0.0253	2608	25	2529	42
PRMP10_219a	1.84	0.0112	0.1862	0.0257	2793	25	2709	42
PRMP10_26a	2.97	0.0450	0.1108	0.0367	1869	73	1813	65
PRMP10_71a	2.83	0.0137	0.1160	0.0297	1950	23	1895	53
PRMP10_149a	2.79	0.0183	0.1177	0.0292	1975	31	1922	51
PRMP10_11a	2.91	0.0300	0.1134	0.0167	1904	49	1854	30
PRMP10_140a	2.80	0.0150	0.1175	0.0283	1969	25	1919	50

PRMP10_151a	2.76	0.0223	0.1193	0.0114	1995	38	1946	20
PRMP10_160a	2.95	0.0223	0.1124	0.0131	1884	36	1839	24
PRMP10_84a	1.85	0.0163	0.1877	0.0281	2790	37	2722	46
PRMP10_12a	2.68	0.0378	0.1226	0.0364	2043	66	1995	63
PRMP10_225a	2.97	0.0191	0.1118	0.0123	1872	31	1828	22
PRMP10_41a	2.83	0.0122	0.1166	0.0285	1948	21	1905	50
PRMP10_141a	2.95	0.0218	0.1126	0.0300	1884	36	1842	53
PRMP10_48a	1.87	0.0426	0.1860	0.0367	2764	95	2707	59
PRMP10_103a	2.53	0.0307	0.1302	0.0145	2145	56	2101	25
PRMP10_131a	2.86	0.0124	0.1159	0.0282	1931	21	1893	50
PRMP10_78a	2.96	0.0234	0.1125	0.0113	1877	38	1840	20
PRMP10_173a	2.89	0.0133	0.1151	0.0283	1917	22	1882	50
PRMP10_207a	1.88	0.0145	0.1847	0.0262	2745	32	2695	43
PRMP10_138a	2.89	0.0237	0.1150	0.0150	1915	39	1880	27
PRMP10_142a	1.84	0.0113	0.1912	0.0292	2803	26	2753	47
PRMP10_201a	2.85	0.0153	0.1164	0.0257	1937	26	1902	45
PRMP10_77a	1.91	0.0233	0.1810	0.0102	2709	51	2662	17
PRMP10_179a	2.98	0.0188	0.1121	0.0264	1864	30	1834	47
PRMP10_40a	3.00	0.0483	0.1116	0.0367	1854	77	1825	65
PRMP10_107a	2.91	0.0235	0.1148	0.0106	1906	39	1878	19
PRMP10_203a	2.84	0.0125	0.1175	0.0256	1947	21	1918	45
PRMP10_157a	1.85	0.0138	0.1901	0.0254	2784	31	2743	41
PRMP10_70a	1.78	0.0240	0.2000	0.0098	2868	55	2826	16
PRMP10_34a	1.88	0.0404	0.1863	0.0170	2749	90	2709	28
PRMP10_53a	1.83	0.0125	0.1937	0.0293	2814	28	2774	47
PRMP10_210a	3.02	0.0194	0.1113	0.0125	1844	31	1820	23
PRMP10_56a	1.83	0.0419	0.1950	0.0186	2816	95	2785	30
PRMP10_188a	1.92	0.0147	0.1830	0.0255	2706	32	2681	42
PRMP10_134a	1.95	0.0202	0.1786	0.0257	2664	44	2640	42
PRMP10_73a	2.98	0.0136	0.1133	0.0294	1867	22	1854	52
PRMP10_67a	3.07	0.0457	0.1104	0.0363	1818	72	1806	65
PRMP10_47a	2.99	0.0180	0.1130	0.0302	1860	29	1848	54
PRMP10_29a	3.03	0.0240	0.1119	0.0124	1839	38	1830	22
PRMP10_209a	1.84	0.0148	0.1943	0.0260	2793	34	2779	42
PRMP10_206a	2.73	0.0210	0.1233	0.0126	2014	36	2004	22
PRMP10_133a	2.94	0.0106	0.1148	0.0292	1885	17	1876	52
PRMP10_76a	3.02	0.0238	0.1122	0.0108	1842	38	1836	19
PRMP10_158a	2.87	0.0116	0.1180	0.0256	1929	19	1925	45
PRMP10_170a	3.03	0.0166	0.1126	0.0263	1840	26	1841	47

PRMP10_23a	2.99	0.0235	0.1137	0.0099	1858	38	1859	18
PRMP10_45a	1.89	0.0229	0.1896	0.0099	2736	51	2739	16
PRMP10_186a	2.27	0.0144	0.1506	0.0258	2351	28	2353	43
PRMP10_43a	1.97	0.0475	0.1793	0.0365	2642	102	2646	59
PRMP10_114a	3.00	0.0120	0.1137	0.0295	1856	19	1859	52
PRMP10_36a	2.77	0.0515	0.1224	0.0384	1986	87	1992	67
PRMP10_63a	2.30	0.0127	0.1502	0.0293	2331	25	2349	49
PRMP10_91a	2.58	0.0116	0.1322	0.0294	2112	21	2128	51
PRMP10_189a	1.87	0.0187	0.1946	0.0115	2757	42	2781	19
PRMP10_65a	3.08	0.0463	0.1122	0.0369	1813	73	1836	65
PRMP10_214a	1.97	0.0186	0.1843	0.0116	2651	40	2692	19
PRMP10_16a	2.80	0.0349	0.1230	0.0180	1968	59	2001	32
PRMP10_82a	2.96	0.0146	0.1170	0.0283	1878	24	1910	50
PRMP10_58a	2.86	0.0140	0.1206	0.0288	1931	23	1966	51
PRMP10_99a	3.02	0.0120	0.1150	0.0295	1845	19	1879	52
PRMP10_57a	2.65	0.0133	0.1314	0.0297	2065	24	2117	51
PRMP10_72a	5.70	0.0220	0.0751	0.0118	1042	21	1071	24
PRMP10_95a	2.95	0.0117	0.1198	0.0295	1884	19	1953	52
PRMP10_128a	1.98	0.0204	0.1899	0.0283	2632	44	2742	46
PRMP10_122a	3.98	0.0121	0.0942	0.0296	1445	16	1512	55
PRMP10_39a	2.21	0.0151	0.1678	0.0280	2405	30	2536	46
PRMP10_62a	3.31	0.0446	0.1110	0.0378	1701	66	1816	67
PRMP10_125a	2.07	0.0268	0.1896	0.0292	2542	56	2739	47
PRMP10_7a	3.21	0.0321	0.1177	0.0165	1749	49	1922	29
> 10% Discordant								
PRMP10_213a	2.03	0.0354	0.2068	0.0280	2586	75	2880	45
PRMP10_75a	2.16	0.0122	0.1898	0.0291	2454	25	2740	47
PRMP10_38a	2.71	0.0163	0.1431	0.0334	2026	28	2265	57
PRMP10_175a	3.59	0.0192	0.1084	0.0115	1583	27	1772	21
PRMP10_112a	4.82	0.0202	0.1042	0.0293	1216	22	1700	53

WETHERIL PLOTS

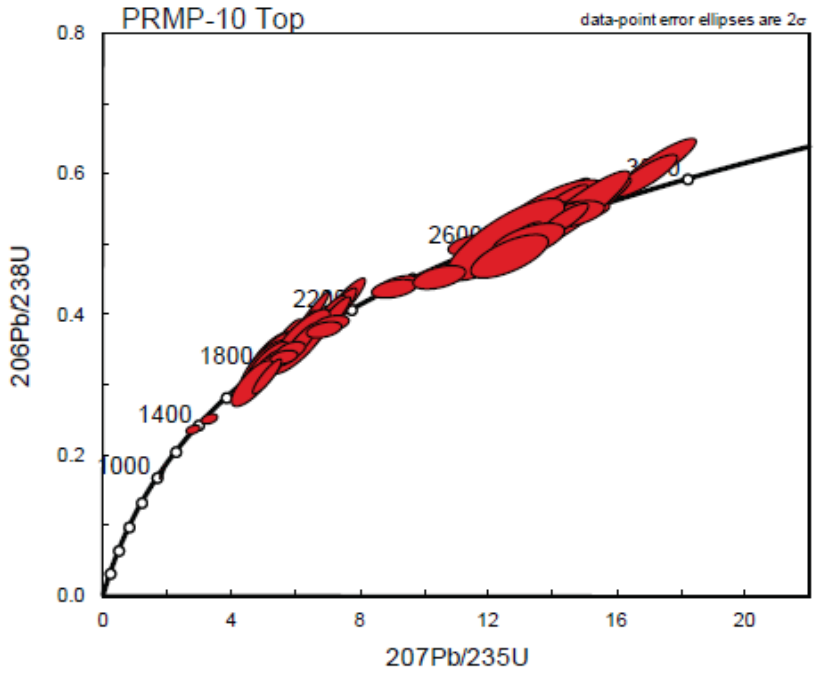

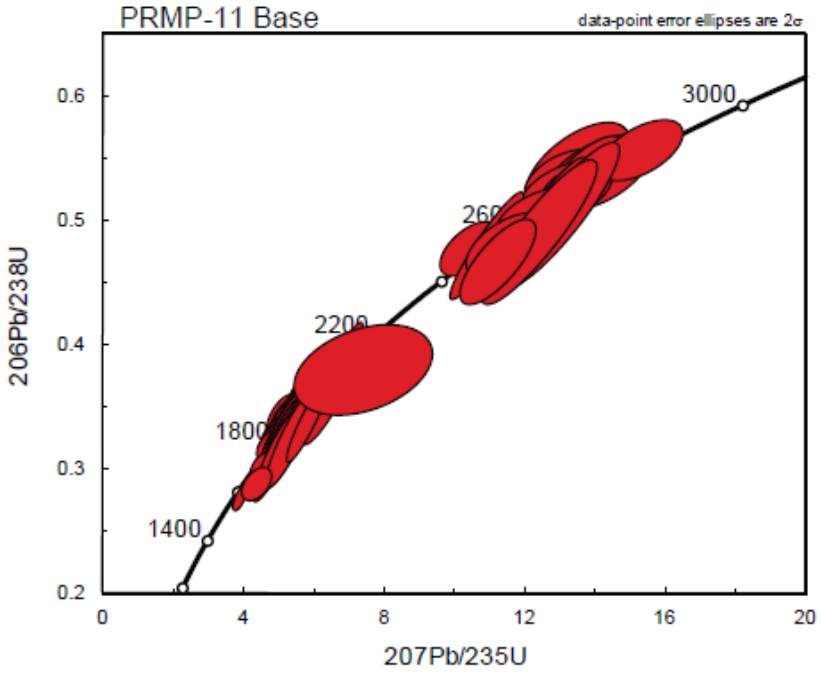

STRATIGRAPHIC SECTION

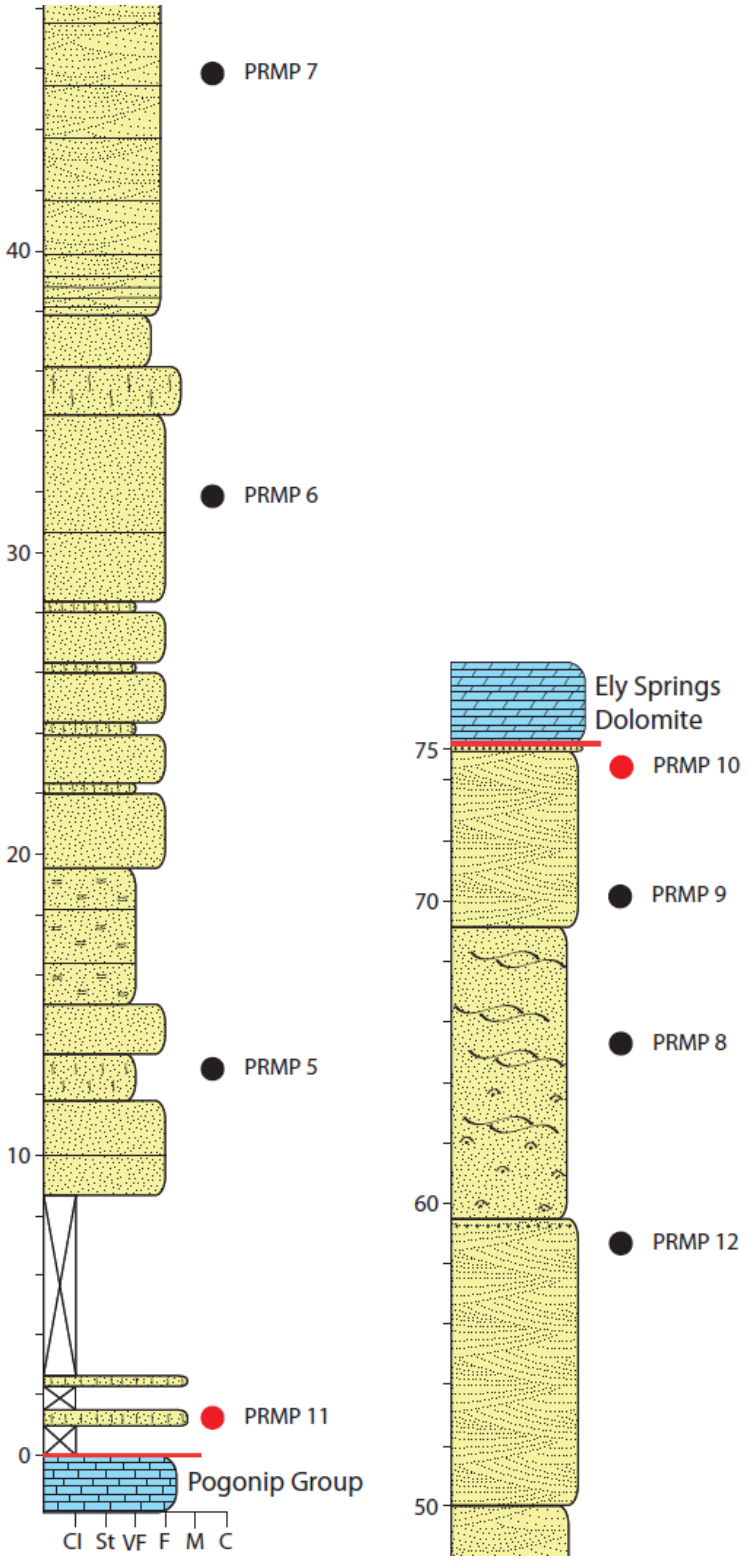

APPENDIX G

SPOTTED RANGE

STRATIGRAPHIC SECTION

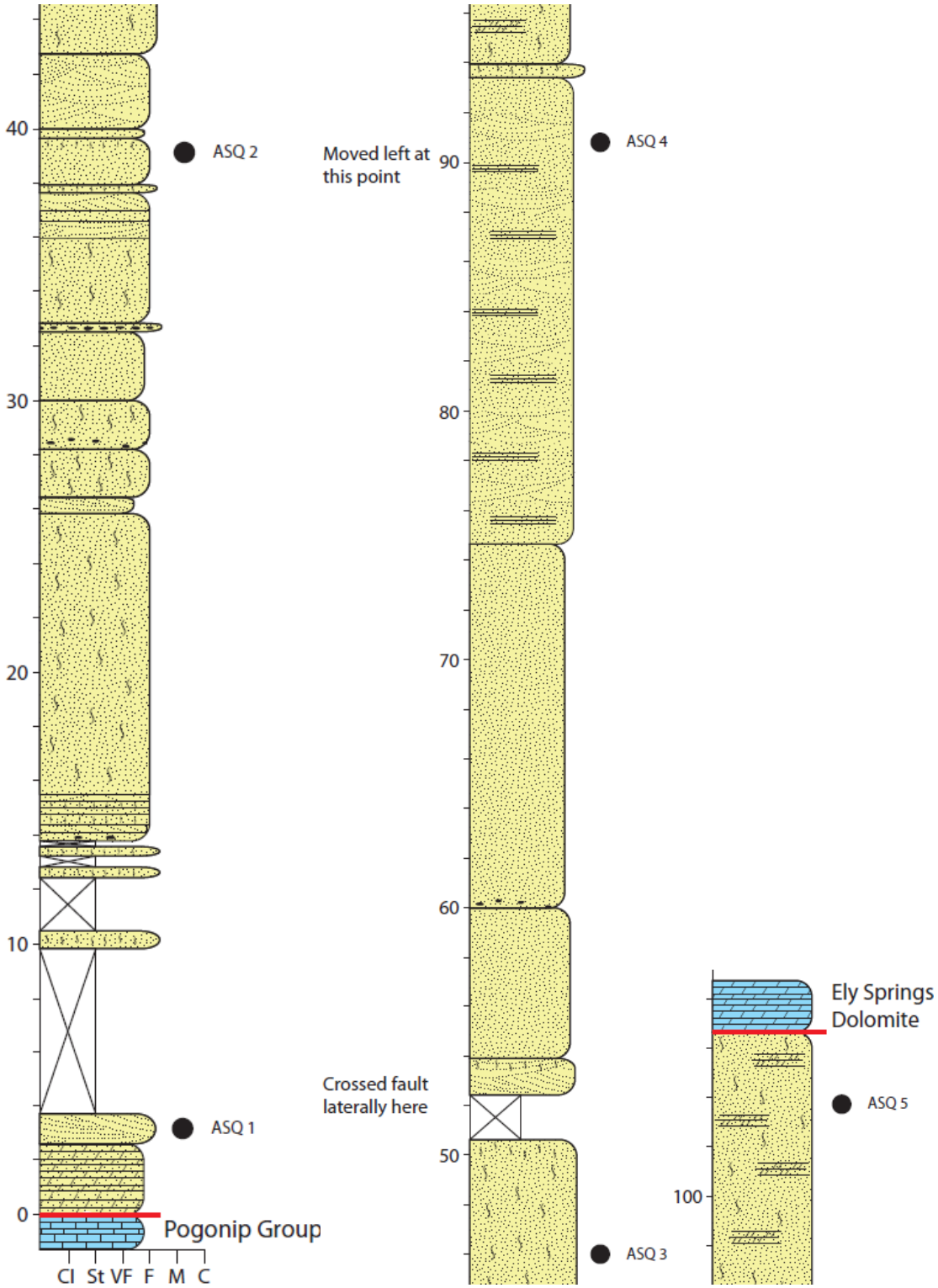

APPENDIX H

NOPAH RANGE

STRATIGRAPHIC SECTION

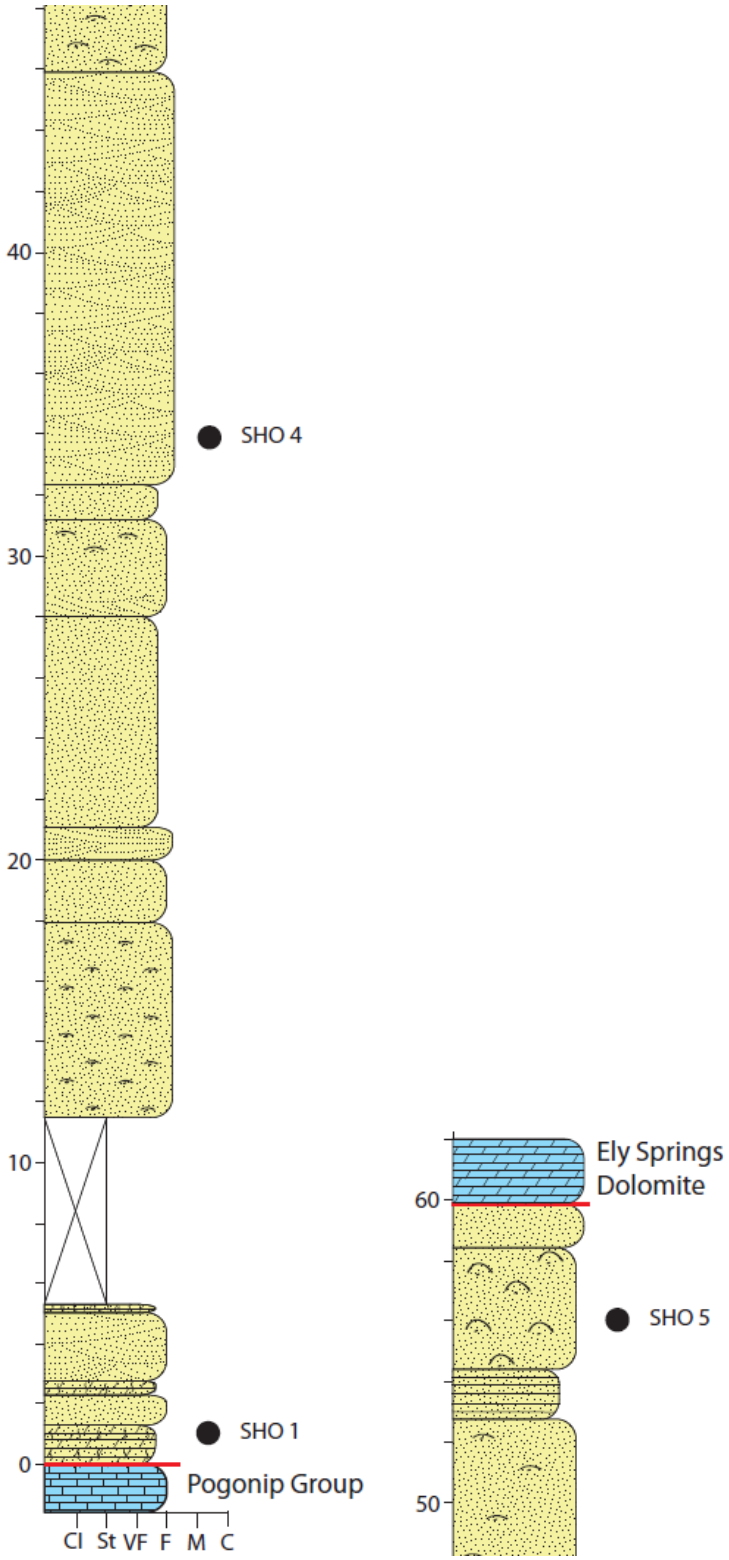

VITA

Name:	Benjamin David Workman
Address:	Department of Geology and Geophysics, MS 3115, Texas A&M University College Station, Texas 77843-3115
Email Address:	workman.ben@gmail.com
Education:	B.S., Geology, Calvin College, 2008 M.S., Geology, Texas A&M University, 2012